

IOWA STATE UNIVERSITY  
Digital Repository

---

Retrospective Theses and Dissertations

Iowa State University Capstones, Theses and  
Dissertations

---

1975

# The multiconfiguration self-consistent field method for many-electron systems and its application to the dissociation of ethylene

Lap Ming Cheung  
*Iowa State University*

Follow this and additional works at: <https://lib.dr.iastate.edu/rtd>



Part of the [Physical Chemistry Commons](#)

---

## Recommended Citation

Cheung, Lap Ming, "The multiconfiguration self-consistent field method for many-electron systems and its application to the dissociation of ethylene" (1975). *Retrospective Theses and Dissertations*. 5464.  
<https://lib.dr.iastate.edu/rtd/5464>

This Dissertation is brought to you for free and open access by the Iowa State University Capstones, Theses and Dissertations at Iowa State University Digital Repository. It has been accepted for inclusion in Retrospective Theses and Dissertations by an authorized administrator of Iowa State University Digital Repository. For more information, please contact [digirep@iastate.edu](mailto:digirep@iastate.edu).



## **INFORMATION TO USERS**

This material was produced from a microfilm copy of the original document. While the most advanced technological means to photograph and reproduce this document have been used, the quality is heavily dependent upon the quality of the original submitted.

The following explanation of techniques is provided to help you understand markings or patterns which may appear on this reproduction.

- 1. The sign or "target" for pages apparently lacking from the document photographed is "Missing Page(s)". If it was possible to obtain the missing page(s) or section, they are spliced into the film along with adjacent pages. This may have necessitated cutting thru an image and duplicating adjacent pages to insure you complete continuity.**
- 2. When an image on the film is obliterated with a large round black mark, it is an indication that the photographer suspected that the copy may have moved during exposure and thus cause a blurred image. You will find a good image of the page in the adjacent frame.**
- 3. When a map, drawing or chart, etc., was part of the material being photographed the photographer followed a definite method in "sectioning" the material. It is customary to begin photoing at the upper left hand corner of a large sheet and to continue photoing from left to right in equal sections with a small overlap. If necessary, sectioning is continued again — beginning below the first row and continuing on until complete.**
- 4. The majority of users indicate that the textual content is of greatest value, however, a somewhat higher quality reproduction could be made from "photographs" if essential to the understanding of the dissertation. Silver prints of "photographs" may be ordered at additional charge by writing the Order Department, giving the cataiog number, title, author and specific pages you wish reproduced.**
- 5. PLEASE NOTE: Some pages may have indistinct print. Filmed as received.**

**Xerox University Microfilms**  
300 North Zeeb Road  
Ann Arbor, Michigan 48106

76-1829

CHEUNG, Lap Ming, 1947-  
THE MULTICONFIGURATION SELF-CONSISTENT FIELD  
METHOD FOR MANY-ELECTRON SYSTEMS AND ITS  
APPLICATION TO THE DISSOCIATION OF ETHYLENE.

Iowa State University, Ph.D., 1975  
Chemistry, physical

Xerox University Microfilms, Ann Arbor, Michigan 48106

THIS DISSERTATION HAS BEEN MICROFILMED EXACTLY AS RECEIVED.

The multiconfiguration self-consistent field method  
for many-electron systems and its application  
to the dissociation of ethylene

by

Lap Ming Cheung

A Dissertation Submitted to the  
Graduate Faculty in Partial Fulfillment of  
The Requirements for the Degree of  
DOCTOR OF PHILOSOPHY

Department: Chemistry  
Major: Physical Chemistry

Approved:

Signature was redacted for privacy.

In Charge of Major Work

Signature was redacted for privacy.

For the Major Department

Signature was redacted for privacy.

For the Graduate College

Iowa State University  
Ames, Iowa

1975

## TABLE OF CONTENTS

	Page
I. INTRODUCTION	1
II. FORMULATION OF THE MCSCF METHOD	11
A. Multiconfiguration Wavefunction	11
B. Generalized Brillouin Theorem	13
C. Natural Orbitals	19
D. Orbital Optimization	22
E. Treatment of Excited States	28
F. Calculation Procedure	30
G. SCF Iterations and Extrapolations	31
H. Implementation	33
I. Conclusions	33
III. DISSOCIATION OF ETHYLENE	35
A. Introduction	35
B. The Orbital and Configurational Reaction Space	39
1. Molecular orbitals	39
2. Configurations of $^1\text{Ag}$ symmetry in terms of symmetry orbitals	41
3. Configurations of $^1\text{Ag}$ symmetry in terms of left and right orbitals	42
4. Separation to infinity	49
C. Calculational Procedure and Basis Set	54
D. The Three Low Lying States of Methylene	56
E. Dissociation of the Ethylene Ground State into Triplet Methylenes	57

	Page
1. Reaction coordinates	57
2. Energetics of dissociation	58
3. Configurational analysis of dissociation	60
4. Orbital analysis of dissociation	62
5. Excited states from ground state MCSCF calculations	63
F. Dissociation of the Lowest $^1\text{A}_g$ ( $\pi^*^2$ ) Excited State of Ethylene into Singlet Methylenes	63
1. Reaction coordinates	63
2. Energetics of dissociation	66
3. Configurational analysis of dissociation	69
4. Orbital analysis of dissociation	70
IV. LITERATURE CITED	90
V. ACKNOWLEDGMENTS	94
VI. APPENDIX A: DESCRIPTION OF THE MCSCF PROGRAM	95
VII. APPENDIX B: CONTRACTED ATOMIC ORBITALS	99
VIII. APPENDIX C: EXPANSIONS OF MOLECULAR ORBITALS IN TERMS OF ATOMIC ORBITALS FOR THE LOWEST TWO $^1\text{A}_g$ STATES OF ETHYLENE	103

## I. INTRODUCTION

Quantum chemistry deals with the theory of atomic and molecular electronic structure. It describes this structure in terms of wave mechanics which was first introduced by Schrödinger in 1926 [1]. The stationary states of an atomic or molecular system are given by the solution to the Schrödinger equation

$$\mathcal{H} \Psi = E\Psi \quad (1.1)$$

where  $\mathcal{H}$  is the non-relativistic Hamiltonian operator. Most of chemistry is implicit in the wavefunction  $\Psi$  and so virtually the whole field of quantum chemistry depends on the explicit solution of the equation. The exact solution is, however, difficult and to date has been possible only for atoms and molecules with one electron. Therefore approximate solution methods must be employed. The most commonly used approximation is the self-consistent field method first developed by Hartree in 1928 [2]. In this approach, each electron moves in an effective potential field arising from the nuclei and the average charge distribution of all other electrons. The many-body problem is thus replaced by an independent particle model where it is possible to define individual electronic wavefunctions  $\phi_i$  (spin orbitals) and energy levels  $\epsilon_i$  (orbital energies) by an equation

$$\mathcal{H}_{\text{eff}} \phi_i = \epsilon_i \phi_i \quad (1.2)$$

where the "effective Hamiltonian"  $\mathcal{H}_{\text{eff}}$  is a sum of the kinetic energy and the effective potential field. Using an assumed charge distribution to start with, the equation can be solved for  $\phi_i$  which in turn is used to determine a new charge distribution from which a new effective potential is evaluated for the next iteration. The process is then repeated until self-consistency is achieved. One then says that the electron moves in a self-consistent field.

An equation of the type (1.2) can be derived from Equation (1.1) by means of the variational treatment on the expectation value of the total energy, if  $\Psi$  is expressed as a product of spin orbitals or a Slater determinant [3]. The latter form is more accurate since the Pauli Exclusion Principle [4] is taken into account. This approach is known as the Hartree-Fock method [5]. The Hartree-Fock equation is similar to Equation (1.2)

$$\mathcal{T} \phi_i = \epsilon_i \phi_i \quad (1.3)$$

where  $\mathcal{T}$  is the Fock operator defined in terms of the nuclei field, coulomb and exchange operators. The Hartree-Fock self-consistent field (HFSCF) method was initially developed for application to atoms. The extension to molecules where the molecular orbitals [6] are expanded as linear combina-

tions of atomic orbitals (LCAO) has been formalized by Roothaan [7]. Given a set of atomic orbitals  $\{X_k\}$  as a basis, the HF orbitals  $\{\phi_i\}$  can be expressed in the form

$$\phi_i = \sum_k X_k C_{ki} \quad (1.4)$$

The coefficients  $\{C_{ki}\}$  are then determined by means of Roothaan's matrix SCF procedure.

This procedure has since then been widely used. Most of the electronic structure calculations in the past are of this variety. In the variational sense, the HF wavefunction is the best one-configuration wavefunction that can be constructed. In addition, the molecular orbital picture presented by the HF model provides a simple and useful conceptual framework for interpreting many molecular phenomena. Also with the advance of fast and large computers, it can be computationally implemented for a vast number of molecular systems. However, the HF approximation neglects the instantaneous (rather than averaged) repulsion between electrons which is called electron correlation. Therefore although molecular properties calculated from HF wavefunctions are often reasonably accurate, it fails in cases where electron correlation is critically important. For example the dipole moment of carbon monoxide calculated from HF wavefunction is completely wrong [8]. Another deficiency

resulted from the total neglect of electron correlation is the inability to describe molecule formation and dissociation properly, since in most cases, electron correlation is not constant with respect to separation. Moreover, the model naturally breaks down in the calculation of potential energy curves for processes where there is a change of electronic configuration. The  $F_2$  molecule was predicted to have a negative dissociation energy [9]. Therefore methods of going beyond the HFSCF approximation are necessary.

The most commonly used method to improve molecular wavefunctions is superposition of configurations or configuration interaction (CI) [10]. For a given basis set, there is a virtual orbital space in addition to the HF orbitals. These virtual orbitals can be used to construct other configurations. A CI function is of the form

$$\Psi = \sum_n a_n \Phi_n \quad (1.5)$$

which is just a linear combination of configurations  $\{\Phi_n\}$  based on orbitals which have not been optimized, but with the expansion coefficients  $\{a_n\}$  variationally determined. Such CI functions were successful in recovering part of the correlation energy neglected by the HF model. However, a reasonably accurate wavefunction often requires a large number of configurations [11] due to poor representation of the

virtual space. This is the major problem with applying the CI procedure to large molecules. Several techniques have been developed to solve this problem of convergence. Some workers have used perturbation techniques [12, 13] to choose those configurations which give significant contribution to the energy. Others have employed various forms of natural orbitals [11, 14, 15] to hasten convergence. But perhaps the most promising approach is the multiconfiguration self-consistent field (MCSCF) method.

The MCSCF method goes beyond the CI method by variationally optimizing the orbitals simultaneously with the mixing coefficients. In this way, there is no ambiguity in the choice of the orbitals from which the configurations are constructed. The result is that the MCSCF wavefunction will be short, compact and easy to interpret. The MCSCF method can also be considered a generalization of the one-configuration HFSCF method. In fact the first MCSCF calculation was done by Hartree himself and coworkers [16]. More recently, there has been a revival of interest. A brief review of the formulation of the problem is given here, following the treatment of Hiraç and Nakatsuji [17].

The MC wavefunction is of the form given in Equation (1.5), where  $\{\Phi_n\}$  are antisymmetric many-electron functions constructed from spin orbitals  $\{\phi_i\}$ . In the MCSCF theory, the expectation value of the total energy is variationally

stationary with respect to all variations of the coefficients  $\{a_n\}$  and of the orbitals  $\{\phi_i\}$

$$\delta E = \delta \langle \Psi | H | \Psi \rangle = 0 \quad (1.6)$$

under the orthonormality constraints

$$\sum_n a_n^2 = 1 \quad (1.7)$$

and

$$\langle \phi_i | \phi_j \rangle = \delta_{ij} \quad (1.8)$$

While the coefficients  $\{a_n\}$  are readily determined from a secular equation, the optimization of the orbitals  $\{\phi_i\}$  is a more difficult problem. One approach involves the use of Lagrangian multipliers  $\{\lambda_{ji}\}$  and leads to the identity

$$\delta E - 2 \delta \sum_{ij} \lambda_{ji} \langle \phi_i | \phi_j \rangle = 0 \quad (1.9)$$

or

$$\begin{aligned} & 2 \sum_i \{ \langle \delta \phi_i | F_i | \phi_i \rangle + \langle \phi_i | F_i | \delta \phi_i \rangle \} \\ & - 2 \sum_{ij} \lambda_{ji} \{ \langle \delta \phi_i | \phi_j \rangle + \langle \phi_i | \delta \phi_j \rangle \} = 0 \end{aligned} \quad (1.10)$$

where  $F_i$  is an effective one-electron Hamiltonian. The first two summations are just adjoints of each other, as are  $\langle \delta \phi_i | \phi_j \rangle$  and  $\langle \phi_i | \delta \phi_j \rangle$ . Consequently,

$$F_i |\phi_i\rangle = \sum_j |\phi_j\rangle \lambda_{ji} \quad (1.11)$$

$$\langle \phi_i | F_i = \sum_j \langle \phi_j | \lambda_{ij} \quad (1.12)$$

Taking the complex conjugate of Equation (1.12) and subtracting from Equation (1.11) indicates that  $\{\lambda_{ij}\}$  are hermitian, viz.,

$$\lambda_{ij}^* = \lambda_{ji} \quad (1.13)$$

Equation (1.11) together with Equation (1.13) are the correct variational conditions. The orbital orthonormality allows them to be rewritten as,

$$F_i |\phi_i\rangle = \sum_j |\phi_j\rangle \langle \phi_j | F_i | \phi_i \rangle \quad (1.14a)$$

$$\langle \phi_j | F_i - F_j | \phi_i \rangle = 0 \quad (1.14b)$$

which eliminate the Lagrangian multipliers. The problem is how to combine these two equations into a simple eigenvalue equation which can be solved for all orbitals. There have been a variety of coupling operator methods developed [18-23], but successful practical applications to molecules are limited [24-26].

The best method so far seems to be the optimized valence configuration (OVC) formalism developed by Das and Wahl [18]. This method was developed with particular emphasis in obtaining chemically accurate potential curves for diatomics

[26], but recently it has been extended to triatomics [27]. Unfortunately the SCF operators proposed by Das and Wahl are improper since the variational condition of Equation (1.14b) is not taken into account [17]. Consequently this method does not necessarily yield optimum solution unless the initial orbitals are accurately chosen. Also this may be the source of poor convergence. However, despite this drawback, the OVC method has been applied to a vast number of molecules successfully.

In conclusion, we find that practical solution of Equations (1.14a) and (1.14b) is difficult by coupling operator technique. Another approach is possible, however. These two Equations (1.14a) and (1.14b) have been shown to be equivalent to the generalized Brillouin Theorem [28] by Hirao and Nakatsuji [17] (see also Section IIB). Since it has been known for some time that HF wavefunctions can be obtained by an iterative procedure based on the Brillouin Theorem [29, 30], the generalization to MC wavefunction is natural and in fact has been applied by Grein and Chang [31] to calculate atomic wavefunctions. The method is simple and easily adapted for numerical solution. However there is one deficiency in the iterative procedure by Grein and Chang which is similar to neglecting Equation (1.14b) in coupling operator technique. The orbitals have to be orthonormalized at each iteration, which may be the source of unoptimum solution or

slow convergence. A new technique is therefore desirable.

In this dissertation, an iterative MCSCF procedure based on the generalized Brillouin Theorem and the application of natural orbitals is developed. Natural orbitals can be used to give a better representation of the orbital space from which a CI wavefunction is constructed. Adams [32] pointed out that in most MCSCF techniques, a common feature is the important role played by natural orbitals. Das and Wahl [18], Veillard and Clementi [21], Hinze and Roothaan [19] all attempted to restrict mixing configurations to differ by at least two spin orbitals, making the molecular orbitals automatically natural orbitals. The generalized valence bond theory [33], a special case of MCSCF theory, was developed by Goddard who used natural orbitals to construct geminals. The iterative natural orbital method [34] suggested by Bender and Davidson and used extensively by Schaefer [35] indicates the power of natural orbitals, although in this method there is no variational condition imposed on the energy. All these facts show the usefulness of natural orbitals in MCSCF calculations.

The novel aspect of the present approach lies in the combined application of the generalized Brillouin Theorem and of natural orbitals. In order to avoid complications due to spin, a novel approach to the handling of the spin eigenfunction problem is used, namely the expansion of the MC wavefunction

in terms of spin adapted antisymmetrized products (SAAP's) [36]. Symmetry is also included to simplify the calculations. As a consequence, the resulting computer program can handle almost any type of MC wavefunction. Hence, the treatment here is more general than previous approaches. This method has been applied to study the dissociation of ethylene.

## II. FORMULATION OF THE MCSCF METHOD

### A. Multiconfiguration Wavefunction

The space basis of a MCSCF wavefunction of a N-electron system is an orthonormal set of spatial symmetry orbitals

$$\{\phi_1^{v\mu}, \phi_2^{v\mu}, \dots, \phi_{\delta_v}^{v\mu}\} \quad v = 1, 2, \dots, K \\ \mu = 1, 2, \dots, I_v$$

with (2.1)

$$\langle \phi_i^{v\mu} | \phi_{i'}^{v'\mu'} \rangle = \delta_{ii'} \delta_{vv'} \delta_{\mu\mu'}$$

$$\sum_v \delta_v = L; \quad 2L \geq N$$

where  $L$  is the total number of space orbitals,  $\delta_v$  the number of orbitals in symmetry specie  $v$ ,  $K$  the number of symmetry species and  $I_v$  the degeneracy of symmetry specie  $v$ . The spin basis is a set of orthonormal spin functions  $\{\theta_\alpha(\text{NSM})\}$  which are simultaneous eigenfunctions of the total spin operator  $\hat{S}^2$  and spin operator  $\hat{S}_z$ , viz.,

$$\hat{S}^2 \theta_\alpha(\text{NSM}) = \hbar^2 S(S+1) \theta_\alpha(\text{NSM}) \quad (2.2a)$$

$$\hat{S}_z \theta_\alpha(\text{NSM}) = \hbar M \theta_\alpha(\text{NSM}) \quad (2.2b)$$

The spin eigenfunctions used here are Serber-type spin functions [37]. From these spatial and spin functions, SAAP's are constructed

$$\psi_{k\alpha}(\text{NSM}) = \sqrt{I_k} [\phi_k \theta_\alpha(\text{NSM})] \quad (2.3)$$

with

$$\Phi_k = f_{k1}(1)f_{k2}(2)\dots f_{kN}(N) \quad (2.4)$$

where  $\Phi$  is the antisymmetrizer and the orbitals  $f_{k1}(1), f_{k2}(2), \dots, f_{kN}(N)$  are certain selections from those listed in Equation (2.1). The SAAP's are good building blocks for a MC wavefunction. They are antisymmetric under the exchange of two electrons, eigenfunctions of  $\hat{S}^2$  and  $\hat{S}_z$ , and are orthonormal because of orbital orthonormality, viz.,

$$\langle \psi_{k\alpha} | \psi_{l\beta} \rangle = \delta_{kl} \delta_{\alpha\beta} \quad (2.5)$$

Therefore the MC wavefunction can be expressed as a linear combination of SAAP's,

$$\Psi = \sum_k \sum_\alpha C_{k\alpha} \psi_{k\alpha} \quad (2.6)$$

The normalization of the MC wavefunction requires

$$\sum_k \sum_\alpha C_{k\alpha}^2 = 1$$

The expansion coefficients  $\{C_{k\alpha}\}$  are obtained variationally by solving the conventional configuration interaction eigenvalue problem

$$\mathbf{H} \mathbf{C} = \mathbf{E} \mathbf{C} \quad (2.7)$$

where  $\mathbf{H}$  is the Hamiltonian matrix defined by

$$H_{k\alpha, l\beta} = \langle \psi_{k\alpha} | \Phi | \psi_{l\beta} \rangle \quad (2.8)$$

Explicit expressions for the matrix elements are defined in reference [36].  $\mathbb{E}$  is the diagonal matrix containing the eigenvalues. MacDonald's Theorem [38] states that the  $n$ th lowest eigenvalue is a rigorous upper bound to the  $n$ th lowest exact energy. With each energy is associated an eigenvector which defines the corresponding MC wavefunction. Since  $\mathbb{H}$  is a totally symmetric operator, eigenvectors of  $\mathbb{H}$  are symmetry-adapted. Therefore if the SAAP's span the space of a specific symmetry species and subspecies solution of the eigenvalue equation gives rise to a MC wavefunction which belongs to an irreducible representation of the point group under consideration. Therefore ground state as well as excited state wavefunctions belonging to the same irreducible representation can be constructed.

### B. Generalized Brillouin Theorem

Suppose the coefficients corresponding to a specific state have been chosen, what are then the conditions for optimal space orbitals? The treatment below follows reference [28]. The energy is given by

$$E = \sum_{k\alpha} \sum_{l\beta} C_{k\alpha} C_{l\beta} \langle \psi_{k\alpha} | \mathbb{H} | \psi_{l\beta} \rangle \quad (2.09)$$

Variation of the energy due to variation of the orbitals in  $\psi_{k\alpha}$  under the orbital orthonormality condition is given by

$$\delta E = 2 \sum_{k\alpha} \sum_{l\beta} C_{k\alpha} C_{l\beta} \langle \delta \psi_{k\alpha} | \mathbb{H} | \psi_{l\beta} \rangle \quad (2.10)$$

where

$$\delta \psi_{k\alpha} = \sum_{i < j}^L X_{ij} [\psi_{k\alpha}(i \rightarrow j) - \psi_{k\alpha}(j \rightarrow i)]$$

Therefore,

$$\delta E = 2 \sum_{i < j}^L X_{ij} \langle \Psi(i+j) | \mathcal{H} | \Psi \rangle \quad (2.12)$$

where we put

$$\Psi(i+j) = \sum_{k\alpha} C_{k\alpha} [\psi_{k\alpha}(i+j) - \psi_{k\alpha}(j+i)] \quad (2.13)$$

If the minimum energy is reached,  $\delta E = 0$ , then

$$\langle \Psi(i+j) | \mathcal{H} | \Psi \rangle = 0 \quad \text{for all } i < j \quad (2.14)$$

This is the generalized Brillouin Theorem for the MCSCF wavefunction. It means that if the orbitals are optimum in the sense of the variation principle, then the matrix elements of the total Hamiltonian between the MC wavefunction and some linear combination of the singly excited (SE) functions,  $\Psi(i+j)$ , vanish.

To understand the meaning of Equation (2.14), it is necessary to discuss the various possible SE functions  $\psi_{k\alpha}(i+j)$ . It is a SAAP or a linear combination of SAAP's. In the SAAP  $\psi_{k\alpha}$ , there are doubly occupied orbitals (doubles) and singly occupied orbitals (singles). All the other orbitals which are not occupied are called virtual orbitals (virtuals). The indices i and j refer to two different space orbitals and  $\psi_{k\alpha}(i+j)$  is obtained from  $\psi_{k\alpha}$  simply by exciting the electron in  $\phi_i^{v\mu}$  to  $\phi_j^{v\mu}$ , or in other words, removing

$\phi_i^{\nu\mu}$  and replacing it with  $\phi_j^{\nu\mu}$ . In order to reserve the overall spatial symmetry of the SAAP, the two orbitals must belong to the same symmetry species and subspecies. Otherwise the generalized Brillouin Theorem is meaningless since the matrix element of a totally symmetric operator between  $\psi_{k\alpha}$  and  $\psi_{k\alpha}(i+j)$  is identically zero if their overall symmetries are different.

The proper preservation of spin symmetries in SE functions is handled as follows. By definition, the orbitals must be arranged in "standard order" in the SAAP's. This means that the doubles are listed first and the singles thereafter. Preservation of this rule is not only necessary for use of our matrix element algorithms, but also guarantees the orthogonality and proper counting of the SAAP's. Now, it is possible that in some SE functions the orbitals do not satisfy this convention. In such a case, let  $P$  be the permutation operator which permutes the orbitals into standard order, i.e.,

$$P\Phi_k(i+j) = \Phi'_k(i+j) \quad (2.15)$$

where  $\Phi'_k(i+j)$  has its orbitals in standard order. Then

$$\begin{aligned} \psi_{k\alpha}(i+j) &= \not\propto [\Phi_k(i+j)\theta_\alpha(\text{NSM})] \\ &= \not\propto [P^{-1}\Phi'_k(i+j)\theta_\alpha(\text{NSM})] \end{aligned}$$

$$\begin{aligned}
 &= \not\propto P^{-1} [\phi_k'(i \rightarrow j) P \theta_\alpha(\text{NSM})] \\
 &= \epsilon(P^{-1}) \sum_{\beta} [P]_{\beta\alpha}^{\text{NS}} \not\propto [\phi_k'(i \rightarrow j) \theta_\beta(\text{NSM})] \\
 &= \epsilon(P^{-1}) \sum_{\beta} [P]_{\beta\alpha}^{\text{NS}} \psi_k'(i \rightarrow j)
 \end{aligned} \tag{2.16}$$

where the index  $\beta$  sums over all the appropriate spin eigenfunctions.  $[P]_{\beta\alpha}^{\text{NS}}$  is the permutation matrix element between spin eigenfunction  $\beta$  and  $\alpha$  and  $\epsilon(P^{-1})$  is +1 when  $P^{-1}$  is even and -1 when  $P^{-1}$  is odd. Note that if the spin eigenfunction  $\theta_\beta(\text{NSM})$  has symmetric geminal spin function in positions where the associated space function in  $\phi_k'(i \rightarrow j)$  is a double, then  $\psi_k'(i \rightarrow j)$  vanishes.

In the single excitations, there exist nine possible cases. But not all of them give contributions. In fact the following five vanish:

- (a) virtual to virtual
- (b) virtual to single
- (c) virtual to double
- (d) single to double
- (e) double to double

The remaining four non-vanishing ones are:

- (f) single to virtual
- (g) single to single
- (h) double to virtual
- (i) double to single.

Of these, (g), (h), and (i) may require orbital permutation.

As mentioned earlier, the generalized Brillouin Theorem has been shown to be equivalent to Equations (1.14a) and (1.14b) by Hirao and Nakatsuji. They have shown that Equation (2.14) can be written in terms of the effective one-electron Hamiltonians.

$$\langle \Psi(i \rightarrow j) | \mathcal{H} | \Psi \rangle = \langle \phi_j^{v\mu} | F_i - F_j | \phi_i^{v\mu} \rangle = 0 \quad (2.17)$$

which is identical to Equation (1.14b). If  $\phi_j^{v\mu}$  is a virtual orbital, then

$$\langle \Psi(i \rightarrow j) | \mathcal{H} | \Psi \rangle = \langle \phi_j^{v\mu} | F_i | \phi_i^{v\mu} \rangle = 0 \quad (2.18)$$

But taking the inner product of  $\phi_j^{v\mu}$  in Equation (1.14a) gives

$$\langle \phi_j^{v\mu} | F_i | \phi_i^{v\mu} \rangle = 0 \quad (2.19)$$

which is identical to Equation (2.18). Therefore the generalized Brillouin Theorem is indeed identical with the conditions derived with the help of Lagrangian multipliers.

The generalized Brillouin Theorem has a remarkable consequence. Suppose the optimal MC wavefunction has been found as regards expansion coefficients and orbitals. Let us now construct SE functions from this MC wavefunction and try to determine an optimal "super CI" approximation,  $\Psi_{\text{super CI}}$ , by linear combination of this MC wavefunction and SE

functions, i.e.,

$$\Psi_{\text{super CI}} = a_{00} \Psi_{\text{MC}} + \sum_{i < j}^L a_{ij} \Psi_{\text{MC}}^{(i+j)} \quad (2.20)$$

Then super CI coefficients,  $a_{00}$ ,  $\{a_{ij}\}$  are determined from the secular equation between  $\Psi_{\text{MC}}$  and  $\Psi_{\text{MC}}^{(i+j)}$ . But because of the generalized Brillouin Theorem, this matrix is block diagonal with respect to the diagonal element  $\langle \Psi_{\text{MC}} | \hat{H} | \Psi_{\text{MC}} \rangle$  and, hence, the lowest root has the solution

$$\Psi_{\text{super CI}} = \Psi_{\text{MC}} \quad (2.21a)$$

$$\langle \Psi_{\text{super CI}} | \hat{H} | \Psi_{\text{super CI}} \rangle = \langle \Psi_{\text{MC}} | \hat{H} | \Psi_{\text{MC}} \rangle \quad (2.21b)$$

This suggests that the linear super CI problem might be used to determine the optimal orbitals. Suppose the optimal MC expansion coefficients are determined, but only approximations to the MC orbitals are known, then the lowest energy of the super CI problem will yield a wavefunction

$\Psi_{\text{super CI}} \neq \Psi_{\text{MC}}$  and

$$\langle \Psi_{\text{super CI}} | \hat{H} | \Psi_{\text{super CI}} \rangle < \langle \Psi_{\text{MC}} | \hat{H} | \Psi_{\text{MC}} \rangle \quad (2.22)$$

It should be possible to use the information embodied in the super CI coefficients  $a_{00}$ ,  $\{a_{ij}\}$  to find better approximations to the optimal MC orbitals. The bridge by which we propose to transfer this information from  $\Psi_{\text{super CI}}$  to

$\Psi_{MC}$  are the natural orbitals which give the most rapidly convergent expansions [11]. Let us first review some of the properties of the natural orbitals.

### C. Natural Orbitals

Natural space orbitals are formed as eigenfunctions of the density operator for the first order spinless density matrix, viz.,

$$\int \rho(x_1, x'_1) \omega_n(x'_1) dx'_1 = \lambda_n \omega_n(x_1) \quad (2.23)$$

where the corresponding eigenvalue  $\lambda_n$  is the occupation number and

$$\rho(x_1, x'_1) = N \int \psi(x_1 s_1, \tau_2, \tau_3 \dots) \psi^*(x'_1 s'_1, \tau_2, \tau_3 \dots) ds_1 d\tau_2 d\tau_3 \dots \quad (2.24)$$

If the wavefunction  $\psi(\tau)$  is represented by a real orbital basis  $\{\phi_i^\mu\}$ , the density operator is in matrix form

$$\rho(x_1, x'_1) = \sum_{i,j} \phi_i(x_1) \phi_j(x'_1) P_{ij} \quad (2.25)$$

where the coefficients  $\{P_{ij}\}$  form a symmetric matrix  $P$ .

The natural orbitals are obtained by diagonalization of the density matrix, namely,

$$\omega_n = \sum_i \phi_i U_{in} \quad (2.26)$$

where

$$\psi^+ \hat{P} \psi = \lambda \quad (2.27a)$$

$$\psi^+ \psi = 1 \quad (2.27b)$$

Therefore the density matrix is reduced to diagonal form

$$\rho(x_1, x'_1) = \sum_n \omega_n(x_1) \omega_n(x'_1) \lambda_n \quad (2.28)$$

In a certain mathematical sense [11, 39], the natural orbitals offer the most rapidly convergent expansion to the density matrix and consequently to the wavefunction. The occupation numbers give a measure of the importance of individual natural orbitals.

The density operator is totally symmetric if the wavefunction  $\psi(\tau)$  belongs to a non-degenerate irreducible representation of the point group of the system under consideration. In this case, applying a symmetry operator  $\hat{O}_R$  to the left of Equation (2.23), it becomes

$$\begin{aligned} \hat{O}_R \int \rho(x_1, x'_1) \omega_n(x'_1) dx'_1 \\ &= \int \rho(R^{-1}x_1, x'_1) \omega_n(x'_1) dx'_1 \\ &= \int \rho(R^{-1}x_1, R^{-1}x''_1) \omega_n(R^{-1}x''_1) d(R^{-1}x''_1) \\ &= \int \rho(x_1, x''_1) \hat{O}_R \omega_n(x''_1) dx''_1 \end{aligned} \quad (2.29)$$

The last step requires  $\rho$  to be totally symmetric. If that is true, then the symmetry operator commutes with the density operator, and therefore the natural orbitals are symmetry-adapted. Thus the density matrix can be written as

$$\rho(x_1, x'_1) = \sum_{v\mu} \sum_n \lambda_n^v \omega_n^{v\mu}(x_1) \omega_n^{v\mu}(x'_1) \quad (2.30)$$

where  $v$  sums over the symmetry species,  $\mu$  the symmetry subspecies in  $v$  and  $n$  the orbitals belonging to symmetry species  $v$  and subspecies  $\mu$ . It follows then that, in terms of the basis orbitals  $\{\phi_i^{v\mu}\}$ , the natural orbitals  $\{\omega_n^{v\mu}\}$  can then be expressed as

$$\omega_n^{v\mu} = \sum_i \phi_i^{v\mu} U_{in}^v \quad (2.31)$$

Equations (2.30) and (2.31) also state the facts that degenerate orbitals have the same occupation numbers and that the transformation of degenerate basis orbitals to natural orbitals are the same. Consequently, the density matrix can be simplified as

$$\begin{aligned} \rho(x_1, x'_1) &= \sum_{v\mu} \sum_n \lambda_n^v \sum_{i i'} \sum_{in} U_{in}^v U_{i' n}^v \phi_i^{v\mu} \phi_{i'}^{v\mu} \\ &= \sum_{v\mu} \sum_{i i'} (\sum_{n} U_{in}^v \lambda_n^v U_{i' n}^v) \phi_i^{v\mu} \phi_{i'}^{v\mu} \\ &= \sum_{v\mu} \sum_{i i'} T_{ii'}^v \phi_i^{v\mu} \phi_{i'}^{v\mu} \end{aligned} \quad (2.32)$$

It can be seen that the density matrix is in block diagonal form.

On the other hand, if the wavefunction which builds up the density matrix does not belong to a non-degenerate irreducible representation, the density matrix will not be totally symmetric and it is expressed as

$$\rho(x_1, x'_1) = \sum_{iv\mu} \sum_{i'v'\mu'} T_{ii'}^{vv'\mu'\mu} \phi_i^v \phi_{i'}^{v'} \quad (2.33)$$

In this case, the totally symmetric component of the density matrix must be projected out in order to obtain the symmetry adapted natural orbitals. It is readily shown that this symmetric component is given by

$$\rho(x_1, x'_1) = \sum_{iv\mu} \sum_{i'v'\mu'} \delta_{vv'} \delta_{\mu\mu'} \left( \frac{1}{I_v} \sum_{i} T_{ii'}^{vv'\mu'\mu} \right) \phi_i^v \phi_{i'}^{v'} \quad (2.34)$$

where  $I_v$  is the degeneracy of symmetry species  $v$ .

#### D. Orbital Optimization

We now describe how the natural orbitals are used as a bridge between the MC and super CI wavefunctions. After the configuration mixing coefficients have been determined for the MC wavefunction, a spinless first order density matrix can be formed [40]. Natural orbitals are then calculated by diagonalization of that matrix, yielding

$$\omega_n^{v\mu} = \sum_i^{\delta_v} \phi_i^{v\mu} U_{in}^v \quad (2.35a)$$

with

$$n = 1, 2, \dots, \delta_v$$

$$v = 1, 2, \dots, K$$

$$\mu = 1, 2, \dots, I_v$$

where  $\delta_v$  is the number of occupied orbitals of symmetry species  $v$  in the MC wavefunction,  $K$  the number of symmetry species, and  $I_v$  the degeneracy in symmetry species  $v$ .

The natural orbitals are symmetry adapted if the MC wavefunction belongs to a one-dimensional irreducible representation of the point group under consideration and hence the density matrix is totally symmetric. If the latter is not true, we project out the totally symmetric component according to Equation (2.34). The eigenvalues obtained are ordered such that  $\lambda_1^{v\mu} \geq \lambda_2^{v\mu} \geq \dots \geq \lambda_{\delta_v}^{v\mu}$ . Thus the natural orbital  $\omega_1^{v\mu}$  will have the highest possible occupation number in symmetry specie  $v$  and subspecie  $\mu$ , i.e., it will be the most important contribution to the overall wavefunction;  $\omega_2^{v\mu}$  will have the highest occupation number of all the orbitals orthogonal to  $\omega_1^{v\mu}$ ; and so on for the remaining orbitals. The same argument applies to the other symmetries.

We now determine the configuration mixing coefficients of the super CI wavefunction by the standard variation technique, i.e., diagonalization of the super CI Hamiltonian matrix.

This matrix is in general quite large and its diagonalization is time-consuming. Fortunately only the lowest eigenvalue and the corresponding eigenvector are required, and Nesbet's algorithm and improvements thereof [41] suits this purpose perfectly.

After the coefficients are determined, the first order spinless super CI density matrix can then be formed. Again, if the matrix is not totally symmetric, its totally symmetric component is projected out and diagonalized to give symmetry-adapted natural orbitals  $\bar{\omega}_n^{v\mu}$

$$\bar{\omega}_n^{v\mu} = \sum_i \phi_i^{v\mu} \bar{U}_{in}^v \quad (2.35b)$$

with

$$n = 1, 2, \dots, \delta_v$$

$$v = 1, 2, \dots, K$$

$$\mu = 1, 2, \dots, I_v$$

where  $\delta_v$  is the total number of space orbitals in symmetry species  $v$ . As before, the eigenvalues obtained are arranged such that  $\lambda_1^{v\mu} \geq \lambda_2^{v\mu} \geq \dots \geq \lambda_{\delta_v}^{v\mu}$ .

Since the natural orbitals obtained from the MC wavefunction and those from the super CI wavefunction are arranged in the same order,  $\omega_n^{v\mu}$  will be identical to  $\bar{\omega}_n^{v\mu}$ ,  $n = 1, 2, \dots, \delta_v$  when the generalized Brillouin Theorem is satisfied. Before convergence, however,  $\bar{x}_n^{v\mu}$  are better orbitals than  $x_n^{v\mu}$  and we

use them to find new molecular orbitals  $\bar{\phi}_i^{\nu\mu}$  which are better than  $\phi_i^{\nu\mu}$ . To this end we note that the transformation of Equation (2.35a) can be inverted to give

$$\phi_i^{\nu\mu} = \sum_n^{\delta_\nu} \omega_n^{\nu\mu} U_{ni}^\nu \quad (2.36)$$

with

$$i = 1, 2, \dots, \delta_\nu$$

Now the new set of occupied orbitals  $\bar{\phi}_i^{\nu\mu}$  can be defined by replacing  $\omega_n^{\nu\mu}$  in Equation (2.36) by  $\bar{\omega}_n^{\nu\mu}$  in Equation (2.35b)

$$\bar{\phi}_i^{\nu\mu} = \sum_n^{\delta_\nu} \bar{\omega}_n^{\nu\mu} U_{ni}^\nu \quad (2.37)$$

where

$$i = 1, 2, \dots, \delta_\nu$$

From Equations (2.35b) and (2.37) we obtain the following transformation from the old molecular orbitals to the new ones

$$\bar{\phi}_i^{\nu\mu} = \sum_j^{\delta_\nu} \phi_j^{\nu\mu} v_{ji}^\nu, \quad i = 1, 2, \dots, \delta_\nu \quad (2.38a)$$

where

$$v_{ji}^\nu = \sum_{n=1}^{\delta_\nu} \bar{U}_{jn}^\nu U_{ni}^\nu \quad (2.39)$$

A new set of virtual orbitals can be simply defined by

$$\bar{\phi}_i^{\nu\mu} = \bar{\omega}_i^{\nu\mu}, \quad i = \delta_\nu + 1, \delta_\nu + 2, \dots, \delta_\nu \quad (2.38b)$$

This new set of orbitals is orthonormal and, hence, satisfies

the variational condition of orbital orthonormality. It is also symmetry adapted.

The new orbitals can be expected to be better approximations to the true MCSCF orbitals because the natural orbitals from the super CI wavefunction are better than those from the approximate MC wavefunction. Moreover, the natural orbitals are arranged in such a way that the dominant orbitals generally become more important and higher virtual orbitals less important. This means that after orbital transformation, the energy contributions from the SE functions are diminishing and the deviations from the generalized Brillouin Theorem are decreasing. Iterating the entire process of forming two sets of natural orbitals and performing the orbital transformation is a special way of optimizing the orbitals. By virtue of the properties of the natural orbitals, rapid convergence is expected. Using the natural orbitals from the super CI wavefunction to replace the natural orbitals from the MC wavefunction improves the latter function and forces convergence. During the iterative process, the MC energy should go down. When successive improvements in the MC energy falls below some threshold, the MC energy and the super CI energy agree within that same threshold. At this point, the generalized Brillouin Theorem is satisfied and the orbitals are variationally determined.

In the execution of this scheme, three problems may

arise. The first concerns the ordering of the natural orbitals, in case some of them have the same or almost the same occupation numbers. The order in  $\{\omega_n^{v\mu}\}$  can remain the same but the order in  $\{\bar{\omega}_n^{v\mu}\}$  may have to be modified so that  $\bar{\omega}_n^{v\mu}$  will correspond to  $\omega_n^{v\mu}$ ,  $n = 1, 2, \dots, \delta_v$ . This is achieved by forming an overlap matrix between the two sets of orbitals

$$S_{nm}^{v\mu} = \langle \omega_n^{v\mu} | \bar{\omega}_m^{v\mu} \rangle \quad (2.40)$$

with

$$n = 1, 2, \dots, \delta_v$$

$$m = 1, 2, \dots, \delta_v$$

$\bar{\omega}_m^{v\mu}$  will correspond to  $\omega_n^{v\mu}$  if the magnitude of  $S_{n'm}^{v\mu}$  is larger than  $S_{n'm}^{v\mu}$  for all other values of m. In this fashion, we can arrange  $\bar{\omega}_m^{v\mu}$  for  $m = 1, 2, \dots, \delta_v$ . The order of  $\bar{\omega}_m^{v\mu}$  for  $m > \delta_v$  is irrelevant.

Secondly, it is well known that all fully occupied shells permit an arbitrary orthogonal transformation of the orbitals. This arbitrariness may be an obstacle to the orbital optimization. Therefore the closed shells are always chosen to be eigenfunctions of the one-electron Hamiltonian operator. This choice enables the orbitals in successive iterations to correspond to each other. The "partners" between successive iterations can again be found by forming an overlap matrix between the two sets of orbitals and matching those with the largest overlap.

Thirdly, it is possible that the SE functions formed as described up to now do not form a linearly independent set. They may not be orthonormal either. Linear dependence can be removed and orthonormality imposed by Schmidt orthonormalization. The orthonormalization procedure is simplified by the following considerations:

- (a) The MC wavefunction is orthogonal to all the SE functions [28].
- (b)  $\Psi_{MC}^{(i \rightarrow j)}$ ,  $i, j = 1, 2, \dots, L$  is orthogonal to  $\Psi_{MC}^{(i' \rightarrow j')}$ ,  $i', j' = 1, 2, \dots, L$  for  $j \neq j'$  if  $\phi_j^{\nu\mu}$  and  $\phi_{j'}^{\nu'\mu'}$  are not occupied in any of the SAAP's in  $\Psi_{MC}$ .
- (c) The SE functions are orthogonal to each other if all the SAAP's in  $\Psi_{MC}$  are composed of doubles only.

#### E. Treatment of Excited States

The described method can also deal with excited states belonging to the same spatial and spin symmetry as the ground state. To obtain, say, the first excited state, we simply choose the second root of the MC-CI problem. This root is always an upper bound to the first excited state [38] and, so, maximal lowering of this second root will approach the excited state most closely. This minimization can now be accomplished in exactly the same way as in the ground

state. Namely: all SE configurations are generated from the MC function belonging to the second MC root, and then the lowest root of the corresponding super CI secular equation is found and its natural orbitals used to replace the natural orbitals of the previous MC approximation, etc. Higher states can be dealt with analogously.

Although the resulting energy is an upper bound, the excited state determined in this manner is in general not orthogonal to the lower states. If orthogonal states are desired, the following for determining simultaneously several states can be used.

Suppose the lowest two states are sought. Then we choose the lowest two roots of the MC-CI problem and form both MC wavefunctions. For each of them, single excitations are formed and the super CI problem is solved for the lowest root. Now there are four density matrices: for the MC wavefunctions of the two states,  $\rho_0$  and  $\rho_1$ , and for the super CI wavefunctions of the two states,  $\bar{\rho}_0$  and  $\bar{\rho}_1$ . At this stage, we form the average density matrices

$$\rho_{ave} = (\rho_0 + \rho_1)/2 \quad (2.41a)$$

$$\bar{\rho}_{ave} = (\bar{\rho}_0 + \bar{\rho}_1)/2 \quad (2.41b)$$

The natural orbitals of these two average density matrices are now used to define new molecular orbitals in terms of the

old molecular orbitals by the method described above. When the procedure converges, both states are formed from the same set of orthogonal molecular orbitals and hence the two states will be orthogonal to each other. Higher excited states can be treated similarly.

#### F. Calculation Procedure

The whole iterative procedure is summarized in the following steps:

- (a) Construct from some initial orbitals and Serber spin eigenfunctions the MC wavefunction in terms of SAAP's. Solve the MC-CI eigenvalue problem by diagonalizing the Hamiltonian matrix and choose the eigenvector corresponding to the energy state desired.
- (b) Construct the super CI wavefunction from the MC wavefunction. Determine the expansion coefficients from the super CI eigenvalue problem. Choose the eigenvector corresponding to the lowest energy.
- (c) Compare the MC energy and the super CI energy. If they agree within some threshold, convergence is achieved and the calculation comes to the end. If not, form natural orbitals from the first order spinless density matrix of the MC wavefunction and that of the super CI wavefunction, respectively.

(d) Perform the orbital transformation to obtain a new set of orbitals. Go back to step (a) with the new orbitals as input.

#### G. SCF Iterations and Extrapolations

The MCSCF method would be efficient only if the number of iterations required to obtain convergence is reduced to a minimum. The initial guess of the orbitals is very important in this respect, but unfortunately there is no general rule or economic way to make a good approximation to the MCSCF orbitals. Another way to hasten convergence is to add an extrapolation feature to the iterative procedure. The method due to Hartree [42, 43] is used for this purpose. This procedure applies to a sequence of values  $y_n$  which approach an unknown limiting value  $y_\infty$ . Hartree basically assumes that  $y_n$  approaches  $y_\infty$  according to the formula

$$y_n = y_\infty + ab^n \quad (2.42)$$

This assumption is such that the three constants  $a$ ,  $b$ ,  $y_\infty$  can be easily extracted from the consecutive values  $y_n$ ,  $y_{n+1}$ ,  $y_{n+2}$ . Indeed, from Equation (2.42) we readily find

$$\frac{y_{n+1} - y_\infty}{y_n - y_\infty} = \frac{y_{n+2} - y_{n+1}}{y_{n+1} - y_n} \quad (2.43)$$

whence

$$y_{\infty} = (y_{n+2}y_n - y_{n+1}^2) / (y_{n+2} - 2y_{n+1} + y_n) \quad (2.44)$$

or

$$y_{\infty} = y_{n+2} - (y_{n+2} - y_{n+1}) / (1 - b^{-1}) \quad (2.45)$$

with

$$b = (y_{n+2} - y_{n+1}) / (y_{n+1} - y_n) \quad (2.46)$$

Equation (2.46) reduces the error of evaluating  $y_{\infty}$  when  $y_n$ ,  $y_{n+1}$ , and  $y_{n+2}$  are nearly equal. It is obvious that the extrapolation scheme leads to convergence only if  $|b| < 1$ . If  $|b| \approx 1$ , the extrapolation breaks down.

We apply the extrapolation to the configuration mixing coefficients of the MC wavefunction as well as to the density matrix elements derived from the super CI wavefunction, after three successive iterations. One caution is that the density matrices to be extrapolated must be expanded in terms of the same set of orbitals. Moreover, the MC wavefunctions and the density matrices must all be normalized. This extrapolation procedure is preferable to extrapolating the orbitals since there are more components in the orbital set and, moreover, the orbitals would be neither orthogonal nor symmetry-adapted after extrapolation. In order to avoid divergence, we extrapolate only those points for which  $|b^{-1}| > 1.1$ . This value gave good results in all cases considered. Generally the extrapolation

seems to work. However, the assumption in Hartree's method may not be valid all the time and consequently the extrapolation may not always give an acceleration. Anyway, in general, the extrapolation is still a good bet.

#### H. Implementation

A Fortran MCSCF program for IBM 360/65 has been developed for both atoms and molecules. A general discussion of the program is given in Appendix A. A number of calculations have been made to test the program and in most cases convergence of the energy to within  $10^{-5}$  % were obtained in less than 10 iterations. In a number of cases, mostly in dealing with excited states, convergence could only be achieved to within  $10^{-3}$  % before fluctuations of the energy occurred. However, in general, the method gives variationally correct energies and wavefunctions.

Applications of the MCSCF method to calculate the dissociation curves of ethylene will be presented in the next chapter.

#### I. Conclusions

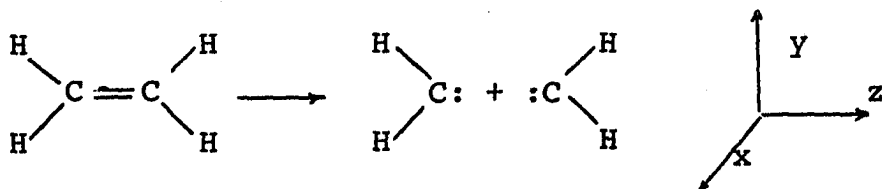
The MCSCF method presented here is a conceptually simple model which can be applied to any atomic or molecular system. The MC wavefunction is an exact eigenfunction of  $\hat{S}^2$  and  $\hat{S}_z$  since it is expanded in terms of SAAP's. It is also

symmetry-adapted as an eigenfunction of the Hamiltonian. There is no restriction to the type of configurations which can be included in the MC wavefunction. The method can deal with ground state as well as excited states belonging to the same irreducible representation and spin multiplicity. In addition, in the calculation of any state, other states are automatically obtained, although the wavefunction of these states are not optimal. The only defect is that in the calculation of an excited state, it is not constrained to be orthogonal to all the lower energy states. Correction, if desired, is possible as discussed.

### III. DISSOCIATION OF ETHYLENE

#### A. Introduction

Consider the dissociation of ethylene into methylenes



Since both reactant and products are planar, the least motion planar reaction path must be considered. The ground state SCF configuration of ethylene ( $D_{2h}$  symmetry) is given by

$$|{}^1A_g\rangle = \Psi [ (1a_g)^2 (1b_{1u})^2 (2a_g)^2 (2b_{1u})^2 (1b_{2u})^2 (3a_g)^2 (1b_{3g})^2 (1b_{3u})^2 \theta_-^8 ] \quad (3.1)$$

where

$$\theta_- = (\alpha\beta - \beta\alpha)/\sqrt{2} \quad (3.2)$$

The dissociation of ethylene involves only the breaking of the carbon carbon bond and so we put the other twelve electrons into a core function. Also in the least motion reaction path, the molecular plane (yz plane) and the xy plane are persisting symmetry elements. Thus it suffices to classify the bond orbitals as  $\sigma$ ,  $\sigma^*$ ,  $\pi$ , or  $\pi^*$  orbitals. So

$$|{}^1A_g\rangle = \Psi [ (\text{core}) \sigma^2 \pi^2 \theta_-^8 ] \quad (3.3)$$

where

$$(\text{core}) = (1a_g)^2 (1b_{1u})^2 (2a_g)^2 (2b_{1u})^2 (1b_{2u})^2 (1b_{3g})^2 \quad (3.4)$$

$$\sigma = 3a_g \quad (3.5)$$

$$\pi = 1b_{3u} \quad (3.6)$$

On the other hand, the configurations of three low lying electronic states of methylene ( $C_{2v}$  symmetry) are given in the SCF approximation by

$$|{}^3B_1\rangle = [(\text{core})\sigma\pi \theta_-^3 \theta_+] \quad (3.7)$$

$$|{}^1A_1, \sigma^2\rangle = [(\text{core})\sigma^2 \theta_-^4] \quad (3.8)$$

$$|{}^1A_1, \pi^2\rangle = [(\text{core})\pi^2 \theta_-^4] \quad (3.9)$$

Here

$$(\text{core}) = (1a_1)^2 (2a_1)^2 (1b_2)^2 \quad (3.10)$$

$$\sigma = 3a_1 \quad (3.11)$$

$$\pi = 1b_1 \quad (3.12)$$

$$\theta_+ = \begin{cases} \alpha\alpha \\ \beta\beta \\ (\alpha\beta + \beta\alpha)/\sqrt{2} \end{cases} \quad (3.13)$$

The last two configurations may interact to yield two  ${}^1A_1$  states which are linear combinations of  $|{}^1A_1, \sigma^2\rangle$  and  $|{}^1A_1, \pi^2\rangle$ . However the lowest singlet state is mostly  $|{}^1A_1, \sigma^2\rangle$  since the interaction is weak. Neglecting the core electrons, the possible dissociation reaction can there-

fore be abbreviated as



According to the symmetry rule of Woodward and Hoffmann [44], if orbital symmetry is conserved between reactant and products, the reaction is a concerted reaction. Therefore should two triplet methylenes combine to form ethylene, the dimerization is a symmetry allowed process, since there are two  $\sigma$  electrons and two  $\pi$  electrons on both the reactant side and product side. On the other hand, the least motion approach of two singlet methylenes is a high energy one. The methylenes possess four  $\sigma$  electrons altogether, but ethylene possesses two  $\sigma$  electrons and two  $\pi$  electrons. Therefore orbital symmetry is not conserved. If one draws the orbital correlation energy diagram, the  $\sigma^*$  and  $\pi$  orbital energies cross during the reaction. This leads to an avoided crossing of the potential energy surfaces, giving rise to a hump in the lower surface which is called the activation energy. In other words, a barrier is present in the least motion approach of two singlet methylenes [45].

Experimentally the dimerization of methylenes has not been observed [46]. Therefore it is interesting to study how the dissociation proceeds. From the above argument, it is

clear that the dissociation of ground state ethylene into two triplet methylenes is the dominant reaction. If that is the case, what happens to the approach of two singlet methylenes?

To describe these reactions, the use of a multiconfiguration wavefunction is essential, since ordinary Hartree Fock wavefunctions would not allow different assignment of electrons to different orbitals at different points along the reaction path. Basch [47] tried to solve this problem using a wavefunction with six configurations. However this function is insufficient to describe the reaction properly; he omitted the spin coupling in the triplet dimerization and this led to an improper dissociation of the ground state ethylene. He also used ground state molecular orbitals to calculate the excited  $^1\text{Ag}$  state which describes separation into singlet methylenes, and because of this he failed to find the metastable extremum in the dimerization curve. These deficiencies prompted the present calculation to be carried out using the new MCSCF program described in the last chapter.

## B. The Orbital and Configurational Reaction Space

### 1. Molecular orbitals

The molecular structure of ethylene can be analyzed in terms of the molecular orbitals which are linear combinations of atomic orbitals. The molecular orbitals can be divided into four classes:

#### (a) Inner core orbitals

$$i(A_g) = (i_L + i_R)/\sqrt{2} \quad (3.16a)$$

$$i^*(B_{1u}) = (i_L - i_R)/\sqrt{2} \quad (3.16b)$$

where  $i_L$  and  $i_R$  are mainly localized left and right orbitals centered on the carbon atoms, although they are not completely localized because they are kept orthogonal. However upon dissociation to infinity,  $i_L$  and  $i_R$  become pure inner core orbitals centered on each of the carbon atoms of the methylenes. Similar arguments also hold for the next three classes of molecular orbitals.

#### (b) CH bonds

$$b_+(A_g) = (b_{+L} + b_{+R})/\sqrt{2} \quad (3.17a)$$

$$b_+^*(B_{1u}) = (b_{+L} - b_{+R})/\sqrt{2} \quad (3.17b)$$

$$b_-(B_{2u}) = (b_{-L} + b_{-R})/\sqrt{2} \quad (3.17c)$$

$$b_-^*(B_{3g}) = (b_{-L} - b_{-R})/\sqrt{2} \quad (3.17d)$$

where

$$b_{+L} = (b_L + b'_L)/\sqrt{2} \quad (3.17e)$$

$$b_{-L} = (b_L - b'_L)/\sqrt{2} \quad (3.17f)$$

$$b_{+R} = (b_R + b'_R)/\sqrt{2} \quad (3.17g)$$

$$b_{-R} = (b_R - b'_R)/\sqrt{2} \quad (3.17h)$$

and  $b_L, b'_L$  are the localized molecular orbitals for the two CH bonds at left and  $b_R, b'_R$  are those at right

(c) CC  $\sigma$  bonds

$$\sigma(A_g) = (\sigma_L + \sigma_R)/\sqrt{2} \quad (3.18a)$$

$$\sigma^*(B_{1u}) = (\sigma_L - \sigma_R)/\sqrt{2} \quad (3.18b)$$

where  $\sigma_L$  and  $\sigma_R$  are the localized  $\sigma$  molecular orbitals centered on the left and right carbon atoms.

(d) CC  $\pi$  bonds

$$\pi(B_{3u}) = (\pi_L + \pi_R)/\sqrt{2} \quad (3.19a)$$

$$\pi^*(B_{2g}) = (\pi_L - \pi_R)/\sqrt{2} \quad (3.19b)$$

where  $\pi_L$  and  $\pi_R$  are the localized  $\pi$  molecular orbitals centered on the left and right carbon atoms.

2. Configurations of  $^1A_g$  symmetry in terms of symmetry orbitals

Intuitively we know that the inner core orbitals and CH bond orbitals must remain occupied during the reaction. Therefore we can keep these shells closed. The only orbitals left are the  $\sigma$ ,  $\sigma^*$ ,  $\pi$ , and  $\pi^*$  functions between the two carbon atoms. We are going to put four electrons into different combinations of these four orbitals. The only ones which obey the Pauli Exclusion Principle and at the same time belong to the irreducible representation  $^1A_g$  are  $\sigma^2\pi^2$ ,  $\sigma^{*2}\pi^2$ ,  $\sigma^2\pi^{*2}$ ,  $\sigma^{*2}\pi^{*2}$ ,  $\sigma^2\sigma^{*2}$ ,  $\pi^2\pi^{*2}$ , and  $\sigma\sigma^*\pi\pi^*$ . Of these only the last one permits a triplet coupling. Using the notation in the previous section, the eight configurations of  $^1A_g$  symmetry are given by

$$|I\rangle = \frac{1}{2} \not{\{F\sigma^2\pi^2\theta_{--}\}} = |\sigma^2\pi^2\rangle \quad (3.20a)$$

$$|II\rangle = \frac{1}{2} \not{\{F\sigma^{*2}\pi^2\theta_{--}\}} = |\sigma^{*2}\pi^2\rangle \quad (3.20b)$$

$$|III\rangle = \frac{1}{2} \not{\{F\sigma^2\pi^{*2}\theta_{--}\}} = |\sigma^2\pi^{*2}\rangle \quad (3.20c)$$

$$|IV\rangle = \frac{1}{2} \not{\{F\sigma^{*2}\pi^{*2}\theta_{--}\}} = |\sigma^{*2}\pi^{*2}\rangle \quad (3.20d)$$

$$|V\rangle = \not{\{F\sigma\sigma^*\pi\pi^*\theta_{--}\}} = |\sigma\sigma^*\pi\pi^*\rangle \quad (3.20e)$$

$$|VI\rangle = \frac{1}{2} \not{\{F\sigma^2\sigma^{*2}\theta_{--}\}} = |\sigma^2\sigma^{*2}\rangle \quad (3.20f)$$

$$|VII\rangle = \frac{1}{2} \not{\{F\pi^2\pi^{*2}\theta_{--}\}} = |\pi^2\pi^{*2}\rangle \quad (3.20g)$$

$$|VIII\rangle = \not{\{F\sigma\sigma^*\pi\pi^*\theta_{++}\}} = |\sigma\sigma^*\pi\pi^*\rangle \quad (3.20h)$$

where

$$F = 2^{-3} i^2 i^*^2 b_+^2 b_+^*^2 b_-^2 b_-^*^2 [(\alpha\beta - \beta\alpha)/\sqrt{2}]^6 \quad (3.21)$$

$$\theta_{--} = [(\alpha\beta - \beta\alpha)\sqrt{2}]^2 \quad (3.22)$$

$$\theta_{++} = \{\alpha\alpha\beta\beta + \beta\beta\alpha\alpha - (\alpha\beta + \beta\alpha)(\alpha\beta + \beta\alpha)\frac{1}{2}\}/\sqrt{3} \quad (3.23)$$

and

$$\mathcal{A} = (\sqrt{16!})^{-1} \sum_P (-1)^P P \quad (3.24)$$

with the sum goes over the symmetric group.  $P$  is a permutation operator.

### 3. Configurations of ${}^1A_g$ symmetry in terms of left and right orbitals

In order to analyze how the methylenes separate from each other, it is useful to span the configuration space in terms of configurations made from left and right orbitals. This leads to the definitions of the following configurations

$$|A\rangle = \frac{1}{2} \mathcal{A} \left\{ F \frac{1}{\sqrt{2}} (\sigma_L^2 \pi_L^2 + \pi_R^2 \sigma_R^2) \theta_{--} \right\} = |\sigma^2 \pi^2| \rightarrow \quad (3.25a)$$

$$|B\rangle = \frac{1}{\sqrt{2}} \mathcal{A} \left\{ F \frac{1}{\sqrt{2}} (\pi_L^2 \sigma_L \sigma_R + \pi_R^2 \sigma_R \sigma_L) \theta_{--} \right\} = |\pi^2 \sigma| \sigma \rangle \quad (3.25b)$$

$$|C\rangle = \frac{1}{\sqrt{2}} \mathcal{A} \left\{ F \frac{1}{\sqrt{2}} (\sigma_L^2 \pi_L \pi_R + \sigma_R^2 \pi_R \pi_L) \theta_{--} \right\} = |\sigma^2 \pi| \pi \rangle \quad (3.25c)$$

$$|D'\rangle = \frac{1}{2} \mathcal{A} \left\{ F \frac{1}{\sqrt{2}} (\sigma_L^2 \pi_R^2 + \pi_L^2 \sigma_R^2) \theta_{--} \right\} = |\sigma^2| \pi^2 \rangle \quad (3.25d)$$

$$|E'\rangle = \frac{1}{2} \mathcal{A} \left\{ F \sigma_L^2 \sigma_R^2 \theta_{--} \right\} = |\sigma^2| \sigma^2 \rangle \quad (3.25e)$$

$$|F'> = \frac{1}{2} \not\{ F \pi_L^2 \pi_R^2 \theta_{--} \} = |\pi^2 \pi^2> \quad (3.25f)$$

$$|G> = \not\{ F \sigma_L \pi_L \sigma_R \pi_R \theta_{--} \} = |\sigma\pi \sigma\pi|S> \quad (3.25g)$$

$$|H> = \not\{ F \sigma_L \pi_L \sigma_R \pi_R \theta_{++} \} = |\sigma\pi \sigma\pi|T> \quad (3.25h)$$

Using the relations between the two sets of molecular orbitals in Section III,B,1, we can show that the two sets of configurations are related by the orthogonal transformation ( $T_1$ ) which is shown on Table 1a.

In order to formulate the separation process, it is furthermore necessary to express the configurations  $|A>$  to  $|H>$  in terms of methylene states. To this end we introduce the following definitions

$$F = F_L F_R \quad (3.26a)$$

where

$$F_L = 2^{-\frac{3}{2}} i_L^2 b_{+L}^2 b_{-L}^2 [(\alpha\beta - \beta\alpha)/\sqrt{2}]^3 \quad (3.26b)$$

$$F_R = 2^{-\frac{3}{2}} i_R^2 b_{+R}^2 b_{-R}^2 [(\alpha\beta - \beta\alpha)/\sqrt{2}]^3 \quad (3.26c)$$

and

$$\theta_{--} = \theta_- \theta_- = [(\theta_- \alpha) \beta - (\theta_- \beta) \alpha] / \sqrt{2} \quad (3.27)$$

$$\theta_{++} = (\theta_+^+ \theta_+^- + \theta_+^- \theta_+^+ - \theta_+^0 \theta_+^0) / \sqrt{3} \quad (3.28a)$$

where

$$\theta_+^+ = \alpha\alpha \quad (3.28b)$$

$$\theta_+^- = \beta\beta \quad (3.28c)$$

$$\theta_+^0 = (\alpha\beta + \beta\alpha) / \sqrt{2} \quad (3.28d)$$

Table 1a. Orthogonal transformation ( $T_1$ )

	$ \sigma^2\pi^2\rangle$	$ \sigma^*\pi^2\rangle$	$ \sigma^2\pi^*\pi^2\rangle$	$ \sigma^*\pi^2\pi^*\pi^2\rangle$	$ \sigma\sigma^*\pi\pi^*S\rangle$	$ \sigma^2\sigma^*\pi^2\rangle$	$ \pi^2\pi^*\pi^2\rangle$	$ \sigma\sigma^*\pi\pi^*T\rangle$
$ \sigma^2\pi^2\rangle$	$\frac{1}{4}\sqrt{2}$	$\frac{1}{4}\sqrt{2}$	$\frac{1}{4}\sqrt{2}$	$\frac{1}{4}\sqrt{2}$	$\frac{1}{2}\sqrt{2}$	0	0	0
$ \pi^2\sigma^*\sigma\rangle$	$\frac{1}{2}$	$-\frac{1}{2}$	$\frac{1}{2}$	$-\frac{1}{2}$	0	0	0	0
$ \sigma^2\pi^*\pi\rangle$	$\frac{1}{2}$	$\frac{1}{2}$	$-\frac{1}{2}$	$-\frac{1}{2}$	0	0	0	0
$ \sigma^2\pi^2\rangle$	$\frac{1}{4}\sqrt{2}$	$\frac{1}{4}\sqrt{2}$	$\frac{1}{4}\sqrt{2}$	$\frac{1}{4}\sqrt{2}$	$-\frac{1}{2}\sqrt{2}$	0	0	0
$ \sigma^2\sigma^2\rangle$	0	0	0	0	0	1	0	0
$ \pi^2\pi^2\rangle$	0	0	0	0	0	0	1	0
$ \sigma\pi^*\sigma\pi^*S\rangle$	$-\frac{1}{4}$	$\frac{1}{4}$	$\frac{1}{4}$	$-\frac{1}{4}$	0	0	0	$-\frac{1}{2}\sqrt{3}$
$ \sigma\pi^*\sigma\pi^*T\rangle$	$-\frac{1}{4}\sqrt{3}$	$\frac{1}{4}\sqrt{3}$	$\frac{1}{4}\sqrt{3}$	$-\frac{1}{4}\sqrt{3}$	0	0	0	$\frac{1}{2}$

Finally if we have a function of N electrons of the form

$$\mathcal{A}(XY) = \mathcal{A}\{X(N_x^1, N_x^2, \dots, N_x^n)Y(N_y^1, N_y^2, \dots, N_y^m)\} \quad (3.29)$$

where

$$n+m = N$$

We can write it as

$$\mathcal{A}(XY) = \mathcal{A}_{xy}\{\mathcal{A}_x(X)\mathcal{A}_y(Y)\} \quad (3.30a)$$

where

$$\mathcal{A}_x = (n!)^{-\frac{1}{2}} \sum_p S_x (-1)^p p \quad (3.30b)$$

$$\mathcal{A}_y = (m!)^{-\frac{1}{2}} \sum_p S_y (-1)^p p \quad (3.30c)$$

$$\mathcal{A}_{xy} = [N!/(n!m!)]^{-\frac{1}{2}} \sum_p S_{xy} (-1)^p p \quad (3.30d)$$

Here  $S_x$  and  $S_y$  are the subgroups of permutations over the electrons  $N_x^1, N_x^2, \dots, N_x^n$  and  $N_y^1, N_y^2, \dots, N_y^m$ , respectively. The last sum goes over a set of coset generators ( $S_{xy}$ ) corresponding to the decomposition  $S_N = S_{xy} \otimes S_x \otimes S_y$ , where  $S_N$  is the symmetric group of N electrons. There are  $N!/(n!m!)$  elements in  $S_{xy}$ , each of which corresponds to one way of dividing N electrons into two groups in such manner that n electrons are in X and the remaining m electrons are in Y. The number n and m depend on the configurations and, hence,  $\mathcal{A}_x$ ,  $\mathcal{A}_y$ , and  $\mathcal{A}_{xy}$  will have a configuration label.

Using these conventions we find, for instance

$$\begin{aligned}
 |\mathbf{A}\rangle &= \frac{1}{2} \not{\star} \left\{ F \frac{1}{\sqrt{2}} (\sigma_L^2 \pi_L^2 + \pi_R^2 \sigma_R^2) \theta_{--} \right\} \\
 &= \frac{1}{2} \not{\star} \left\{ \frac{1}{\sqrt{2}} (F_L \sigma_L^2 \pi_L^2 F_R + F_L F_R \pi_R^2 \sigma_R^2) \theta_{--} \right\} \\
 &= \not{\star}_{xy}^A \left\{ \frac{1}{2} \not{\star}_x^A (F_L \sigma_L^2 \pi_L^2 \theta_{--}) \not{\star}_y^A (F_R) + \right. \\
 &\quad \left. \frac{1}{2} \not{\star}_x^A (F_R \sigma_R^2 \pi_R^2 \theta_{--}) \not{\star}_y^A (F_L) \right\} / \sqrt{2} \quad (3.31)
 \end{aligned}$$

The factors inside the parentheses represent the following two configurations of the methylene ( $2+$ ) and ( $2-$ ) ions:

$$\frac{1}{2} \not{\star}_x^A (F_L \sigma_L^2 \pi_L^2 \theta_{--}) = |\text{CH}_2^{--}, {}^1\text{A}_1\rangle_L \quad (3.32a)$$

$$\not{\star}_y^A (F_L) = |\text{CH}_2^{++}, {}^1\text{A}_1\rangle_L \quad (3.32b)$$

and similarly for the factors containing the right orbitals. Hence we can write,

$$|\mathbf{A}\rangle = |\sigma^2 \pi^2| \rightarrow = \not{\star}_{10,6} \not{\star}_{LR} |\text{CH}_2^{--}, {}^1\text{A}_1\rangle_L |\text{CH}_2^{++}, {}^1\text{A}_1\rangle_R \quad (3.33a)$$

where  $\not{\star}_{LR}$  is the "left-right symmetrizer",

$$\not{\star}_{LR} = \{1 + (L \rightarrow R, R \rightarrow L)\} / \sqrt{2}. \quad (3.34)$$

and  $\not{\star}_{10,6}$  is the coset antisymmetrizer  $\not{\star}_{xy}$  corresponding to a division into 10 and 6 electrons:  $x \in (1, 2, \dots, 10)$ ,  $y \in (11, 12, \dots, 16)$ .

The configurations  $|\mathbf{B}\rangle$  to  $|\mathbf{H}\rangle$  can be treated in a

similar manner. In this way, we obtain

$$|B\rangle = |\pi^2\sigma|\sigma\rangle = \frac{1}{\sqrt{2}}_{LR}\{|\text{CH}_2^-, {}^2\text{A}_1^+>_L|\text{CH}_2^+, {}^2\text{A}_1^->_R \\ - |\text{CH}_2^-, {}^2\text{A}_1^->_L|\text{CH}_2^+, {}^2\text{A}_1^+>_R\}/\sqrt{2} \quad (3.33b)$$

$$|C\rangle = |\sigma^2\pi|\pi\rangle = \frac{1}{\sqrt{2}}_{LR}\{|\text{CH}_2^-, {}^2\text{B}_1^+>_L|\text{CH}_2^+, {}^2\text{B}_1^->_R \\ - |\text{CH}_2^-, {}^2\text{B}_1^->_L|\text{CH}_2^+, {}^2\text{B}_1^+>_R\} \quad (3.33c)$$

$$|D\rangle = |\sigma^2|\pi^2\rangle = \frac{1}{\sqrt{2}}_{LR}|\text{CH}_2, {}^1\text{A}_1\sigma^2>_L|\text{CH}_2, {}^1\text{A}_1\pi^2>_R \quad (3.33d)$$

$$|E\rangle = |\sigma^2|\sigma^2\rangle = \frac{1}{\sqrt{2}}_{LR}|\text{CH}_2, {}^1\text{A}_1\sigma^2>_L|\text{CH}_2, {}^1\text{A}_1\sigma^2>_R \quad (3.33e)$$

$$|F\rangle = |\pi^2|\pi^2\rangle = \frac{1}{\sqrt{2}}_{LR}|\text{CH}_2, {}^1\text{A}_1\pi^2>_L|\text{CH}_2, {}^1\text{A}_1\pi^2>_R \quad (3.33f)$$

$$|G\rangle = |\sigma\pi|\sigma\pi|S\rangle = \frac{1}{\sqrt{2}}_{LR}|\text{CH}_2, {}^1\text{B}_1>_L|\text{CH}_2, {}^1\text{B}_1>_R \quad (3.33g)$$

$$|H\rangle = |\sigma\pi|\sigma\pi|T\rangle = \frac{1}{\sqrt{3}}_{LR}\{|\text{CH}_2, {}^3\text{B}_1^+>_L|\text{CH}_2, {}^3\text{B}_1^->_R \\ + |\text{CH}_2, {}^3\text{B}_1^->_L|\text{CH}_2, {}^3\text{B}_1^+>_R \\ - |\text{CH}_2, {}^3\text{B}_10>_L|\text{CH}_2, {}^3\text{B}_10>_R\} / \sqrt{3} \quad (3.33h)$$

where the configurations of the left methylene are defined as follows

$$|\text{CH}_2^{--}, {}^1\text{A}_1 >_L = \frac{1}{2} \not{\star}_x^A (F_L \sigma_L^2 \pi_L^2 \theta_{--}) \quad (3.35a)$$

$$|\text{CH}_2^{++}, {}^1\text{A}_1 >_L = \not{\star}_y^A (F_L) \quad (3.35b)$$

$$|\text{CH}_2^-, {}^2\text{A}_1^+ >_L = \frac{1}{\sqrt{2}} \not{\star}_x^B (F_L \pi_L^2 \sigma_L \theta_{-\alpha}) \quad (3.35c)$$

$$|\text{CH}_2^-, {}^2\text{A}_1^- >_L = \frac{1}{\sqrt{2}} \not{\star}_x^B (F_L \pi_L^2 \sigma_L \theta_{-\beta}) \quad (3.35d)$$

$$|\text{CH}_2^+, {}^2\text{A}_1^+ >_L = \frac{1}{\sqrt{2}} \not{\star}_y^B (F_L \sigma_L^\alpha) \quad (3.35e)$$

$$|\text{CH}_2^+, {}^2\text{A}_1^- >_L = \frac{1}{\sqrt{2}} \not{\star}_y^B (F_L \sigma_L^\beta) \quad (3.35f)$$

$$|\text{CH}_2^-, {}^2\text{B}_1^+ >_L = \frac{1}{\sqrt{2}} \not{\star}_x^C (F_L \sigma_L^2 \pi_L \theta_{-\alpha}) \quad (3.35g)$$

$$|\text{CH}_2^-, {}^2\text{B}_1^- >_L = \frac{1}{\sqrt{2}} \not{\star}_x^C (F_L \sigma_L^2 \pi_L \theta_{-\beta}) \quad (3.35h)$$

$$|\text{CH}_2^+, {}^2\text{B}_1^+ >_L = \frac{1}{\sqrt{2}} \not{\star}_x^C (F_L \pi_L^\alpha) \quad (3.35i)$$

$$|\text{CH}_2^+, {}^2\text{B}_1^- >_L = \frac{1}{\sqrt{2}} \not{\star}_y^C (F_L \pi_L^\beta) \quad (3.35j)$$

$$\begin{aligned} |\text{CH}_2, {}^1\text{A}_1 \sigma^2 >_L &= \frac{1}{\sqrt{2}} \not{\star}_x^D (F_L \sigma_L^2 \theta_-) \\ &= \frac{1}{\sqrt{2}} \not{\star}_x^E (F_L \sigma_L^2 \theta_-) \end{aligned} \quad (3.35k)$$

$$\begin{aligned} |\text{CH}_2, {}^1\text{A}_1 \pi^2 >_L &= \frac{1}{\sqrt{2}} \not{\star}_x^D (F_L \pi_L^2 \theta_-) \\ &= \frac{1}{\sqrt{2}} \not{\star}_x^F (F_L \pi_L^2 \theta_-) \end{aligned} \quad (3.35l)$$

$$|\text{CH}_2, {}^1\text{B}_1>_L = \alpha_x^G (F_L \sigma_L \pi_L \theta_-) \quad (3.35m)$$

$$|\text{CH}_2, {}^3\text{B}_1^+>_L = \alpha_x^H (F_L \sigma_L \pi_L \theta_+^+) \quad (3.35n)$$

$$|\text{CH}_2, {}^3\text{B}_1^->_L = \alpha_x^H (F_L \sigma_L \pi_L \theta_-^-) \quad (3.35o)$$

$$|\text{CH}_2, {}^3\text{B}_1^0>_L = \alpha_x^H (F_L \sigma_L \pi_L \theta_+^0) \quad (3.35p)$$

The configurations of the right methylene are defined analogously. All these configurations of methylene are orthogonal to each other.

#### 4. Separation to infinity

Every one of the configurations  $|A\rangle$  to  $|H\rangle$  is of the form

$$|U\rangle = \alpha_{xy} \alpha_{LR} (\sum_i k_i |U_L^i\rangle |U_R^i\rangle); \quad \sum_i k_i^2 = 1 \quad (3.36)$$

where  $U_L^i$  and  $U_R^i$  are certain configurations of the left and right methylene. It is evident that at infinite separation, configuration U corresponds to two separate methylenes, which are confined to give the  ${}^1\text{A}_g$  symmetry of U, and between which the electrons are formally antisymmetrized. It is also readily shown that the total energy of U at infinite separation is given by

$$\langle U | \mathcal{H} | U \rangle = \sum_i k_i^2 \{ \langle U_L^i | \mathcal{H}_L | U_L^i \rangle + \langle U_R^i | \mathcal{H}_R | U_R^i \rangle \} \quad (3.37)$$

where  $\mathcal{H}_L, \mathcal{H}_R$  are the sub-Hamiltonians for the left and right methylene respectively, and  $\mathcal{H} = \mathcal{H}_L + \mathcal{H}_R + \mathcal{H}_{LR}$ . In the case at hand, the energies  $\langle U_L^i | \mathcal{H}_L | U_L^i \rangle$  and  $\langle U_R^i | \mathcal{H}_R | U_R^i \rangle$  are furthermore independent of  $i$ , so that we have

$$\langle U | \mathcal{H} | U \rangle = \langle U_L^i | \mathcal{H}_L | U_L^i \rangle + \langle U_R^i | \mathcal{H}_R | U_R^i \rangle \quad (3.38)$$

where  $i$  can be arbitrarily chosen. Thus we get indeed the sum of the methylene energies at infinite separation.

All configurations  $U_L^i$  and  $U_R^i$  as given by Equation (3.35) describe certain states of an isolated methylene system, with the only exception of  $|\text{CH}_2, {}^1\text{A}_1 \sigma^2\rangle$  and  $|\text{CH}_2, {}^1\text{A}_1 \pi^2\rangle$  which belong to the same irreducible representation. Clearly a calculation of these  ${}^1\text{A}_1$  states of methylene in the approximation of the given orbital bases will yield two  ${}^1\text{A}_1$  states that are linear combination of  $\sigma^2$  and  $\pi^2$ .

$$|\text{CH}_2, {}^1\text{A}_1, 1\rangle = \cos\gamma |\text{CH}_2, {}^1\text{A}_1 \sigma^2\rangle + \sin\gamma |\text{CH}_2, {}^1\text{A}_1 \pi^2\rangle \quad (3.39a)$$

$$|\text{CH}_2, {}^1\text{A}_1, 2\rangle = -\sin\gamma |\text{CH}_2, {}^1\text{A}_1 \sigma^2\rangle + \cos\gamma |\text{CH}_2, {}^1\text{A}_1 \pi^2\rangle \quad (3.39b)$$

which we can write

$$|\text{CH}_2, {}^1\text{A}_1, 1\rangle = \frac{1}{\sqrt{2}} |\text{CH}_2 \{F_L a_1 \theta_-\} \rangle \quad (3.40a)$$

$$|\text{CH}_2, {}^1\text{A}_1, 2\rangle = \frac{1}{\sqrt{2}} |\text{CH}_2 \{F_L a_2 \theta_-\} \rangle \quad (3.40b)$$

where  $a_1$  and  $a_2$  are the geminals

$$a_1 = \cos \gamma \sigma^2 + \sin \gamma \pi^2 \quad (3.41a)$$

$$a_2 = -\sin \gamma \sigma^2 + \cos \gamma \pi^2 \quad (3.41b)$$

From the foregoing, it follows that at infinite separation, each of the configurations  $|A\rangle$ ,  $|B\rangle$ ,  $|C\rangle$ ,  $|G\rangle$  and  $|H\rangle$  represents an eigenstate of the system of two separated methylenes. However,  $|D'\rangle$ ,  $|E'\rangle$  and  $|F'\rangle$  do not.

By contrast the configurations

$$|D\rangle = \Psi_{8,8} |LR| \text{CH}_2, {}^1A_1, 1\rangle_L |CH_2, {}^1A_1, 2\rangle_R = |a_1|a_2\rangle \quad (3.42a)$$

$$|E\rangle = \Psi_{8,8} |CH_2, {}^1A_1, 1\rangle_L |CH_2, {}^1A_1, 1\rangle_R = |a_1|a_1\rangle \quad (3.42b)$$

$$|F\rangle = \Psi_{8,8} |CH_2, {}^1A_1, 2\rangle_L |CH_2, {}^1A_1, 2\rangle_R = |a_2|a_2\rangle \quad (3.42c)$$

do become eigenstates of the system at infinite separation.

It is therefore appropriate to replace the configurations  $|D'\rangle$ ,  $|E'\rangle$ ,  $|F'\rangle$  by the configurations  $|D\rangle$ ,  $|E\rangle$ ,  $|F\rangle$ . For, then, every one of the molecular eigenstates will go into one of the configurations  $|A\rangle$  to  $|H\rangle$  at infinity.

It is readily seen that the new configurations  $|D\rangle$ ,  $|E\rangle$  and  $|F\rangle$  can also be written in the form

$$|D\rangle = \frac{1}{2} \Psi \left\{ F \frac{1}{\sqrt{2}} (a_{1L}a_{2R} + a_{2L}a_{1R}) \theta_{--} \right\} \quad (3.43a)$$

$$|E\rangle = \frac{1}{2} \Psi \left\{ F a_{1L}a_{1R} \theta_{--} \right\} \quad (3.43b)$$

$$|F\rangle = \frac{1}{2} \Psi \left\{ F a_{2L}a_{2R} \theta_{--} \right\} \quad (3.43c)$$

Using the relations (3.41) in these expressions we find that

$|D\rangle$ ,  $|E\rangle$  and  $|F\rangle$  are related to  $|D'\rangle$ ,  $|E'\rangle$  and  $|F'\rangle$  by the orthogonal transformation ( $T_2$ )

	$ D'\rangle$	$ E'\rangle$	$ F'\rangle$
$ D\rangle$	$\cos 2\gamma$	$-\frac{1}{2} \sqrt{2} \sin 2\gamma$	$\frac{1}{2} \sqrt{2} \sin 2\gamma$
$ E\rangle$	$\frac{1}{2} \sqrt{2} \sin 2\gamma$	$\cos^2 \gamma$	$\sin^2 \gamma$
$ F\rangle$	$-\frac{1}{2} \sqrt{2} \sin 2\gamma$	$\sin^2 \gamma$	$\cos^2 \gamma$

Combining this transformation with the one given in Section III,B,3 ( $T_1$ ), we find the following transformation ( $T_3$ ) which is shown on Table 1b. The constants

$$a = \frac{1}{4}\sqrt{2} \cos 2\gamma \quad (3.44a)$$

$$b = \frac{1}{4} \sin 2\gamma \quad (3.44b)$$

$$c = \cos^2 \gamma \quad (3.44c)$$

$$d = \sin^2 \gamma \quad (3.44d)$$

are obtained from a separate calculation on methylene.

Thus, if we calculate the eight molecular states in terms of the configurations  $|I\rangle$  to  $|VIII\rangle$  and then re-express them in terms of configurations  $|A\rangle$  to  $|H\rangle$  by means this orthogonal transformation ( $T_3$ ), then the transformation from  $|A\rangle$  to  $|H\rangle$  to the molecular states should become identity upon dissociation.

Basch [47] omitted configurations  $|V\rangle$  and  $|VIII\rangle$ . As can be seen from the transformation matrix ( $T_3$ ), configuration

Table 1b. Orthogonal transformation ( $T_3$ )

	$ \sigma^2\pi^2\rangle$	$ \sigma^*\pi^2\rangle$	$ \sigma^2\pi^*\pi^2\rangle$	$ \sigma^*\pi^*\pi^2\rangle$	$ \sigma\sigma^*\pi\pi^*S\rangle$	$ \sigma^2 \sigma^*2\rangle$	$ \pi^2\pi^*\pi^2\rangle$	$ \sigma\sigma^*\pi\pi^*T\rangle$
$ \sigma^2\pi^2  \rangle$	$\frac{1}{4}\sqrt{2}$	$\frac{1}{4}\sqrt{2}$	$\frac{1}{4}\sqrt{2}$	$\frac{1}{4}\sqrt{2}$	$\frac{1}{2}\sqrt{2}$	0	0	0
$ \pi^2\sigma \sigma\rangle$	$\frac{1}{2}$	$-\frac{1}{2}$	$\frac{1}{2}$	$-\frac{1}{2}$	0	0	0	0
$ \sigma^2\pi \pi\rangle$	$\frac{1}{2}$	$\frac{1}{2}$	$-\frac{1}{2}$	$-\frac{1}{2}$	0	0	0	0
$ a_1 a_2\rangle$	a	a	a	a	-2a	$-2\sqrt{2}b$	$2\sqrt{2}b$	0
$ a_1 a_1\rangle$	b	b	b	b	-2b	c	d	0
$ a_2 a_2\rangle$	-b	-b	-b	-b	2b	d	c	0
$ \sigma\pi \sigma\pi S\rangle$	$-\frac{1}{4}$	$\frac{1}{4}$	$\frac{1}{4}$	$-\frac{1}{4}$	0	0	0	$-\frac{1}{2}\sqrt{3}$
$ \sigma\pi \sigma\pi T\rangle$	$-\frac{1}{4}\sqrt{3}$	$\frac{1}{4}\sqrt{3}$	$\frac{1}{4}\sqrt{3}$	$-\frac{1}{4}\sqrt{3}$	0	0	0	$\frac{1}{2}$

|VIII> is very important in describing the molecular states upon separation to infinity. Therefore his dissociation curves are quantitatively erroneous.

### C. Calculational Procedure and Basis Set

The MCSCF procedure used for the calculations was described in the last chapter. It is well known that the MCSCF procedure would be much more efficient if the initial orbitals were chosen close to the MCSCF orbitals. Therefore it is worthwhile to determine a good set of molecule orbitals before proceeding to the MCSCF calculations. In the present work, separated pair independent particle (SPIP) [48] calculations were used to determine such orbitals. The SPIP model is a compromise between the Hartree Fock method and the general MCSCF method. Although the types of configurations it can handle are limited, the SPIP implementation was a much faster procedure than our MCSCF implementation due to simplification in the transformation to generate molecular electron repulsion integrals. A SPIP function is an antisymmetrized product of spin germinals for pair electrons and spin orbitals for unpaired electrons. Orbital optimization is carried out using a technique similar to the MCSCF method presented in the last chapter.

If the SPIP function is very close to the MCSCF function, the SPIP orbitals are very good initial guess to the MCSCF orbitals. Sometimes if high accuracy is not desired, a plain CI calculation using these orbitals yields a very good

approximation. An approximation intermediate in accuracy between the CI model and the full MCSCF optimization is obtained by a MCSCF calculation using only the occupied orbitals from the SPIP calculation, i.e., omitting the virtual orbitals. This means that the orbital space and hence the correlation gained by the orbital optimization is limited. However, a considerable saving of computer time can be achieved since the number of molecular electron repulsion integrals is greatly reduced. We call this approximation limited MCSCF calculation.

As basis set, even-tempered cartesian gaussian atomic orbitals [49] were used in the calculations. The carbon atom basis was of size (9s 6p) contracted to (3s 2p). The hydrogen atom basis was (4s/2s). The parameters were determined by optimizing the ground state Hartree-Fock energy of ethylene [50] assuming an experimental geometry [51] ( $R_{CC} = 2.517$  a.u.,  $R_{CH} = 2.0478$  a.u. and  $\angle HCH = 115.62^\circ$ ). Contraction coefficients were obtained by the scheme given in Appendix B. The bases are shown in Table 2. The final optimal Hartree Fock energy obtained for ethylene is -77.9942 a.u. which is probably ~0.05 a.u. above the Hartree-Fock limit [47].

#### D. The Three Low Lying States of Methylene

The methylene molecule has been extensively studied in the literature [52-55] and these calculations served as a check for our methylene calculations. Using the atomic orbital basis set given in Section III,C, SCF calculations were made for the  $^3B_1$  and two  $^1A_1$  states ( $\sigma^2$  and  $\pi^2$ ) as a function of the angle. The CH bond distance was taken from the ethylene molecule and kept constant for all calculations. From these calculations optimal angles and energies were determined. The results are shown in Table 3.

Since the two singlet configurations can interact to give two states which are linear combinations of  $|^1A_1\sigma^2\rangle$  and  $|^1A_1\pi^2\rangle$ . They can be written as functions of the form

$$|^1A_1, 1\rangle = \{(\text{core})\Omega_1(\sigma, \pi) \theta_{--}\} \quad (3.45a)$$

$$|^1A_1, 2\rangle = \{(\text{core})\Omega_2(\sigma, \pi) \theta_{--}\} \quad (3.45b)$$

where

$$\Omega_1(\sigma, \pi) = \cos\gamma\sigma^2 + \sin\gamma\pi^2 \quad (3.45c)$$

$$\Omega_2(\sigma, \pi) = -\sin\gamma\sigma^2 + \cos\gamma\pi^2 \quad (3.45d)$$

Using these functions, calculations were made as functions of the angle. Optimal angle and energy were also determined for  $|^1A_1, 1\rangle$ . The results are shown in Table 3.

## E. Dissociation of the Ethylene Ground State into Triplet Methylenes

### 1. Reaction coordinates

The first consideration in calculating the dissociation curve are the reaction coordinates. The reaction path, which was assumed to be coplanar and least motion, just translates the methylene groups away from each other. Therefore there were, in addition to the carbon carbon bond distance  $R_{CC'}$ , two parameters to be considered, viz., the CH bond distance ( $R_{CH}$ ) and HCH angle. The change of  $R_{CH}$  is small and does not change the energy significantly during the reaction; so it was held constant. However we had to vary the HCH angle since the experimental angle of ethylene ( $115.62^\circ$ ) is quite different from the optimal angle of methylene ( $130.00^\circ$ ). Therefore to perform the calculations we first chose nine different values of  $R_{CC'}$ . They are those listed in Table 4 except for the third one. The optimal angles were then determined at several points by repeated calculations of the energies. Angles for the other points were then determined by interpolating the reaction coordinate curve. Since the variation of energy is not too sensitive to the angle, MCSCF calculations were not used. This saved computer time. Instead SPIP calculations followed by limited MCSCF calculations using eight configurations were performed. The

SPIP function is of the form

$$\Phi_0 = \nabla \{ F \Omega(\sigma, \sigma^*) \Omega(\pi, \pi^*) \theta_{\perp} \} \quad (3.46a)$$

where

$$\Omega(\sigma, \sigma^*) = c_1 \sigma^2 + c_2 \sigma^{*2} \quad (3.46b)$$

$$\Omega(\pi, \pi^*) = c_3 \pi^2 + c_4 \pi^{*2} \quad (3.46c)$$

which is similar to a linear combination of configurations  $|\sigma^2 \pi^2\rangle$ ,  $|\sigma^*2 \pi^2\rangle$ ,  $|\sigma^2 \pi^{*2}\rangle$  and  $|\sigma^*2 \pi^{*2}\rangle$ . On studying the transformation matrix ( $T_3$ ) in Section III, B, 4, it can be seen that these four configurations are very important in describing the dissociation of ethylene. Therefore it is not surprising that the SPIP orbitals are very close to the MCSCF orbitals.

The reaction coordinates are shown in Table 4 and graphically in Figure 1. The curve is fairly simple. The angle gradually opens up to the equilibrium angle of a triplet methylene. It is almost a linear function of the internuclear distance. As the carbon carbon bond distance increases, the electron repulsion between the left and right CH groups decreases, allowing the angle to increase steadily.

## 2. Energetics of dissociation

With these coordinates, the dissociation curve was determined by computing the energies using the MCSCF procedure. The MCSCF energies are also listed in Table 4, along with the

SPIP energies, plain CI energies and the limited MCSCF energies. Comparison of the energies indicates that in this case, the plain CI energy and the limited MCSCF energy at each point are identical to four decimals. The difference between the limited MCSCF energy and the MCSCF energy at each point is less than  $10^{-3}$  a.u. This indicates how good the SPIP orbitals are. The SPIP and MCSCF energy curves are shown in Figure 2. It can be seen that the SPIP curve gives the correct shape, but omission of four configurations leads to the incorrect energy of the separated products. The same criticism applies to Basch's calculations [47].

The MCSCF energy at infinite separation is -77.8008 a.u., which is exactly twice the triplet methylene energy listed in Table 3. This confirms that the molecule separates properly using the configurations proposed in Section III,B. From the curve it is apparent that the ethylene ground state dissociates smoothly and without any barrier into methylene triplets, in agreement with the Woodward Hoffmann rules.

In order to find the reaction energy, we determined the minimum of the dissociation curve. This was done keeping  $R_{CH}$  constant and  $\angle HCH$  at  $116.05^\circ$ , the optimal angle for  $R_{CC} = 2.517$  a.u. (experimental CC bond distance). Limited MCSCF energies were calculated at two additional points near  $R_{CC} = 2.517$  a.u. The minimum was then predicted by a parabola fit to be 2.567 a.u. The MCSCF energy calculated at the

predicted minimum is shown in the third row of Table 4.

The reaction energy, computed by taking the difference between this energy and the energy at infinite separation, was found to be 0.2492 a.u. or 156.5 kcal/mole, in close agreement with the experimental value [56]. The reaction energy calculated by Hartree-Fock approximation was 0.1934 a.u. or 121.4 kcal/mole. The correlation energy recovered was 35.1 kcal/mole, which is quite significant.

### 3. Configurational analysis of dissociation

The expansion coefficients  $\{C_i\}$ , where  $i$  denotes the configuration, of the ground state for various internuclear distance are shown in Table 5. Also the  $\{C_i^2\}$  are plotted against  $R_{CC}$  for all the configurations in Figure 3. From the curves, the contribution of different configurations at different internuclear distances to the ground state wavefunction of ethylene can be seen.

We can roughly divide the plot into three regions. The first region is from  $\Delta R$  ( $\Delta R = R_{CC} - R_e$ , where  $R_e = 2.517$  a.u.) = -0.5 a.u. to  $\Delta R = 0.5$  a.u. Here the most dominant configuration is  $|\sigma^2\pi^2\rangle$ . The only other configuration of significance is  $|\sigma^2\pi^{*2}\rangle$ , which accounts for most of the pair correlation energy of the  $\pi$  electrons. The second region is from  $\Delta R = 0.5$  a.u. to  $\Delta R = 3.5$  a.u. In this region the importance of  $|\sigma^2\pi^2\rangle$  decreases but that of  $|\sigma^2\pi^{*2}\rangle$  increases

significantly. These two configurations are dominant and their coefficients are approaching equality in magnitude, suggesting that the  $\pi$  bond is broken before the  $\sigma$  bond. The contributions from  $|\sigma^*|^2 \pi^2\rangle$ ,  $|\sigma^*|^2 \pi^*|^2\rangle$ , and  $|\sigma\sigma^*\pi\pi^*T\rangle$  become larger. Finally for  $\Delta R > 3.5$  a.u., the function approaches that of two methylenes. At  $\Delta R = 15.0$  a.u., the wavefunction is seen to be practically identical with  $-|\sigma\pi|\sigma\pi|T\rangle$ , as given in the transformation matrix ( $T_3$ ) in Section III,B,4. Thus the result deduced for  $\Delta R = \infty$  is reached for  $\Delta R = 15.0$  a.u. The coefficients of the first four configurations are equal in magnitude, so the  $\sigma$  and  $\sigma^*$  orbitals are equally weighed, as are the  $\pi$  and  $\pi^*$  orbitals. The last configuration has the largest coefficient, confirming the importance of the triplet coupling.

The ground state wavefunctions can be expressed in configurations made from the localized orbitals by means of the transformation matrix ( $T_3$ ) in Section III,B,4. The parameter  $\gamma$  occurring in this transformation has to be taken from a calculation of the  $|^1A_1, 1\rangle$  excited state of an isolated methylene. Carried out at  $\langle HCH = 130^\circ$ , the equilibrium angle of the ground state, and with the molecular orbitals that we optimized for the ground state, it is found to be  $-21.48^\circ$  and differs somewhat from the corresponding value in Table 3. The ethylene energy for this excited  ${}^1A_1$  wavefunction is -38.8459 a.u. The resulting

contributions from the different configurations can be seen from Figure 5. where the squares of the expansion coefficients are plotted against the internuclear distance. There is conceivable mixing at small separations, but as  $R_{CC}$  gets larger, the wavefunction becomes quickly dominated by  $|\sigma\pi|\sigma\pi|T\rangle$ .

#### 4. Orbital analysis of dissociation

Since all the configurations in the wavefunction differ from each other by more than one orbital, the first order density matrix is diagonal, and so the symmetry orbitals are natural orbitals. The variations of the occupation numbers of the  $\sigma$ ,  $\sigma^*$ ,  $\pi$ , and  $\pi^*$  orbitals with respect to the internuclear distance are shown graphically in Figure 5. The occupation numbers of all four orbitals are unity at infinite separation, however, the  $\pi$  and  $\pi^*$  orbitals become unity before the  $\sigma$  and  $\sigma^*$  orbitals do. This means that the  $\pi$  bond breaks before the  $\sigma$  bond. At small separations, the  $\pi^*$  orbital is more important than the  $\sigma^*$  orbital, implying that there is more  $\pi$  correlation than  $\sigma$  correlation. There is no sudden change in occupation numbers as the methylene groups separate from each other, and this is characteristic of a concerted reaction.

### 5. Excited states from ground state MCSCF calculations

The ground state MCSCF calculations yield of course energy curves for eight  $^1A_g$  states, resulting from the MC-CI calculations in terms of the ground state orbitals. They are shown in Figure 6. Using the transformation ( $T_3$ ) in Section III,B,4, all of these states can be expressed in terms of the configurations made from localized orbitals. In agreement with the theoretical prediction, each one of these eight molecular states became identical with exactly one of the localized configurations at  $\Delta R = 15.0$  a.u. The limiting localized configurations are indicated in Figure 6 for each state.

### F. Dissociation of the Lowest $^1A_g$ ( $\pi^*2$ ) Excited State of Ethylene into Singlet Methylenes

#### 1. Reaction coordinates

The procedure is similar to the calculation of the ground state dissociation curve and based on the same eight  $^1A_g$  configurations defined in Section III,B. The only difference is that we now used the second root of the MC-CI problem for generating the super CI problem. From Figure 6, it is apparent that for infinite separation, the wavefunction goes into the  $|a_1|a_1\rangle$  state of methylene. The first consideration was again the reaction coordinates. We used a similar technique as before except different values were

chosen for the carbon carbon internuclear distances because we expected a barrier approximately in the region from  $\Delta R = 1.0$  a.u. to  $\Delta R = 2.5$  a.u. and so more points were needed in this region. Also large values of  $\Delta R$  were not included since we know for sure that the separated species are singlet methylenes.

Again it would be too time-consuming to use the MCSCF procedure to determine the optimum angle along the reaction path. Here we used a 1-geminal SPIP function to determine the reaction coordinates. It is of the form

$$\Phi_1 = \alpha \{ F \sigma^2 \Omega(\pi^*, \sigma^*) \theta_{\dots} \} \quad (3.47a)$$

where

$$\Omega(\pi^*, \sigma^*) = c_a \pi^{*2} + c_b \sigma^{*2} \quad (3.47b)$$

Since two separated methylene singlets have the Hartree Fock representation

$$|{}^1A_1\sigma^2\rangle |{}^1A_1\sigma^2\rangle = \alpha \{ F \sigma^2 \sigma^{*2} \theta_{\dots} \} \quad (3.48)$$

The wavefunction  $\Phi_1$  is clearly flexible enough to describe the dissociation of the  $\pi^2$  state of ethylene to singlet methylenes. It is true that the separated fragments will be pure  $\sigma^2$  singlet methylenes. But, as seen from Table 3, the mixing of  $|{}^1A_1\sigma^2\rangle$  and  $|{}^1A_1\pi^2\rangle$  states is small and therefore  $\Phi_1$  is sufficiently accurate for the determination of the

reaction coordinates. The results are shown in Table 6. They are also shown graphically in Figure 1.

The curve in Figure 1 seems strange at first sight. The angle of the  $\pi^*^2$  state of ethylene at  $\Delta R = 0$  is  $113.62^\circ$  and that of singlet methylene is  $108.34^\circ$ . Therefore we might expect the angle to decrease gradually upon dissociation. But the curve is not so simple. It can be understood by examining the variations of the occupation numbers of the orbitals which is shown in figure 7. It suggests the division of the reaction coordinates roughly into three regions. The region from  $\Delta R = 0.0$  a.u. to  $\Delta R = 1.5$  a.u. is region 1;  $\Delta R = 1.5$  a.u. to  $\Delta R = 2.0$  a.u., region 2; and  $\Delta R = 2.0$  a.u. to  $\Delta R = 5.0$  a.u., region 3. In region 1, there is not much change in occupation number. The molecular wavefunction is dominated by the molecular SCF function  $\{F\sigma^2\pi^*^2\theta_{--}\}$  which dissociates into an average of several ionic or molecular species, as indicated by the transformation matrix ( $T_3$ ) in Section III,B,4, and for small separations the dominant product probably has a large angle. Thus the initial rise in the value of  $\langle HCH \rangle$  can be interpreted as the natural response of the molecule to the reaction it is following. In other words, when the dissociation begins, the system starts to separate to different products. The behavior in region 3 can be understood when we start with two separated  $|{}^1A_1\sigma^2\rangle$  configurations of methylene, whose HCH angle is  $108.34^\circ$ . As they

approach each other, some of the electronic population moves from the  $\sigma^*$  orbital to the  $\pi^*$  orbital, and hence from the  $\sigma_L$  to the  $\pi_L$  localized orbital (or  $\sigma_R$  to  $\pi_R$ ). The admixture of the  $\pi_L^2$  configuration to the  $\sigma_L^2$  configuration decreases the HCH angle as can be seen from the fact that this angle is smaller in the  $|^1A_1, 1\rangle$  state than in the  $|^1A_1, \sigma^2\rangle$  configuration (compare this value in Table 3 with that of  $108.34^\circ$ ). In the intermediate region 2, finally the wavefunction rapidly changes from that of excited ethylene to that of the separated methylenes. Concomitantly the HCH angle rapidly changes from the behavior in region 1 to that in region 3.

## 2. Energetics of dissociation

Having determined the reaction coordinates, we calculated more accurate wavefunctions. We first calculated the dissociation curve using a SPIP function of the form

$$\Phi_2 = \mathcal{A}\{\mathbf{F}\Omega(\sigma, \pi)\Omega(\pi^*, \sigma^*)\theta_{\_\_}\} \quad (3.49)$$

which is similar to a linear combination of configurations  $|\sigma^*{}^2\pi^2\rangle$ ,  $|\sigma^2\pi^*{}^2\rangle$ ,  $|\sigma^2\sigma^*{}^2\rangle$ , and  $|\pi^2\pi^*{}^2\rangle$ . On studying the transformation matrix ( $T_3$ ) in Section III,B,4, it can be seen that these four configurations are important in describing the dissociation, although those three which had been left out are important too. Still this was worth

doing since the orbitals determined would be better approximations to the MCSCF orbitals. Subsequent to the SPIP calculations, plain CI calculations, limited MCSCF calculations and MCSCF calculations were then carried out. It is interesting to compare the results from each calculation and they are shown in Table 6. The 2-geminal SPIP and MCSCF energy curves are shown graphically in Figure 8.

There were some convergence problems in the MCSCF calculations. The problem might be due to the fact that the first excited state is not so well-defined as the ground state. Still the energies are valid up to 0.001 Hartree.

On studying Table 6, we can see that the 1-geminal SPIP energy is very close to the 2-geminal SPIP energy at each point. The additional geminal gives pair correlation, the order of magnitude of which is  $10^{-2}$  a.u. Both calculations predict the barrier near  $\Delta R = 1.6$  a.u. The barrier is caused by orbital symmetry change as predicted by Woodward Hoffmann rules.

In the CI calculations, the SPIP orbitals were allowed to relax among each other. On studying the 2-geminal SPIP and MCSCF energy curves in Figure 8, we see that the MCSCF procedure did modify the dissociation curve in a quantitative manner. The barrier was sharpened and shifted by the additional configurations. The MCSCF calculations predicted the minimum at around  $\Delta R = 1.5$  a.u. and this is the geometry

at which the metastable  $\pi^*^2$  state of ethylene might exist. The height of the barrier is about 0.02 a.u., at around  $\Delta R = 1.85$  a.u. The essential feature of both curves, however, is a barrier to the formation of the molecule as both functions predict the existence of  $\pi^*^2$  state of ethylene as a metastable entity.

In comparing the limited MCSCF and MCSCF energies in Table 6, we find the lowering in energy by the MCSCF procedure is quite significant at small separations, but decreases at larger separations. Comparison of the plain CI energies and limited MCSCF energies in Table 6 indicates that the limited MCSCF procedure produced a significant energy lowering over the plain CI calculations. It also resolved ambiguities in the order of the states which is the cause of the erratic behavior of the CI energies for larger separations.

In this series of calculations, we note that the SPIP orbitals are not as good as in the dissociation of the ethylene ground state. This is so because the SPIP wavefunction is a poorer approximation in this case, little correlation energy is recovered by this function.

Finally it is of interest to compare these results with those that are obtained when the ground state MCSCF molecular orbitals are used to calculate the excited state. The energy curve for the lowest excited state is that of the second of the eight roots plotted in Figure 6. This curve

is also indicated as a dotted line in Figure 8. The numerical values are given in the last column of Table 4. The incorrect limiting value for the separated methylenes is due not only to the different orbitals, but also to the different limiting HCH angles. More seriously, it is apparent that, with the ground state orbitals, the calculation does not yield a barrier and no metastable  $^1A_g$  state results.

The smoothness of the dissociation curves and the presence of a barrier contrast Basch's erratic curves [47]. It shows the importance of the adequate choice of configurations and of orbital optimization.

### 3. Configurational analysis of dissociation

The expansion coefficients  $\{c_i\}$ , where  $i$  denotes the configuration, of the first excited state of ethylene at various internuclear distances are shown in Table 7. Also  $\{c_i^2\}$  are plotted against  $\Delta R$  for all configurations in Figure 9. From the graph it can be seen that configuration  $|\sigma^2\pi^*|^2\rangle$  dominates the wavefunction at small separations while configuration  $|\sigma^2\sigma^*|^2\rangle$  is dominant at larger separations. In the region around the barrier, the most important configurations are:  $|\sigma^2\pi^*|^2\rangle$ ,  $|\sigma^2\sigma^*|^2\rangle$ ,  $|\sigma^2\pi^2\rangle$  and  $|\sigma\sigma^*\pi\pi^*S\rangle$ . This indicates the strong interaction from the  $\pi$  orbital.

Using the value of  $\gamma$  from Table 3, the transformation

matrix ( $T_3$ ) in Section III,B,4 was evaluated. Using this transformation, the wavefunctions were then expressed in terms of configurations  $|A\rangle$  to  $|H\rangle$ . The contributions of different configurations can be seen from Figure 10, where the squares of the expansion coefficients are plotted against the internuclear distance. The mixing of configurations is quite considerable at small separations, but as  $R_{CC}$  gets larger, the wavefunction is dominated by  $|a_1|a_1\rangle$ .

The expansion coefficients of  $|a_1|a_1\rangle$  at infinite separation is read off from the evaluated transformation matrix ( $T_3$ ) and is given as

$$\begin{aligned} |a_1|a_1\rangle = & -0.0830\{|\sigma^2\pi^2\rangle + |\sigma^*\pi^2\rangle + |\sigma^2\pi^*\pi^2\rangle + |\sigma^*\pi^2\pi^*\rangle\} \\ & + 0.1550|\sigma\sigma^*\pi\pi^*S\rangle + 0.9716|\sigma^2\sigma^*\pi^2\rangle \\ & + 0.0284|\pi^2\pi^*\pi^2\rangle \end{aligned}$$

The molecular wavefunction at  $R = 5.0$  a.u. is approaching configuration  $|a_1|a_1\rangle$ . They would become identical at infinity.

#### 4. Orbital analysis of dissociation

Similar information can be obtained by studying the occupation numbers of  $\sigma$ ,  $\sigma^*$ ,  $\pi$  and  $\pi^*$  orbitals as functions of internuclear distance shown in Figure 11. From Figure 11 as well as Figure 9 it is apparent that in the neighborhood

the barrier, the occupation of the  $\pi$  orbital indicates that the admixture of the  $|\sigma\sigma^*\pi\pi^*S\rangle$  configuration is not negligible, even though they are relatively unimportant in ethylene and for the dissociated conformation. At infinite separation, the  $\sigma$  and  $\sigma^*$  orbitals are equally weighed, and so are the  $\pi$  and  $\pi^*$  orbitals.

Table 2a. Even-tempered atomic orbitals for carbon in ethylene

Primitive exponents  $\alpha=0.024294$        $\beta=3.20387$

Contraction coefficients

<u>s</u>	<u>s'</u>	<u>s''</u>
-0.021041	0.105687	2.560314
0.083853	-1.006528	-2.196177
0.029610	-0.561905	-0.419553
0.246900	0.425782	0.218253
0.441448	0.438538	0.209440
0.212623	0.186396	0.057135
0.067217	0.055892	0.018348
0.014354	0.011936	0.003189
0.005894	0.004834	0.000894

Primitive exponents  $\alpha=0.025190$        $\beta=3.01742$

Contraction coefficients

<u>p</u>	<u>p'</u>
0.116312	-0.632380
0.412027	-0.602350
0.420862	0.820816
0.154511	0.225189
0.042740	0.071517
0.011077	0.017547

Table 2b. Even-tempered atomic orbitals for hydrogen in ethylene

Primitive exponents  $\alpha=0.039062$        $\beta=4.31999$

Contraction coefficients

<u>s</u>	<u>s'</u>
0.417830	-1.731918
0.504366	1.174174
0.107554	0.503923
0.024630	0.081823

Table 3. Geometries and energies for methylene<sup>a</sup>

$\angle \text{HCH}$	$E(^3\text{B}_1)$	$E(^1\text{A}_1, 1)$	$E(^1\text{A}_1, 2)$	$E(^1\text{A}_1, \sigma^2)$	$E(^1\text{A}_1, \pi^2)$	$-\gamma$
80°	-38.8396	-38.8382	-38.5974	-38.8220	-38.6136	9.991
90°	-38.8639	-38.8525	-38.6393	-38.8370	-38.6548	9.788
100°	-38.8813	-38.8597	-38.6746	-38.8450	-38.6893	9.676
110°	-38.8925	-38.8606	-38.7040	-38.8466	-38.7180	9.762
120°	-38.8986	-38.8565	-38.7286	-38.8433	-38.7418	14.35
130°	<u>-38.9004</u>	-38.8500	-38.7475	-38.8363	-38.7612	18.96
140°	-38.8989	-38.8427	-38.7613	-38.8274	-38.7766	24.32
150°	-38.8951	-38.8364	-38.7703	-38.8182	-38.7885	31.00
160°	-38.8904	-38.8325	-38.7749	-38.8105	-38.7969	37.99
170°	-38.8865	-38.8309	-38.7765	-38.8054	-38.8020	43.15
180°	-38.8849	-38.8305	-38.7769	-38.8037	<u>-38.8037</u>	45.00
106.6°		<u>-38.8609</u>				9.694
108.3°				<u>-38.8467</u>		

<sup>a</sup>All values are in atomic units. The optimal energies are underlined.

Table 4. Reaction coordinates and energies for the dissociation of ethylene ground state into triplet methylenes<sup>a</sup>

$\Delta R^b$	$\langle HCH \rangle$	E (SPIP) <sup>c</sup>	E (CI) <sup>d</sup>	E (limited MCSCF) <sup>e</sup>	E (MCSCF) <sup>f</sup>	E (excited) <sup>g</sup>
-0.5	112.28°	-77.8822	-77.8939	-77.8939	-77.8943	-76.8217
0.0	116.05°	-78.0338	-78.0489	-78.0489	-78.0495	-77.3729
0.05	116.05°	-78.0342	-78.0497	-78.0497	-78.0502	-77.4019
0.5	119.82°	-77.9951	-78.0127	-78.0127	-78.0133	-77.5625
1.5	127.36°	-77.8653	-77.8838	-77.8838	-77.8842	-77.6533
2.5	129.80°	-77.7946	-77.8203	-77.8203	-77.8209	-77.6675
3.0	130.00°	-77.7782	-77.8090	-77.8090	-77.8097	-77.6733
3.5	130.00°	-77.7695	-77.8040	-77.8040	-77.8046	-77.6788
7.5	130.00°	-77.7616	-77.8002	-77.8002	-77.8007	-77.6905
15.0	130.00°	-77.7618	-77.8003	-77.8003	-77.8008	-77.6922

<sup>a</sup>All values are in atomic units.

<sup>b</sup> $\Delta R = R_{CC} - R_e$ , where  $R_e = 2.517$  a.u.

<sup>c</sup>Separated-pair independent particle calculation.

<sup>d</sup>Plain CI with SPIP orbitals.

<sup>e</sup>Orbitals optimized within space of occupied SPIP orbitals.

<sup>f</sup>Complete MCSCF.

<sup>g</sup>First excited state resulting from ground state MCSCF calculation.

Table 5. Expansion coefficients of ethylene ground state wavefunctions at various internuclear distances

$\Delta R^a$	$ \sigma^2\pi^2\rangle$	$ \sigma^*\pi^2\rangle$	$ \sigma^2\pi^*\rangle$	$ \sigma^*\pi^*\rangle$	$ \sigma\sigma^*\pi\pi^*S\rangle$	$ \sigma^2\sigma^*\rangle$	$ \pi^2\pi^*\rangle$	$ \sigma\sigma^*\pi\pi^*T\rangle$
-0.5	0.9893	-0.0328	-0.1237	0.0073	-0.0637	-0.0095	-0.0085	-0.0232
0.0	0.9763	-0.0565	-0.1833	0.0184	-0.0881	-0.0133	-0.0109	-0.0396
0.05	0.9745	-0.0592	-0.1900	0.0201	-0.0905	-0.0137	-0.0112	-0.0418
0.5	0.9531	-0.0872	-0.2559	0.0402	-0.1098	-0.0179	-0.0134	-0.0666
1.5	0.8536	-0.1735	-0.4239	0.1297	-0.1086	-0.0262	-0.0141	-0.1792
2.5	0.6753	-0.2893	-0.5120	0.2562	-0.0459	-0.0175	-0.0065	-0.3605
3.0	0.5967	-0.3345	-0.5063	0.3062	-0.0228	-0.0101	-0.0033	-0.4258
3.5	0.5412	-0.3660	-0.4904	0.3432	0.0105	-0.0051	-0.0015	-0.4634
7.5	0.4376	-0.4296	-0.4364	0.4284	0.0000	0.0000	0.0000	-0.4999
15.0	0.4330	-0.4330	-0.4330	0.4330	0.0000	0.0000	0.0000	-0.5000

<sup>a</sup> $\Delta R = R_{CC} - R_e$ , where  $R_e = 2.517$  a.u.

Table 6. Reaction coordinates and energies for the dissociation of ethylene  $\pi^2$  excited state into singlet methylenes<sup>a</sup>

$\Delta R^b$	$\angle HCH$	$E(\Phi_1)^c$	$E(\Phi_2)^d$	$E(CI)^e$	$E(\text{limited MCSCF})^{f,g}$	$E(\text{MCSCF})^{g,h}$
0.0	113.62	-77.4748	-77.4806	-77.4679	-77.4689	-77.4967
1.0	123.77	-77.5948	-77.5988	-77.6160	-77.6388	-77.6602
1.4	126.03	-77.5830	-77.5868	-77.6542	-77.6599	-77.6695
1.5	125.92	-77.5792	-77.5830	-77.6568	-77.6623	-77.6704
1.7	107.47	-77.5806	-77.5838	-77.6167	-77.6502	-77.6563
2.0	104.15	-77.6052	-77.6083	-77.6458	-77.6560	-77.6591
2.4	104.64	-77.6375	-77.6404	-77.6628	-77.6748	-77.6765
3.0	105.45	-77.6608	-77.6635	-77.5625	-77.6917	-77.6930
5.0	107.39	-77.6868	-77.6893	-77.3405	-77.7108	-77.7103

<sup>a</sup>All values are in atomic units.

<sup>b</sup> $\Delta R = R_{CC} - R_e$ , where  $R_e = 2.517$  a.u.

<sup>c</sup>1-geminal separated pair independent particle calculation.

<sup>d</sup>2-geminal separated pair independent particle calculation.

<sup>e</sup>Plain CI with SPIP orbitals.

<sup>f</sup>Orbitals optimized within space of occupied SPIP orbitals.

<sup>g</sup>Fourth decimal is uncertain.

<sup>h</sup>Complete MCSCF.

Table 7. Expansion coefficients of ethylene  $\pi^*^2$  excited state wavefunctions at various internuclear distances

$\Delta R^a$	$ \sigma^2\pi^2\rangle$	$ \sigma^*\pi^2\rangle$	$ \sigma^2\pi^*\pi^2\rangle$	$ \sigma^*\pi^2\pi^*\pi^2\rangle$	$ \sigma\sigma^*\pi\pi^*S\rangle$	$ \sigma^2\sigma^2\rangle$	$ \pi^2\pi^*\pi^2\rangle$	$ \sigma\sigma^*\pi\pi^*T\rangle$
0.0	0.1907	0.0083	0.9582	-0.0490	-0.1715	-0.0318	-0.0821	0.0762
1.0	0.3083	0.0746	0.8289	-0.0566	-0.3769	-0.1193	-0.1319	0.1882
1.4	0.3584	0.1186	0.7274	-0.0382	-0.4440	-0.1945	-0.1566	0.2598
1.5	0.3713	0.1287	0.6962	-0.0311	-0.4567	-0.2206	-0.1610	0.2772
1.7	0.3687	0.1488	0.5715	-0.0032	-0.4558	-0.4832	-0.1378	0.2347
2.0	0.3083	0.1518	0.4343	0.0268	-0.4099	-0.7006	-0.1197	0.1393
2.4	0.2236	0.1398	0.2878	0.0567	-0.3341	-0.8497	-0.0917	0.0489
3.0	0.1639	0.1246	0.2009	0.0735	-0.2747	-0.9119	-0.0689	0.0119
5.0	0.1142	0.1082	0.1246	0.0957	0.2210	-0.9483	-0.0492	-0.0007

<sup>a</sup> $\Delta R = R_{CC} - R_e$ , where  $R_e = 2.517$  a.u.

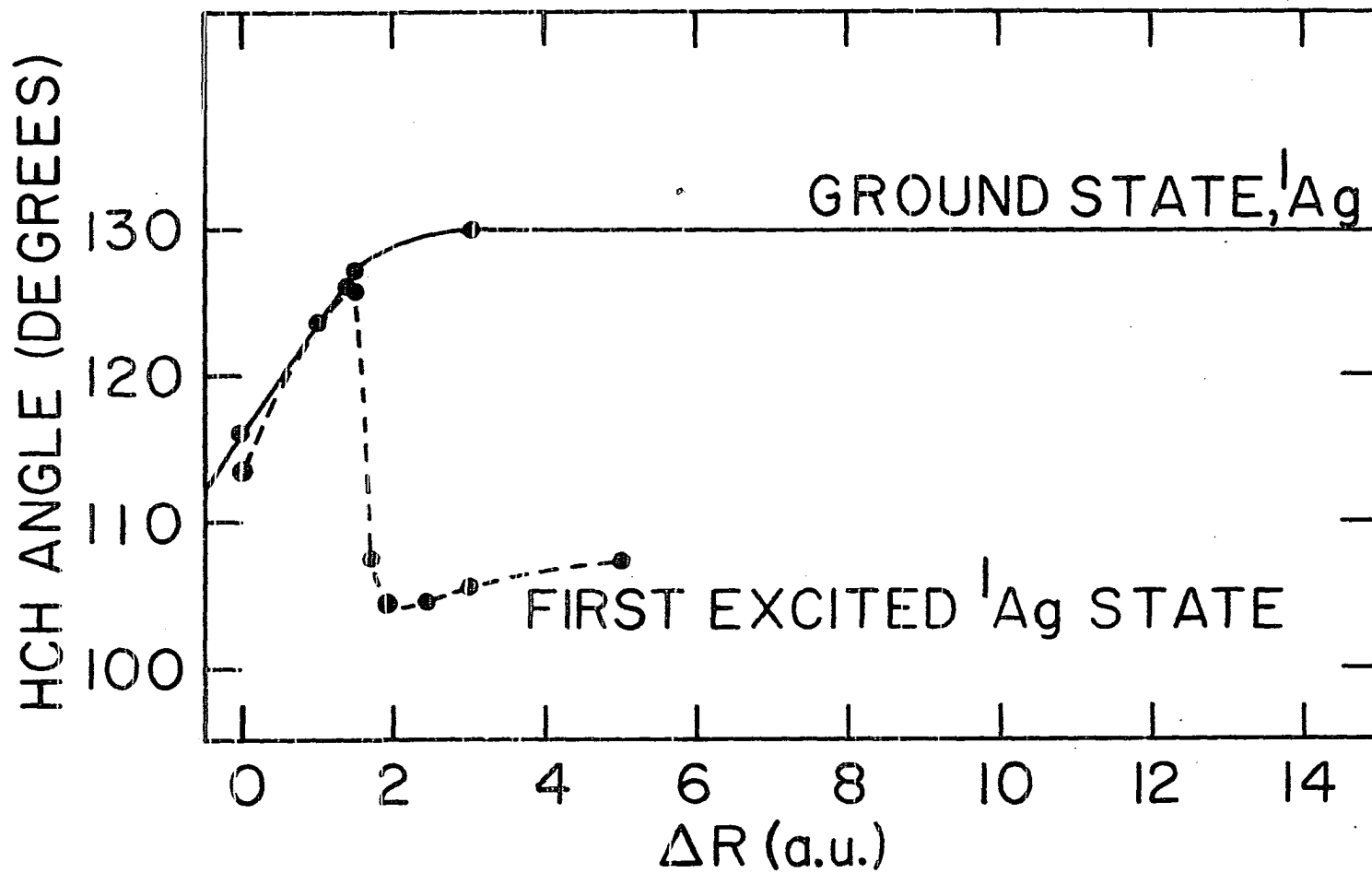


Figure 1. Variation of HCH angle in ethylene,  $\Delta R = R_{\text{CC}} - R_e$ ,  $R_e = 2.517$  a.u.

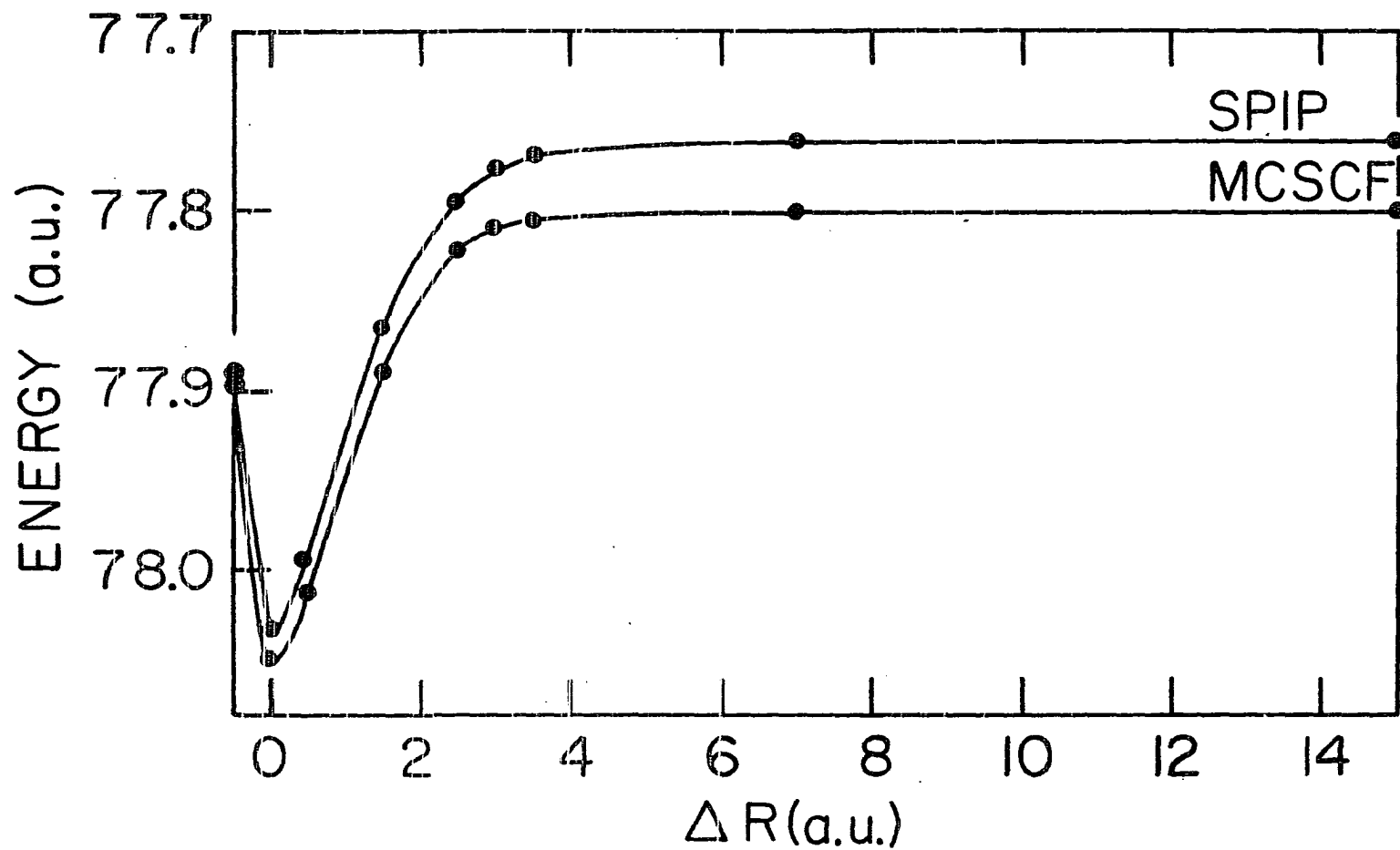


Figure 2. Dissociation of ethylene ground state,  $\Delta R = R_{CC} - R_e$ ,  $R_e = 2.517$  a.u.

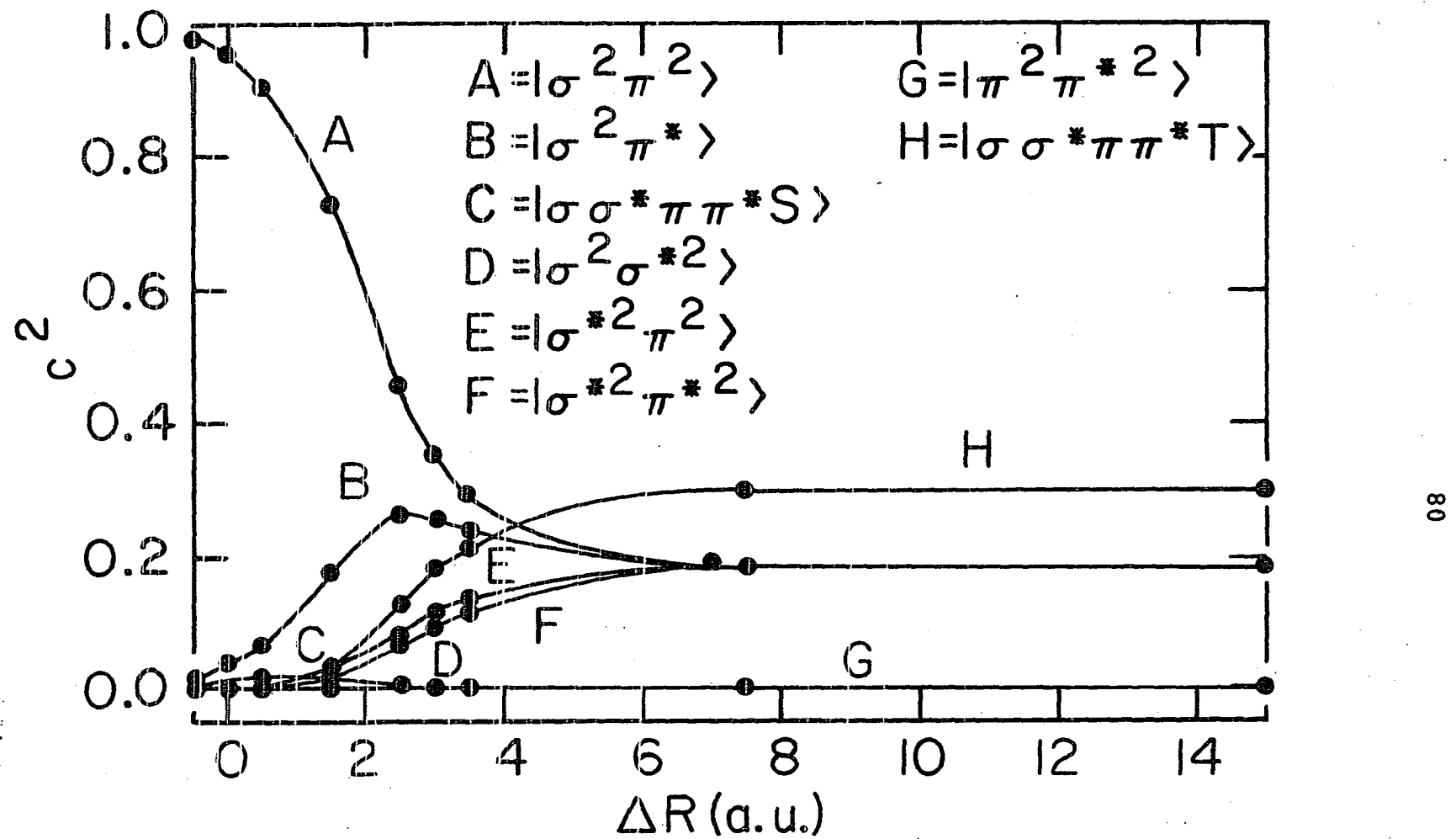


Figure 3. Ethylene ground state: occupations of delocalized configurations,  
 $\Delta R = R_{CC} - R_e$ ,  $R_e = 2.517$  a.u.

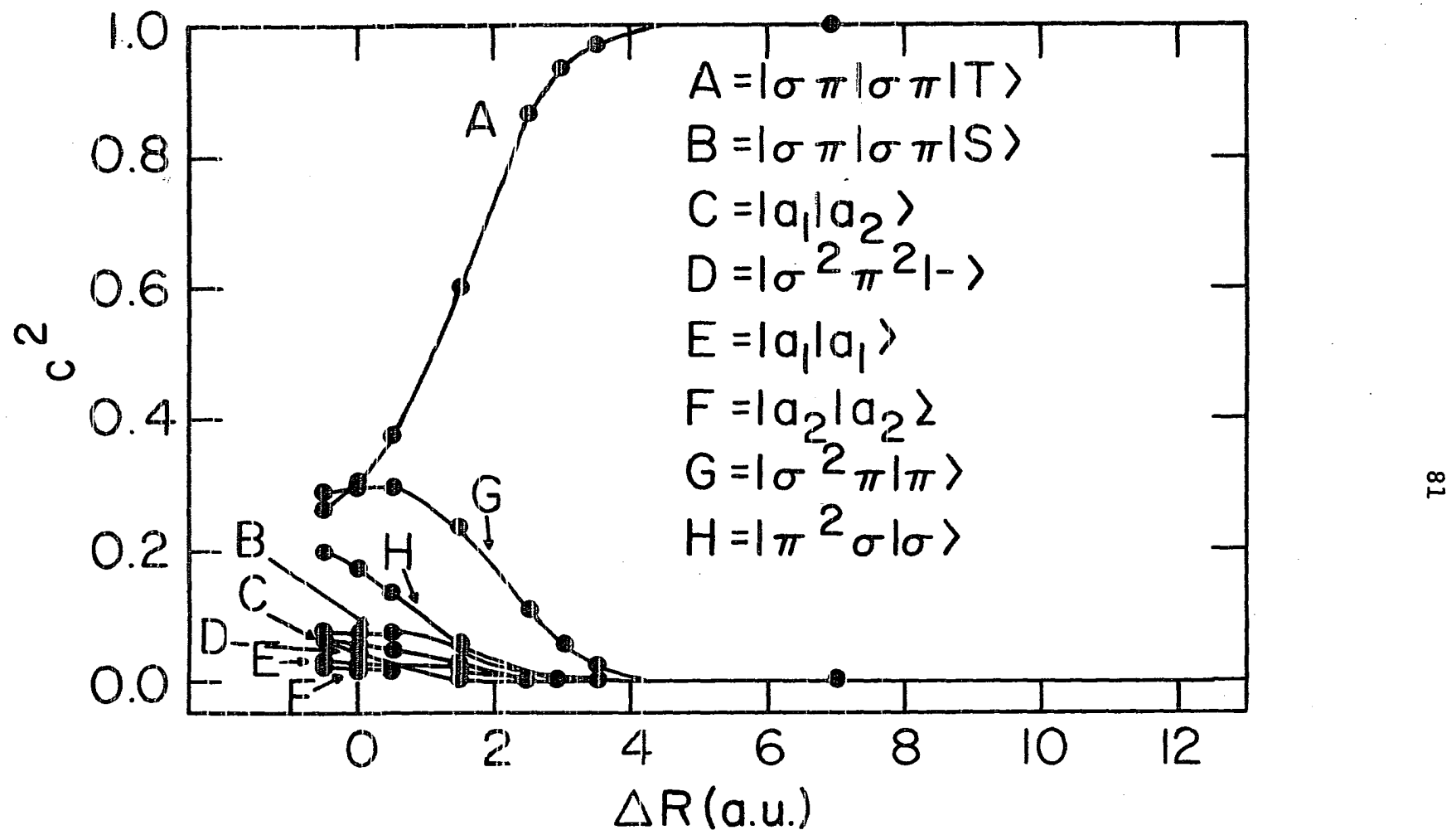


Figure 4. Ethylene ground state: occupations of localized configurations,  
 $\Delta R = R_{CC} - R_e$ ,  $R_e = 2.517$  a.u.

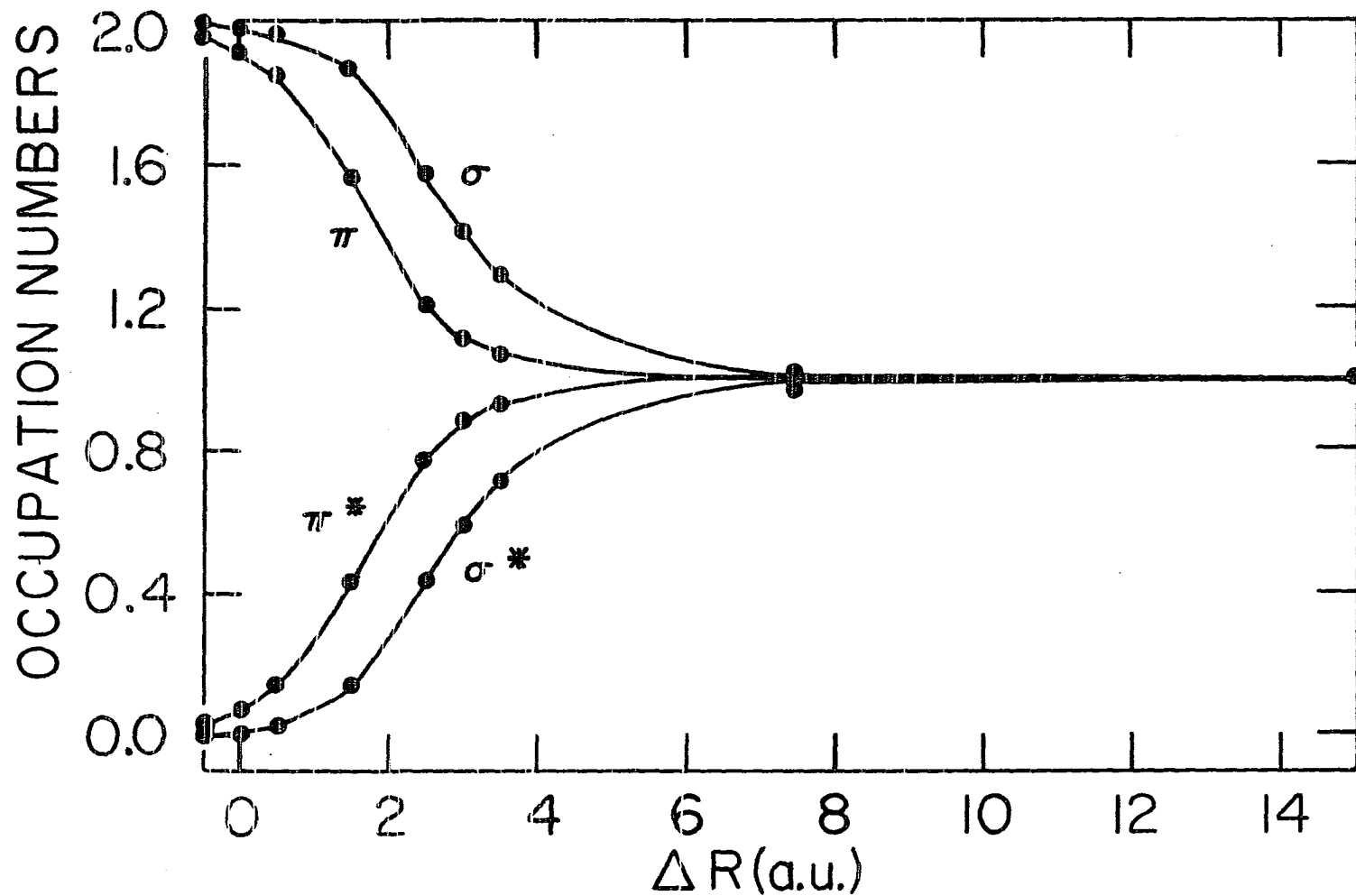


Figure 5. Ethylene ground state: orbital occupation numbers,  $\Delta R = R_{CC} - R_e$ ,  $R_e = 2.517$  a.u.

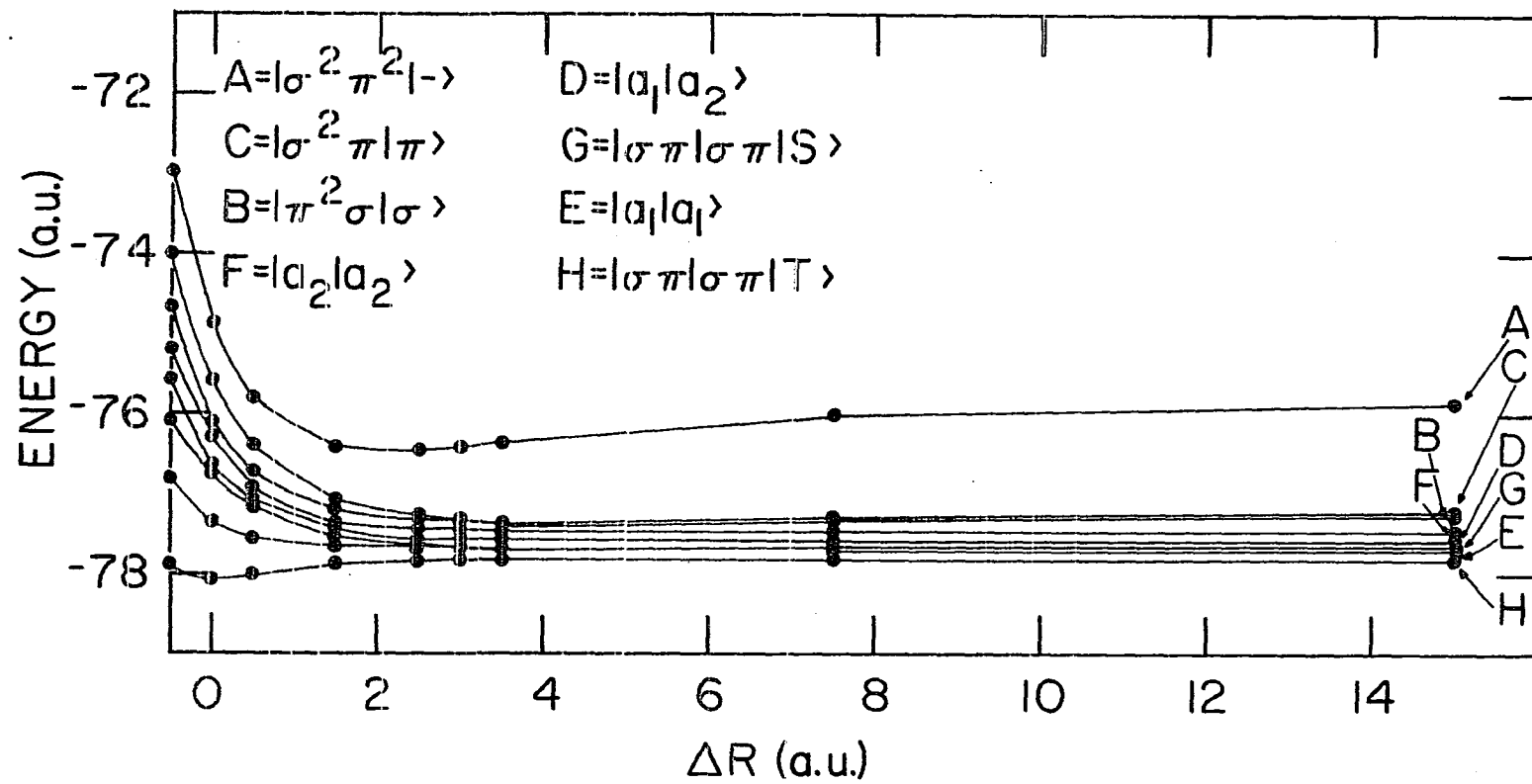


Figure 6. Dissociation of ground and excited  ${}^1\text{Ag}$  states of ethylene,  $\Delta R = R_{\text{CC}} - R_e$ ,  $R_e = 2.517$  a.u.

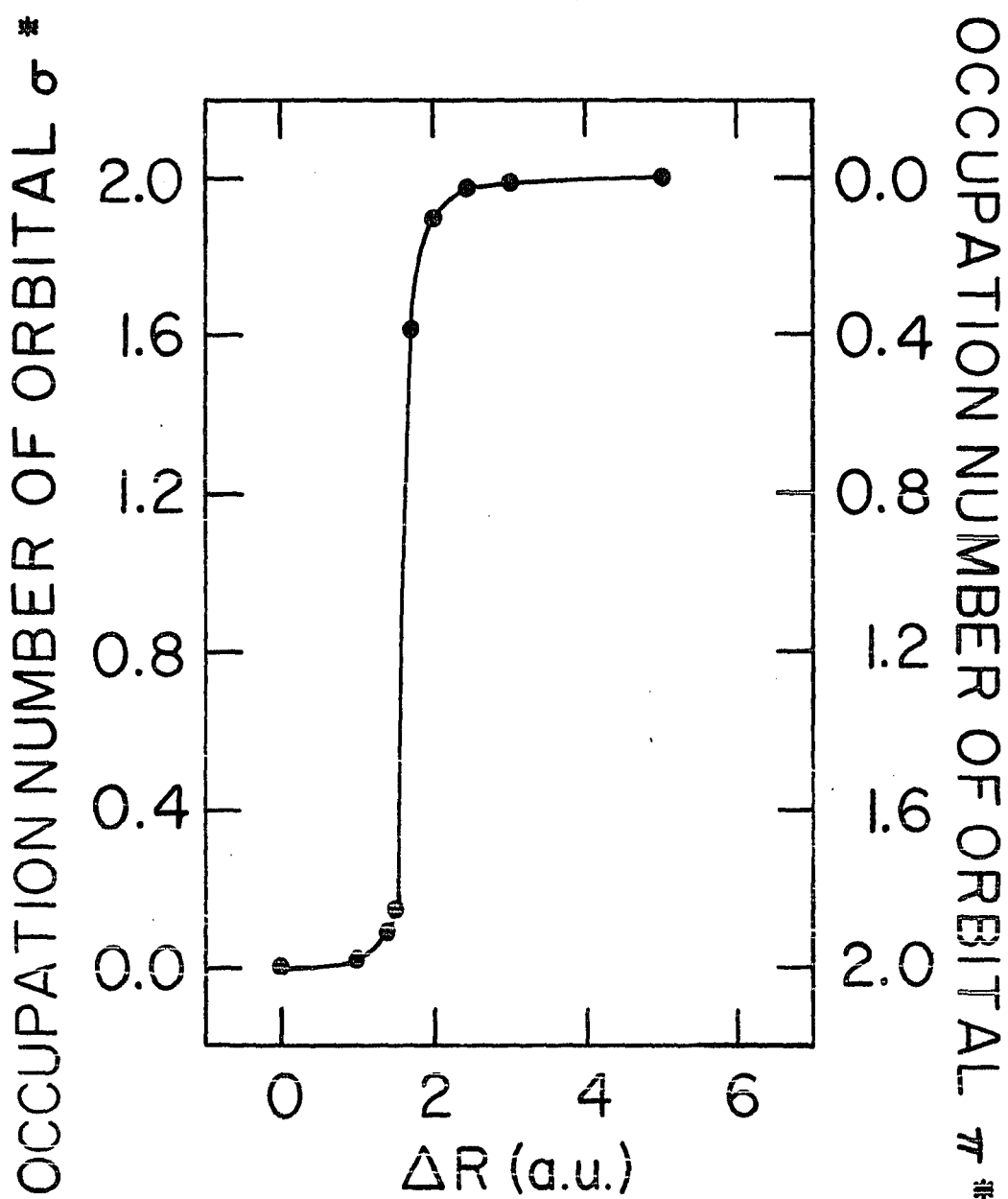


Figure 7. Orbital occupation numbers for 1-geminal SPIP calculations of the dissociation of ethylene  $\pi^*{}^2$  excited state,  $\Delta R = R_{CC} - R_e$ ,  $R_e = 2.517$  a.u.

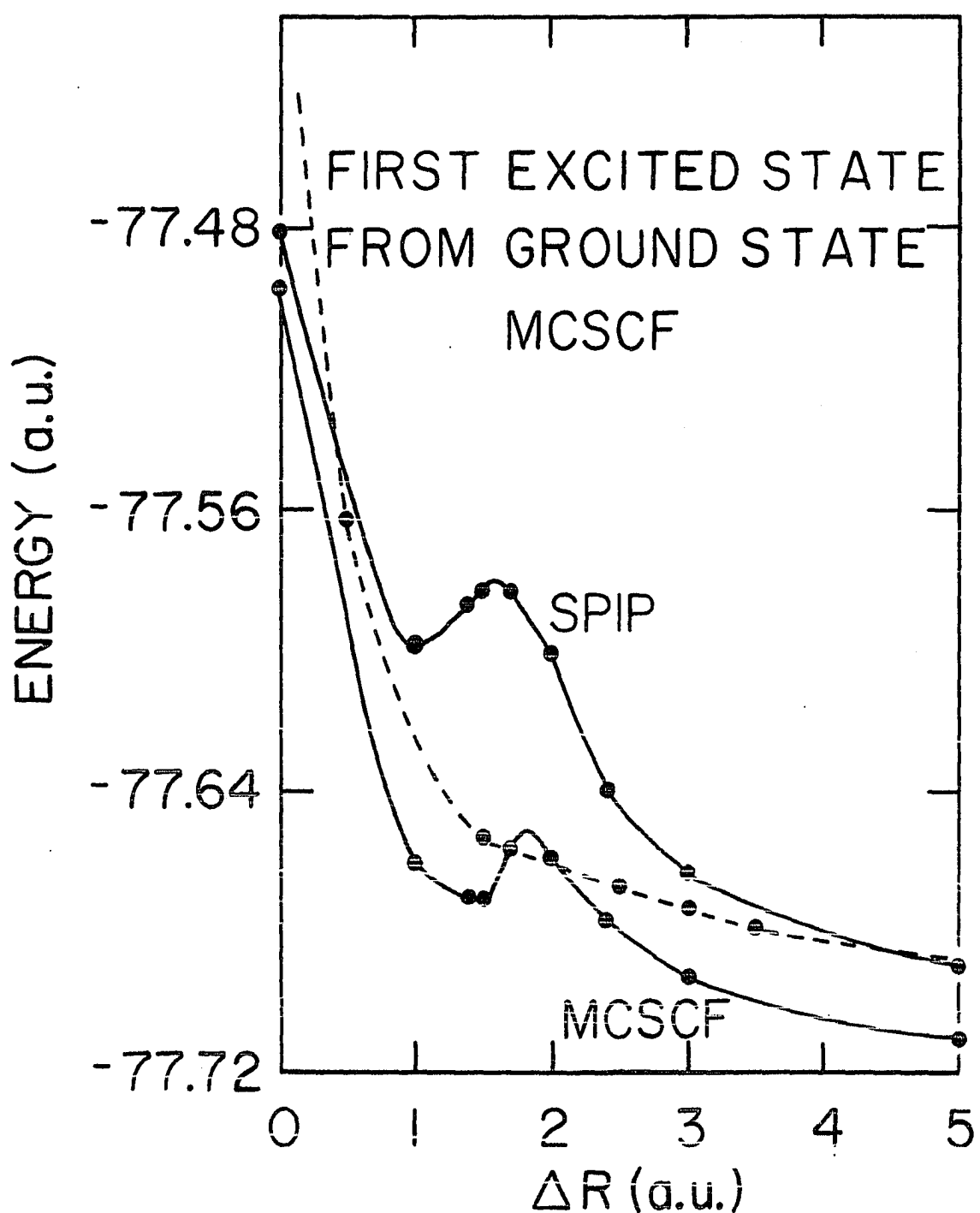


Figure 8. Dissociation of ethylene  $\pi^*{}^2$  excited state,  
 $\Delta R = R_{CC} - R_e$ ,  $R_e = 2.517$  a.u.

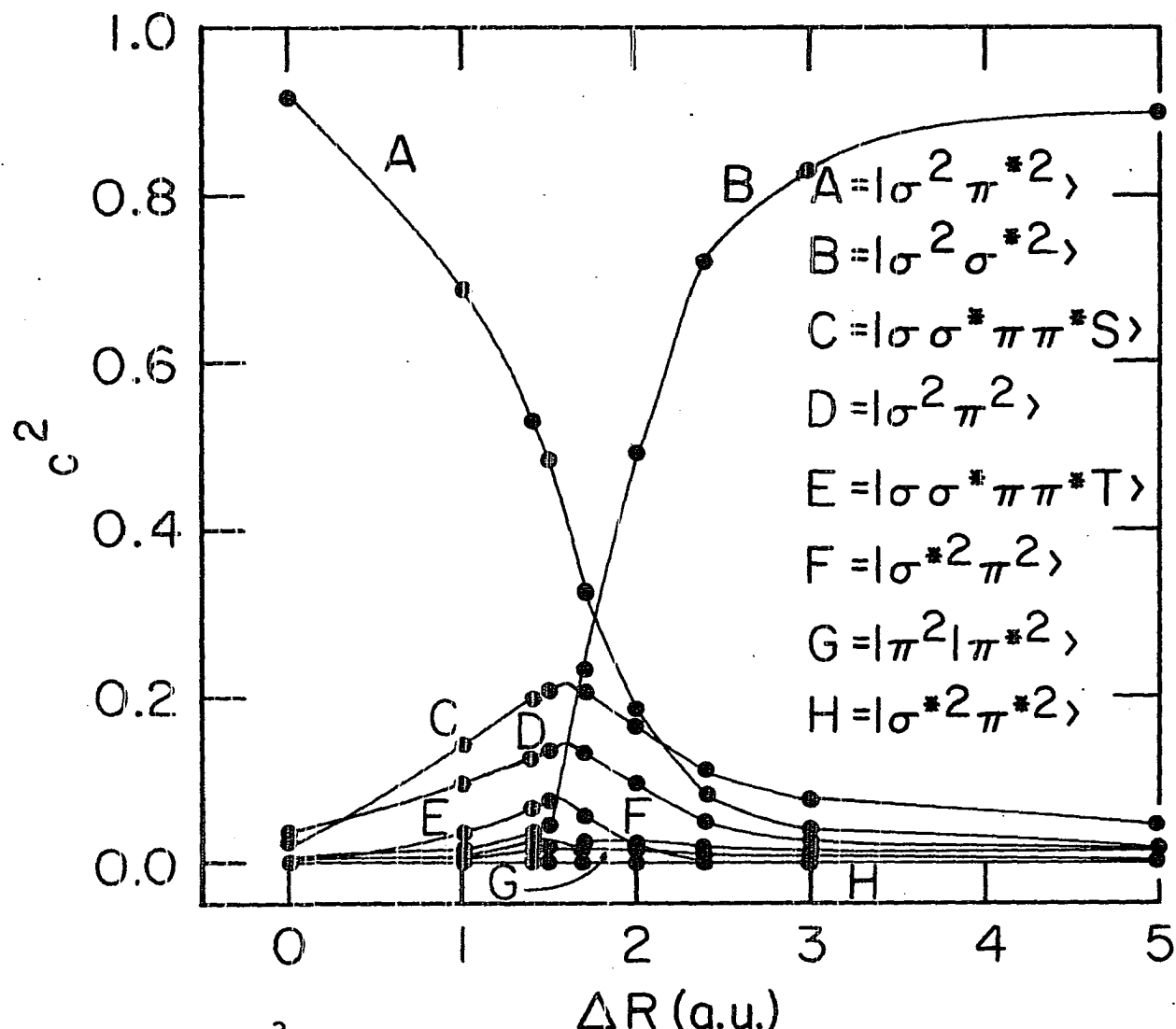


Figure 9. Ethylene  $\pi^*{}^2$  excited state: occupations of delocalized configurations,  
 $\Delta R = R_{CC} - R_e$ ,  $R_e = 2.517$  a.u.

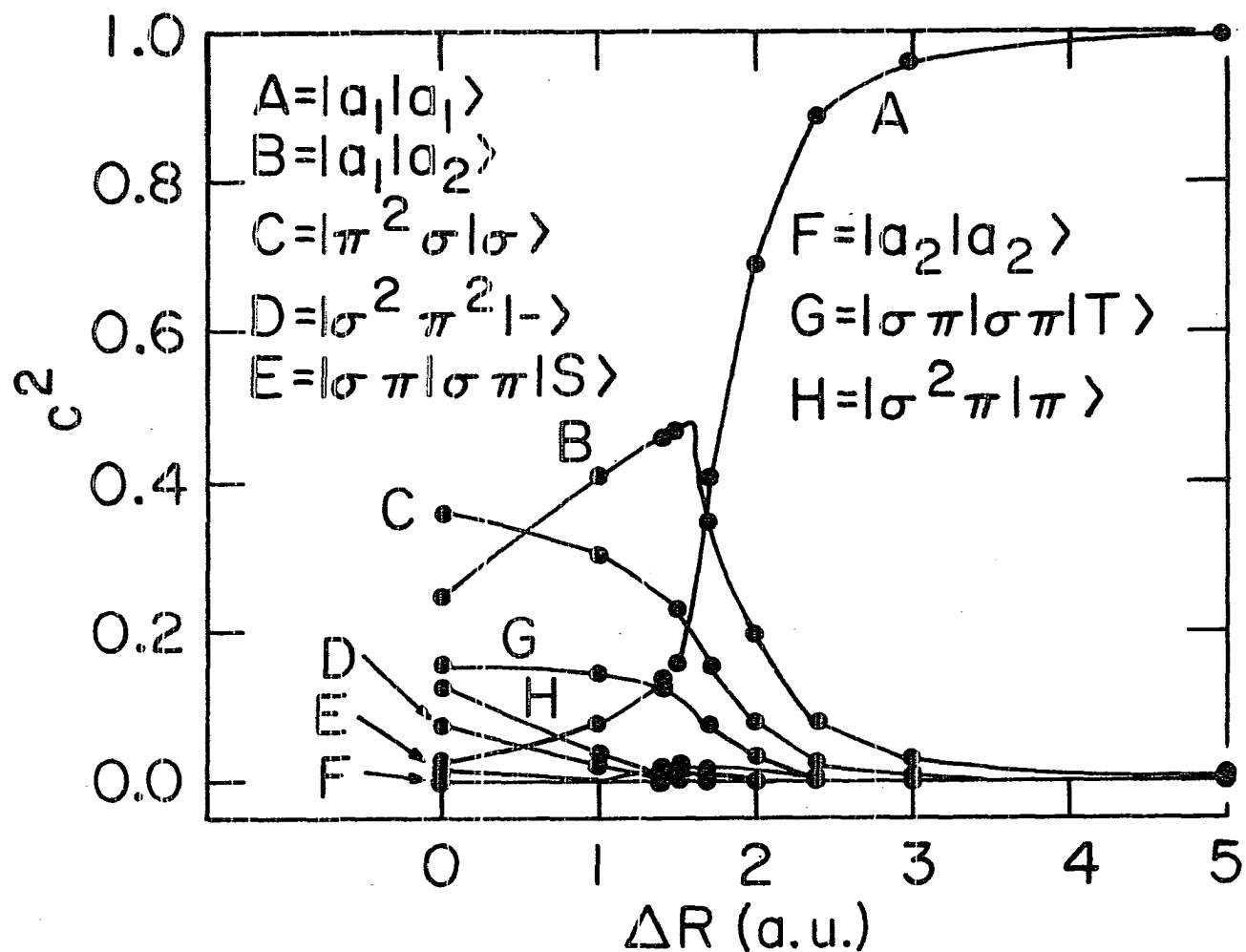


Figure 10. Ethylene  $\pi^*|^2$  excited state: occupations of localized configurations,  
 $\Delta R = R_{CC} - R_e$ ,  $R_e = 2.517$  a.u.

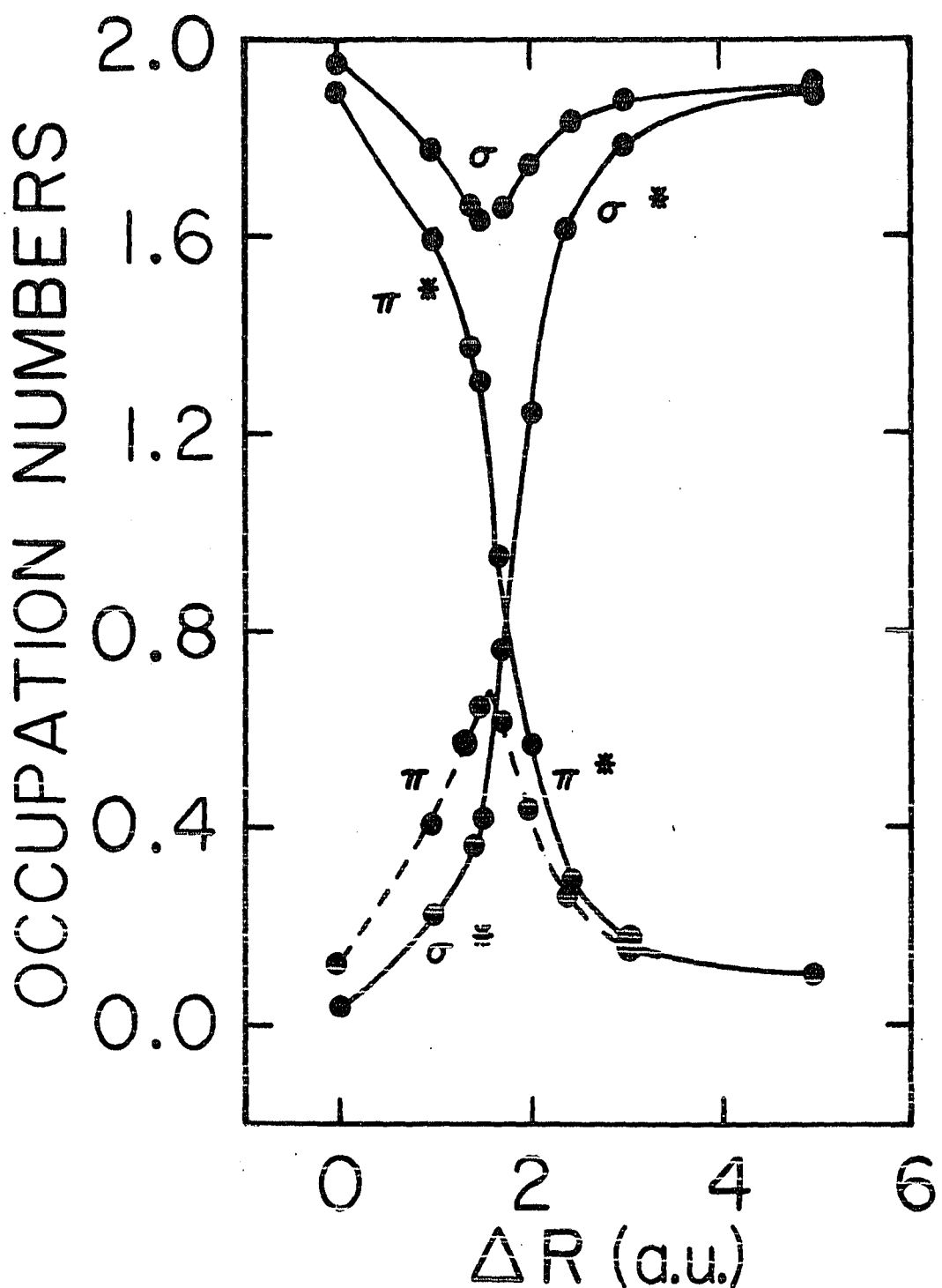


Figure 11. Ethylene  $\pi^*^2$  excited state: orbital occupation numbers,  $\Delta R = R_{CC} - R_e$ ,  $R_e = 2.517$  a.u.

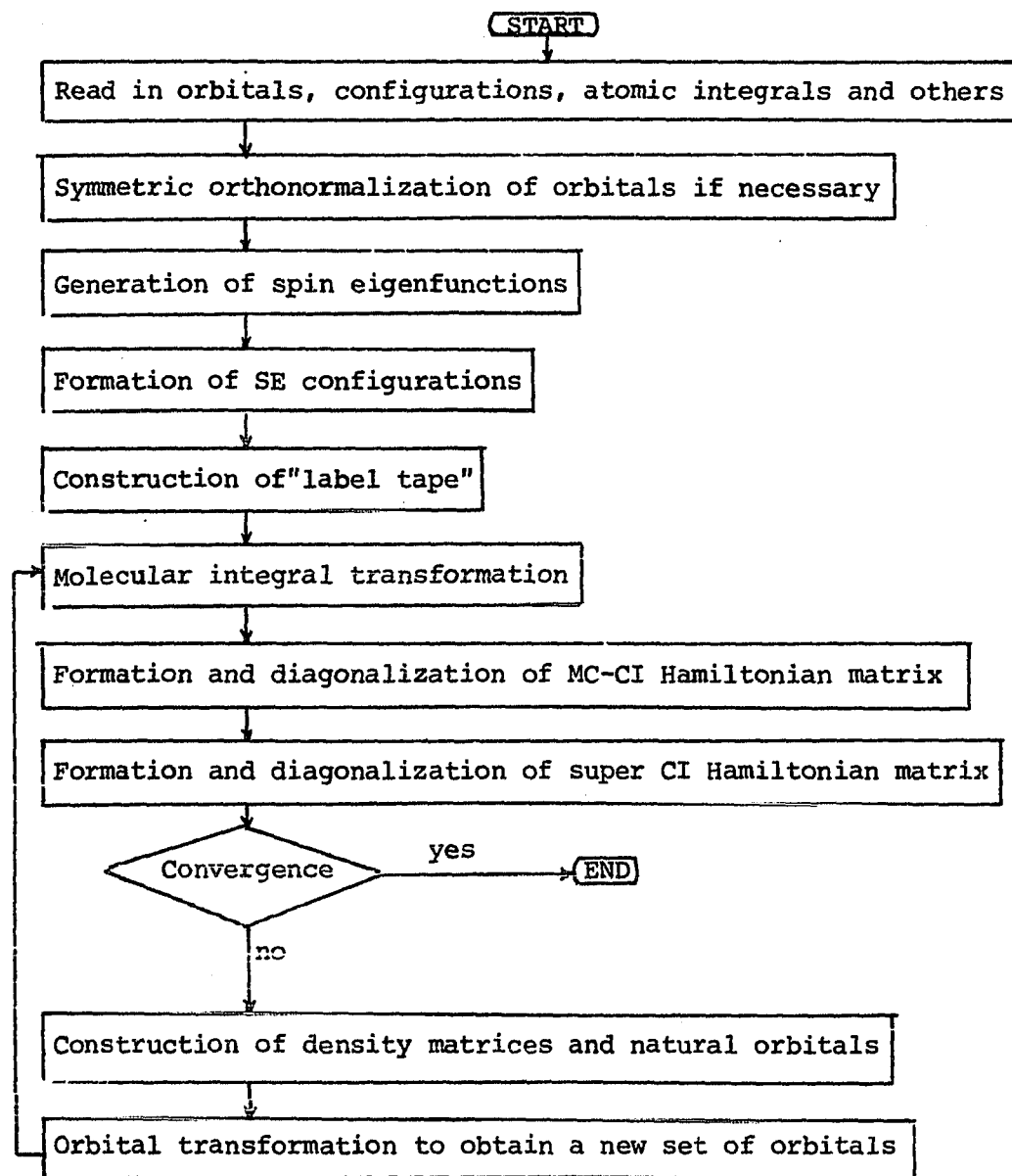


Figure 12. Organization of MCSCF program

## IV. LITERATURE CITED

1. E. Schrödinger, Ann. Physik. 79, 361, 489, 734; 81, 109 (1926); Phys. Rev. 28, 1049 (1926).
2. D. R. Hartree, Proc. Cambridge Phil. Soc. 24, 89 (1928).
3. J. C. Slater, Phys. Rev. 34, 1293 (1929).
4. W. Pauli, Z. Physik. 31, 765 (1925).
5. V. Fock, Z. Physik. 61, 126 (1930); and J. C. Slater, Phys. Rev. 34, 210 (1930).
6. R. S. Mulliken, Phys. Rev. 32, 186, 388, 761 (1928).
7. C. C. J. Roothaan, Rev. Mod. Phys. 23, 69 (1951).
8. M. Yoshimine and A. D. McLean, Int. J. Quantum Chem. 1S, 313 (1967).
9. A. C. Wahl, J. Chem. Phys. 41, 2600 (1964).
10. E. A. Hylleraas, Z. Physik. 48, 469 (1928).
11. P. O. Löwdin, Phys. Rev. 97, 1474 (1955).
12. Z. Gershgorn and I. Shavitt, Int. J. Quantum Chem. 2, 751 (1968).
13. S. Green, J. Chem. Phys. 54, 827 (1971).
14. C. F. Bender and E. R. Davidson, Phys. Rev. 183, 23 (1969).
15. C. Edmiston and M. Krauss, J. Chem. Phys. 45, 1833 (1966).
16. D. R. Hartree, W. Hartree, and B. Swirles, Phil. Trans. Roy. Soc. (London) A238, 229 (1939).
17. K. Hirao and H. Nakatsuji, J. Chem. Phys. 59, 1457 (1973).

18. G. Das and A. C. Wahl, J. Chem. Phys. 44, 87 (1966).
19. J. Hinze and C. C. J. Roothaan, Prog. Theor. Phys. Suppl. 40, 37 (1967).
20. M. L. Benston and D. P. Chong, Mol. Phys. 14, 449 (1968).
21. A. Veillard and E. Clementi, Theoret. Chim. Acta 7, 133 (1967).
22. T. L. Gilbert, Phys. Rev. A6, 580 (1972).
23. J. Hinze, T. Chem. Phys. 59, 6424 (1973).
24. K. K. Docken and J. Hinze, J. Chem. Phys. 57, 4928 (1972).
25. N. G. Mukherjee and R. McWeeny, Int. J. Quantum Chem. 4, 97 (1970).
26. See for example: A. C. Wahl, P. J. Bertoncini, G. Das, and T. L. Gilbert, Int. J. Quantum Chem. 1S, 123 (1967), P. Sutton, P. Bertoncini, G. Das, T. L. Gilbert, and A. C. Wahl, Int. J. Quantum Chem. 35, 479 (1970), P. J. Bertoncini, G. Das, and A. C. Wahl, J. Chem. Phys. 52, 5112 (1970).
27. A. Karo, M. Krauss, and A. C. Wahl, Int. J. Quantum Chem. 7S, 143 (1973).
28. B. Levy and G. Berthier, Int. J. Quantum Chem. 2, 307 (1968).
29. R. Lefebvre and C. M. Moser, J. de Chimie Physique 53, 393 (1956).
30. R. Lefebvre, J. de Chimie Physique 54, 168 (1957); Cahiers de Physique 13, 1 (1959).
31. F. Grein and T. C. Chang, Chem. Phys. Lett. 12, 44 (1971).
32. W. H. Adams, Phys. Rev. 183, 37 (1969).
33. W. J. Hunt, P. J. Hay and W. A. Goddard, J. Chem. Phys. 57, 738 (1972).

34. C. F. Bender and E. R. Davidson, J. Phys. Chem. 70, 2675 (1966).
35. See for example: H. F. Schaefer III, J. Chem. Phys. 54, 2207; 55, 176 (1971).
36. W. I. Salmon and K. Ruedenberg, J. Chem. Phys. 57, 2776 (1972).
37. W. I. Salmon, K. Ruedenberg, and L. M. Cheung, J. Chem. Phys. 57, 2787 (1972).
38. J. K. L. MacDonald, Phys. Rev. 43, 830 (1933).
39. A. J. Coleman, Rev. Mod. Phys., 35, 668 (1963).
40. K. Ruedenberg and R. D. Poshusta, Adv. Quantum Chem. 6, 267 (1972).
41. I. Shavitt, J. Comp. Phys. 6, 124 (1970).
42. D. R. Hartree, Proc. Camb. Phil. Soc. 45, 230 (1948).
43. C. C. J. Roothaan and P. S. Bagus, Methods in Computational Physics 2, 47 (1963).
44. R. B. Woodward and R. Hoffmann, The Conservation of Orbital Symmetry, (Academic, New York, 1970).
45. R. Hoffmann, R. Gleiter, and F. B. Mallory, J. Am. Chem. Soc. 92, 1460 (1970).
46. H. M. Frey, Progr. Reaction Kinetics 2, 131 (1964).
47. H. Basch, J. Chem. Phys. 55, 1700 (1971).
48. K. R. Sundberg and K. Ruedenberg, (to be published).
49. K. Ruedenberg, R. C. Raffenetti, and R. D. Bardo, "Energy Structure and Reactivity", Proceedings of the 1972 Boulder Conference on Theoretical Chemistry (Wiley 1973), p. 164.
50. D. F. Feller, (unpublished).
51. L. S. Bartell and R. A. Bonham, J. Chem. Phys. 31, 400 (1959).

52. J. M. Foster and S. F. Boys, Rev. Mod. Phys. 32, 305 (1960).
53. J. F. Harrison and L. C. Allen, J. Am. Chem. Soc. 91, 807 (1969).
54. C. F. Bender and H. F. Schaefer, J. Am. Chem. Soc. 92, 4984 (1970).
55. S. V. O'Neil, H. F. Schaefer, and C. F. Bender, J. Chem. Phys. 55, 162 (1971).
56. J. A. Kerr, Chem. Rev. 66, 465 (1966).
57. R. C. Raffenetti, (unpublished).
58. G. H. F. Diercksen, Theor. Chim. Acta 33, 1 (1974).
59. R. D. Bardo and K. Ruedenberg, J. Chem. Phys. 60, 918 (1974).

**V. ACKNOWLEDGMENTS**

The author is indebted to Professor Klaus Ruedenberg for his suggestion and guidance of this work. He wishes to thank Mr. Kenneth R. Sundberg for helpful discussions and for his SPIP computer program. Special thanks also go to Dr. Richard C. Raffenetti for his molecular SCF computer program.

VI. APPENDIX A: DESCRIPTION OF THE  
MCSCF PROGRAM

Figure 12 presents a flow diagram of the organization of the program outlined in Section II,F. Some essential detailed features are discussed briefly in the following:

- (a) Generation of the spin eigenfunctions: The procedure is based on the SAAP method of Salmon and Ruedenberg [37]. One important point is that for a  $N$ -electron system, if there are  $M$  doubles in the space orbital product, the spin eigenfunction is a product of  $M$  antisymmetric geminal functions in positions where the associated space functions are doubles and a spin eigenfunction of a  $(N-2M)$ -electron system.
- (b) Formation of the SE functions: The super CI wavefunction is defined in Equation (2.20). It is a linear combination of the MC wavefunction and all the appropriate SE functions. It is obvious that the SE functions depend on the expansion coefficients of the MC wavefunction which have to be determined at each iteration. However, the SAAP's which span the SE functions are fixed throughout the iterative process and so they can be generated in the early stage of the program; and all the information con-

cerning them, such as the corresponding coefficient indices, can be stored for later use.

- (c) Construction of the "label tape": The MC wavefunction as well as the super CI wavefunction are linear combinations of SAAP's. Once all the information concerning about the SAAP's are known, the Hamiltonian matrix elements between them can be evaluated if the molecular integrals are available. The molecular integrals are different from iteration to iteration, but the coefficients of one- and two-electron integrals which appear in the energy formulae [36] remain the same throughout the iterative process. Therefore the coefficients can be calculated first and stored on the "label tape" for later use.
- (d) Transformation of the two-electron repulsion integrals: This is the most time-consuming step in the program. Atomic integrals are obtained from the BIGGMOLI package developed by Raffenetti [57]. The transformation is a modified version of the algorithm presented by Diercksen [58]. It is of the order of  $N^5$  in multiplications and additions ( $N$  is the number of basis orbitals). Integral indices need not be stored throughout the transformation process. The final integral list is in

canonical order. Symmetry is utilized in iterations beyond the first one. In second or higher iterations, the current molecular orbitals are expanded in terms of the molecular orbitals in the previous iteration. Since these orbitals are symmetry-adapted, the orbital transformation matrix is in block diagonal form. Consequently the number of multiplications and additions in the transformation from the "old" molecular integrals to the current molecular integrals is much reduced. Such simplification is not applicable to the first iteration since the transformation is from atomic integrals to molecular integrals.

- (e) Formation of the Hamiltonian matrix: Once the molecular integrals are calculated, they are combined with the coefficients in the label tape to form the Hamiltonian matrix in terms of the SAAP's. The expansion coefficients of the MC wavefunction are then determined by diagonalization of one block of the matrix which contains all the matrix elements between the SAAP's in the MC wavefunction. The diagonalization is carried out using the Jacobi method. After the coefficients are determined, the SE functions are also determined. They are then Schmidt orthonormalized. The Hamiltonian matrix is

then transformed to the basis of the SE functions instead of the SAAP's. The resulting matrix is usually much smaller. Solution to obtain the super CI coefficients and energy is carried out using the modified Nesbet method [41].

- (f) Construction of the density matrix: Explicit formulae for the matrix elements are given in reference [40]. The coefficients of the one-electron integrals, which are stored in the label tape, are used to evaluate the matrix elements. The density matrix is in block diagonal form due to symmetry. Diagonalization is carried out by the Jacobi method.

## VII. APPENDIX B: CONTRACTED ATOMIC ORBITALS

In molecular calculations, it is too time-consuming to use primitive gaussians as independent basis functions. However a smaller number of contracted atomic orbitals (i.e., fixed superpositions of primitives) can be used as the actual basis set with insignificant loss of quality in the resulting wavefunction. To determine good contracted atomic orbitals we follow a recent approach by Bardo and Ruedenberg [59] which gives molecule-optimized contracted even-tempered gaussian atomic orbital (MOCETGAO) bases. A brief discussion is presented here.

For a given molecule, an uncontracted SCF calculation is made. Using the expansion coefficients  $\{C_v\}$  of the occupied molecular orbitals in terms of the primitive gaussians, the spherically-projected, local density matrix is formed.

$$\rho(A) = \sum_l \left\{ \sum_{ab} P(Aal|Ab_l) \left[ \sum_m g(Alm) g(Alm)^\dagger \right] \right\} \quad (B.1)$$

where A denotes the atom, a and b sum over the primitives  $\{g\}$ , l and m are the angular quantum numbers, and

$$P(Aal|Ab_l) = (2l+1)^{-1} \sum_m \left[ 2 \sum_v C_v(Aalm) C_v^\dagger(\bar{A}blm) \right] \quad (B.2)$$

The matrix is then diagonalized separately for each value of l, whence

$$P(A_{al}|A_{bl}) = \sum_k \lambda_k(l) T_{ak}(Al) T_{bk}(Bl) \quad (B.3)$$

where  $\{\lambda_k\}$  are the eigenvalues and  $\{T_{ak}\}$  is the transformation matrix. Substituting back into Equation (B.1) gives

$$\rho(A) = \sum_l \sum_k \lambda_k(l) [\sum_m \phi_k(Alm) \phi_k(Alm)] \quad (B.4)$$

with the contracted atomic orbitals

$$\phi_k(Alm) = \sum_a g(Aalm) T_{ak}(l) \quad (B.5)$$

However these orbitals are not orthogonal. Orthogonalization by standard methods will distort the contracted orbital space slightly. Therefore we modified this method to give orthogonal contracted atomic orbitals directly from the local densities.

Consider the eigenvalue problem for one symmetry

$$\hat{\rho}(A) \bar{\phi}_k(Alm) = \lambda_k^*(l) \bar{\phi}_k(Alm) \quad (B.6)$$

where  $\{\bar{\phi}_k\}$  are the desired orthogonal contracted atomic orbitals and the operator  $\hat{\rho}(A)$  is defined by

$$\hat{\rho}(A)f = \sum_l \sum_{ab} P(A_{al}|A_{bl}) \sum_m g(A_{alm}) \langle g(A_{blm}) | f \rangle \quad (B.7)$$

If we expand

$$\bar{\phi}_k(Alm) = \sum_{b'} g(A_{b'lm}) U_{b'k}(Al) \quad (B.8)$$

then

$$\hat{\rho}(A) \sum_{b'} g(Ab'lm) U_{b'k} (Al) = \lambda_k^i (1) \sum_{b'} g(Ab'lm) U_{b'k} (Al) \quad (B.9)$$

Taking the inner product with  $g(Aa'lm)$  gives

$$\begin{aligned} \sum_{b'} & \langle g(Aa'lm) \rho(A) g(Ab'lm) \rangle U_{b'k} (Al) \\ &= \lambda_k^i (1) \sum_{b'} \langle g(Aa'lm) | g(Ab'lm) \rangle U_{b'k} (Al) \end{aligned} \quad (B.10)$$

Deleting the sums over  $l$  and  $m$  in Equation (B.1) and substitute into Equation (B.10) gives

$$\begin{aligned} \sum_{b'} \sum_{ab} & S_{a'a} (Al) \cdot P(Aal|Ab'l) S_{bb'} (Al) U_{b'k} (Al) \\ &= \lambda_k^i (1) \sum_{b'} S_{a'b'} (Al) U_{b'k} (Al) \end{aligned} \quad (B.11)$$

where

$$S_{ab} (Al) = \langle g(Aalm) | g(Ab'l'm) \rangle \quad (B.12)$$

In matrix notation

$$\begin{matrix} S & P & S & U \end{matrix} = \begin{matrix} S & U & \lambda \end{matrix} \quad (B.13)$$

Therefore

$$\begin{pmatrix} \frac{1}{2} & \frac{1}{2} & \frac{1}{2} \\ \frac{1}{2} & \frac{1}{2} & \frac{1}{2} \\ \frac{1}{2} & \frac{1}{2} & \frac{1}{2} \end{pmatrix} \begin{pmatrix} S & U & \lambda \end{pmatrix} = \begin{pmatrix} \frac{1}{2} \\ \frac{1}{2} \\ \frac{1}{2} \end{pmatrix} \begin{pmatrix} S & U & \lambda \end{pmatrix} \quad (B.14)$$

$$\begin{pmatrix} \frac{1}{2} & \frac{1}{2} \\ \frac{1}{2} & \frac{1}{2} \\ \frac{1}{2} & \frac{1}{2} \end{pmatrix} R = R \begin{pmatrix} \frac{1}{2} \\ \frac{1}{2} \\ \frac{1}{2} \end{pmatrix} \quad (B.15)$$

where

$$\rho = \frac{1}{S^2} u$$

The matrix  $\rho$  can be obtained by diagonalizing the matrix  $(\frac{1}{S^2} \rho \frac{1}{S^2})$ , and the expansion coefficients of the contracted atomic orbitals are then given by

$$u = S^{-\frac{1}{2}} \rho \quad (B.16)$$

or

$$u_{a'k}(Al) = \sum_{b'} S^{-\frac{1}{2}}(Al) D_{b'k}(Al) \quad (B.17)$$

If the eigenvalues  $\{\lambda_k\}$  are ordered according to decreasing magnitude, the contributions of the corresponding atomic orbitals to the density matrix and, hence, to the molecular wavefunction decrease in importance. It is generally found that retention of the contracted functions  $\phi_k(Alm)$  corresponding to the largest three eigenvalues reproduces the molecular energy to an accuracy of  $5 \times 10^{-3}$

a.u.

VIII. APPENDIX C: EXPANSIONS OF MOLECULAR ORBITALS  
 IN TERMS OF ATOMIC ORBITALS FOR THE  
 LOWEST TWO  $^1A_g$  STATES OF ETHYLENE

The tables on the following pages give the expansion coefficients for the optimal molecular orbitals in terms of the contracted atomic orbitals of Table 2. The molecular orbitals (MO's) are those from which the configurations in Equation (3.20) are formed. These MO's are defined in Equations (3.16) to (3.19) and are the following ones:

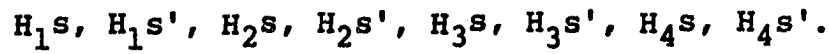
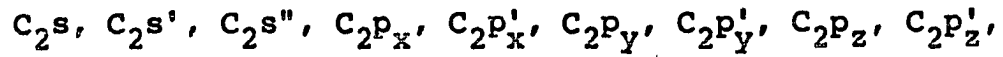
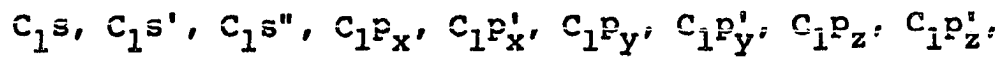
$$1a_g = i, \quad 2a_g = b_+, \quad 3a_g = \sigma,$$

$$1b_{1u} = i^*, \quad 2b_{1u} = b_+^*, \quad 3b_{1u} = \sigma^*,$$

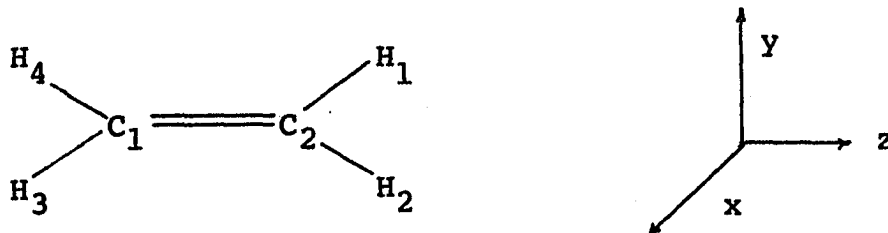
$$1b_{2u} = b_-, \quad 1b_{3u} = \pi,$$

$$1b_{3g} = b_-^*, \quad 1b_{2g} = \pi^*,$$

Each table contains 26 columns of 26 rows. Each column furnishes the expansion coefficients of one MO in terms of the 26 AO's. The sequence of rows corresponds to the following order of the AO's:



where the atoms are labelled as follows:



The sequence of columns corresponds to the following MO's:

$1a_g, 2a_g, \dots, 7a_g, 1b_{1u}, 2b_{1u}, \dots, 7b_{1u}$ ,

$1b_{3g}, 2b_{3g}, 3b_{3g}, 4b_{3g}, 1b_{2u}, 2b_{2u}, 3b_{2u}, 4b_{2u}$ ,

$1b_{3u}, 2b_{3u}, 1b_{2g}, 2b_{2g}$ .

Consequently the MO's that are occupied in the MC wavefunction are those in columns 1, 2, 3, 8, 9, 10, 15, 19, 23, and 25.

The first ten tables correspond to the  $^1A_g$  ground state at 10 different values of  $R_{CC}$ . The subsequent 9 tables correspond to the first excited  $^1A_g$  state at 9 different values of  $R_{CC}$ .  $R_{CC}$  is defined as

$$R_{CC} = (\Delta R + 2.517) \text{a.u.}$$

where  $\Delta R$  is given in each table heading.

Table 8. MO expansions for ground state at  $\Delta R = -0.5$  a.u.

**Table 8** (continued)

**Table 8** (continued)

Table 9. MO expansions for  $A_g$  ground state at  $AR = 0.0$  a.u.

**Table 9 (Continued)**

-1.1215638	1.1297654	-0.9791958	1.8693587	0.0	0.0	0.0	0.0	0.0	0.0	0.0
2.4010051	-2.2694225	2.0971790	-3.8452447	0.0	0.0	0.0	0.0	0.0	0.0	0.0
-1.3514374	1.6424697	-1.8794973	3.2498533	0.0	0.0	0.0	0.0	0.0	0.0	0.0
0.0	0.0	0.0	0.0	0.0	0.0	0.0	0.0	0.0	0.0	0.0
0.0	0.0	0.0	0.0	0.0	0.0	0.0	0.0	0.0	0.0	0.0
0.0	0.0	0.0	0.0	0.0	0.0	0.0	0.0	0.0	0.0	0.0
0.0	0.0	0.0	0.0	0.0	0.0	0.0	0.0	0.0	0.0	0.0
-0.2533638	1.5927264	-1.3784245	-0.0650321	0.0	0.0	0.0	0.0	0.0	0.0	0.0
0.0356210	-1.4173626	1.1683328	-0.0051968	0.0	0.0	0.0	0.0	0.0	0.0	0.0
1.1215638	-1.1297654	0.9791958	-1.8693587	0.0	0.0	0.0	0.0	0.0	0.0	0.0
-2.4010051	2.2694225	-2.0971790	3.8452447	0.0	0.0	0.0	0.0	0.0	0.0	0.0
1.3514374	-1.6424697	1.8794973	-3.2498533	0.0	0.0	0.0	0.0	0.0	0.0	0.0
0.0	0.0	0.0	0.0	0.0	0.0	0.0	0.0	0.0	0.0	0.0
0.0	0.0	0.0	0.0	0.0	0.0	0.0	0.0	0.0	0.0	0.0
0.0	0.0	0.0	0.0	0.0	0.0	0.0	0.0	0.0	0.0	0.0
-0.2533638	1.5927264	-1.3784245	-0.0650321	0.0	0.0	0.0	0.0	0.0	0.0	0.0
0.0356210	-1.4173626	1.1683328	-0.0051968	0.0	0.0	0.0	0.0	0.0	0.0	0.0
-0.3903420	-0.7443633	0.5411316	0.7409868	-0.3080370	-0.0533677	1.8198560	-1.4158542	0.2384551	0.2292936	
-0.0033250	0.0267959	-0.5905801	-0.8224168	0.0099222	0.2375159	-0.8124812	1.1041983	-0.0003445	0.1505319	
-0.3903420	-0.7443633	0.5411316	0.7409868	0.3080273	0.0533677	-1.2398560	1.4158542	-0.2384651	-0.2292966	
-0.0033250	0.0267959	-0.5905801	-0.8224168	-0.0099222	-0.2375159	0.8124812	-1.1041983	0.0003445	-0.1505319	
0.3903420	0.7443633	-0.5411316	-0.7409868	-0.3080270	-0.0533677	1.8198560	-1.4158542	-0.2384651	-0.2292966	
0.0033250	-0.0267959	0.5905801	0.8224168	0.0099222	0.2375159	-0.8124812	1.1041983	0.0003445	-0.1505319	
0.3903420	0.7443633	-0.5411316	-0.7409868	0.3080273	0.0533677	-1.2398560	1.4158542	0.2384651	0.2292966	
0.0033250	-0.0267959	0.5905801	0.8224168	-0.0099222	-0.2375159	0.8124812	-1.1041983	-0.0003445	0.1505319	

**Table 9 (Continued)**

Table 10. MO expansions for  ${}^1A_g$  ground state at  $\Delta R = 0.05$  a.u.

0.08666662	-0.1226119	-0.0838454	0.1927734	0.5288693	0.1929447	0.6476793	0.6871114	-0.1152626	7.4308331
0.0728407	0.4061626	0.3384567	-0.4910396	-1.0028437	-0.4296694	-1.7224261	0.7727624	0.3657277	-1.9864186
0.0561266	-0.0388576	-0.0208536	0.0161644	0.1117151	0.5167217	1.3221638	0.667838	0.0136991	0.1421437
0.c	0.c	0.c	0.c	0.c	0.c	0.c	0.c	0.c	0.c
0.0	0.0	0.0	0.0	0.0	0.0	0.0	0.0	0.0	0.0
0.0	0.0	0.0	0.0	0.0	0.0	0.0	0.0	0.0	0.0
0.0	0.0	0.0	0.0	0.0	0.0	0.0	0.0	0.0	0.0
0.0561561	0.2251929	-0.6608239	-0.2913629	-0.6158287	-0.2287178	-0.3226088	0.0049834	0.2162342	0.5185981
0.0010582	0.0075319	0.0726425	-0.3984628	0.8087636	0.3137978	0.3046251	-0.002451	0.0069772	0.1367819
0.0866662	-0.1226118	-0.0838454	0.1927734	0.5288693	0.1929447	0.6476793	0.6871114	0.1152626	-0.4908331
0.0728407	0.4061626	0.3384567	-0.4910396	-1.0028437	-0.4296694	-1.7224261	0.7727624	0.3657277	-0.2864186
0.0058166	-0.0388576	-0.0208536	0.0161644	0.1117151	0.5167217	1.3221638	0.667838	-0.0136991	-0.1421437
0.c	0.c	0.c	0.c	0.c	0.c	0.c	0.c	0.c	0.c
0.0	0.0	0.0	0.0	0.0	0.0	0.0	0.0	0.0	0.0
0.0	0.0	0.0	0.0	0.0	0.0	0.0	0.0	0.0	0.0
-0.0058166	-0.2251929	-0.6608239	-0.2913629	-0.6158287	-0.2287178	-0.3226088	0.0049834	0.2162342	0.5185981
-0.0010582	-0.0075319	0.0726425	0.3984628	-0.8087636	0.3137978	0.3046251	-0.002451	0.0069772	0.1367819
-0.0058166	-0.2251929	0.1098862	-0.4694656	-0.4467522	-0.3806276	-0.6225768	0.0048774	0.2120239	0.0926315
0.0006472	-0.002061678	-0.0180266	-0.0210328	0.1901613	-0.1651069	0.6688966	-0.0002151	0.0031826	-0.0504833
-0.0058166	-0.2251929	0.1098862	-0.4694656	-0.4467522	-0.3806276	-0.6225768	0.0048774	0.2120239	0.0926315
0.0006472	-0.002061678	-0.0180266	-0.0210328	0.1901613	-0.1651069	0.6688966	-0.0002151	0.0031826	-0.0504833
-0.0058166	-0.2251929	0.1098862	-0.4694656	-0.4467522	-0.3806276	-0.6225768	0.0048774	0.2120239	0.0926315
0.0006472	-0.002061678	-0.0180266	-0.0210328	0.1901613	-0.1651069	0.6688966	-0.0002151	0.0031826	-0.0504833
-0.0058166	-0.2251929	0.1098862	-0.4694656	-0.4467522	-0.3806276	-0.6225768	0.0048774	0.2120239	0.0926315
0.0006472	-0.002061678	-0.0180266	-0.0210328	0.1901613	-0.1651069	0.6688966	-0.0002151	0.0031826	-0.0504833
-0.0058166	-0.2251929	0.1098862	-0.4694656	-0.4467522	-0.3806276	-0.6225768	0.0048774	0.2120239	0.0926315
0.0006472	-0.002061678	-0.0180266	-0.0210328	0.1901613	-0.1651069	0.6688966	-0.0002151	0.0031826	-0.0504833

三

**Table 10** (Continued)

**Table 10 (Continued)**

0.0	0.0	0.0	0.0	0.0	0.0
0.0	0.0	0.0	0.0	0.0	0.0
0.0	0.0	0.0	0.0	0.0	0.0
0.0	0.0	0.6100046	0.1667106	0.0367149	-0.4857484
0.0	0.0	-0.0396991	0.6116813	0.0203162	1.0299710
-0.6612735	0.7173540	0.0	0.0	0.0	0.0
0.7688206	-0.6750161	0.0	0.0	0.0	0.0
0.0	0.0	0.0	0.0	0.0	0.0
0.0	0.0	0.0	0.0	0.0	0.0
0.0	0.0	0.0	0.0	0.0	0.0
0.0	0.0	0.0	0.0	0.0	0.0
0.0	0.0	0.0	0.0	0.0	0.0
0.0	0.0	0.6100046	0.1667106	-0.0367149	0.4857484
0.0	0.0	-0.0396991	0.6116813	-0.0203162	-1.0299710
-0.6612735	0.7173540	0.0	0.0	0.0	0.0
0.7688206	-0.6750161	0.0	0.0	0.0	0.0
0.0	0.0	0.0	0.0	0.0	0.0
0.0	0.0	0.0	0.0	0.0	0.0
0.0	0.0	0.0	0.0	0.0	0.0
0.0	0.0	0.0	0.0	0.0	0.0
-0.3590201	0.9249773	0.0	0.0	0.0	0.0
-0.6728348	0.6572164	0.0	0.0	0.0	0.0
0.1990201	-0.9249773	0.0	0.0	0.0	0.0
-0.6728348	0.6572164	0.0	0.0	0.0	0.0
0.1990201	-0.9249773	0.0	0.0	0.0	0.0
0.6728348	-0.6572164	0.0	0.0	0.0	0.0
-0.1990201	0.9249773	0.0	0.0	0.0	0.0

Table 11. MO expansions for  ${}^1A_g$  ground state at  $\Delta R = 0.5$  a.u.

0.6858557	-0.1309871	-0.0884556	-0.1661522	0.4933450	0.1883007	0.9322114	0.8862594	-0.1278537	-0.3626733
0.0752210	0.4258911	0.3123003	0.4304433	-0.9781414	-0.4370811	-1.7033854	0.0745920	0.4191844	0.8578618
0.0055916	-0.0386897	-0.0203239	-0.0197190	0.0796241	0.5525793	1.3128482	0.0061841	-0.0003861	-0.1381950
0.0	0.0	0.0	0.0	0.0	0.0	0.0	0.0	0.0	0.0
0.0	0.0	0.0	0.0	0.0	0.0	0.0	0.0	0.0	0.0
0.0	0.0	0.0	0.0	0.0	0.0	0.0	0.0	0.0	0.0
0.0	0.0	0.0	0.0	0.0	0.0	0.0	0.0	0.0	0.0
0.034005	0.2117214	-0.4926297	0.3032622	-0.6444355	-0.2924446	-0.3379487	0.0043773	0.1902602	-0.6277324
0.003568	0.0659590	0.0238240	0.0415037	0.7302817	0.3075821	0.3240589	0.0001087	0.0075000	-0.0715083
0.6858557	-0.1309871	-0.0884556	-0.1661522	0.4933450	0.1883007	0.9322114	-0.6862594	0.1278537	0.3626733
0.0752210	0.4258911	0.3123003	0.4304433	-0.9781414	-0.4370811	-1.7033854	-0.0745920	-0.4191844	0.8578618
0.0055916	-0.0386897	-0.0203239	-0.0197190	0.0796241	0.5525793	1.3128482	0.0061841	0.0003861	0.1381950
0.0	0.0	0.0	0.0	0.0	0.0	0.0	0.0	0.0	0.0
0.0	0.0	0.0	0.0	0.0	0.0	0.0	0.0	0.0	0.0
0.0	0.0	0.0	0.0	0.0	0.0	0.0	0.0	0.0	0.0
0.0	0.0	0.0	0.0	0.0	0.0	0.0	0.0	0.0	0.0
-0.0034005	-0.2117214	0.4926297	-0.3032622	0.4444355	0.2924446	0.3379487	0.0043773	0.1902602	-0.6277324
-0.003568	-0.0659590	-0.0238240	-0.0415037	-0.7302817	-0.3075821	-0.3240589	0.0001087	0.0075000	-0.0715083
-0.0045419	-0.2056818	0.0981794	0.4427094	-0.4616029	-0.3793699	-0.8175098	0.0049178	0.2081165	-0.0880941
0.0002568	-0.0016054	-0.0103277	0.0279358	0.1638113	-0.1481187	0.8739781	-0.0002584	0.0028914	0.0004474
-0.0045419	-0.2056818	0.0981794	0.4427094	-0.4616029	-0.3793699	-0.8175098	0.0049178	0.2081165	-0.0880941
0.0002568	-0.0016054	-0.0103277	0.0279358	0.1638113	-0.1481187	0.8739781	-0.0002584	0.0028914	0.0004474
-0.0045419	-0.2056818	0.0981794	0.4427094	-0.4616029	-0.3793699	-0.8175098	0.0049178	-0.2081165	0.0880941
0.0002568	-0.0016054	-0.0103277	0.0279358	0.1638113	-0.1481187	0.8739781	-0.0002584	-0.0028914	-0.0004474
-0.0045419	-0.2056818	0.0981794	0.4427094	-0.4616029	-0.3793699	-0.8175098	0.0049178	-0.2081165	0.0880941
0.0002568	-0.0016054	-0.0103277	0.0279358	0.1638113	-0.1481187	0.8739781	0.0002584	-0.0028914	-0.0004474

**Table 11 (Continued)**

-0.9079871	0.7905172	0.6595518	1.7744276	0.0	0.0	0.0	0.0	0.0	0.0	0.0
1.9711160	-1.6290587	-1.2679330	-3.7514346	0.0	0.0	0.0	0.0	0.0	0.0	0.0
-1.6742986	1.3360706	1.3628648	3.1221788	0.0	0.0	0.0	0.0	0.0	0.0	0.0
0.0	0.0	0.0	0.0	0.0	0.0	0.0	0.0	0.0	0.0	0.0
0.0	0.0	0.0	0.0	0.0	0.0	0.0	0.0	0.0	0.0	0.0
0.0	0.0	0.0	0.0	0.0	0.0	0.0	0.0	0.0	0.0	0.0
0.0	0.0	0.0	0.0	0.0	0.0	0.0	0.0	0.0	0.0	0.0
-0.1876826	1.5190440	1.0511099	0.1652384	0.0	0.0	0.0	0.0	0.0	0.0	0.0
0.7710347	-1.4222889	-0.9161601	-0.1778708	0.0	0.0	0.0	0.0	0.0	0.0	0.0
0.9079871	-0.7905172	-0.3595518	-1.7744276	0.0	0.0	0.0	0.0	0.0	0.0	0.0
-1.9711160	0.6290587	1.2679330	3.7514346	0.0	0.0	0.0	0.0	0.0	0.0	0.0
1.6742986	-1.3360706	-1.3628648	-3.1221788	0.0	0.0	0.0	0.0	0.0	0.0	0.0
0.0	0.0	0.0	0.0	0.0	0.0	0.0	0.0	0.0	0.0	0.0
0.0	0.0	0.0	0.0	0.0	0.0	0.0	0.0	0.0	0.0	0.0
0.0	0.0	0.0	0.0	0.0	0.0	0.0	0.0	0.0	0.0	0.0
-0.1876826	1.5190440	1.0511099	0.1652384	0.0	0.0	0.0	0.0	0.0	0.0	0.0
0.7710347	-1.4222889	-0.9161601	-0.1778708	0.0	0.0	0.0	0.0	0.0	0.0	0.0
-0.4464481	-0.6853730	-0.3527600	0.7597195	-0.3014778	-0.0165628	1.6928307	-1.2830596	0.2589283	0.2479659	
0.177682	0.0535349	0.5310497	-0.8133681	0.0098172	0.2307886	-0.4835848	1.0651415	-0.0050827	0.1313286	
-0.4464481	-0.6853730	-0.3527600	0.7597195	0.3014778	0.0165628	-1.6928307	1.2830596	-0.2589283	-0.2479659	
0.0177682	0.0535349	0.5310490	-0.8133681	-0.0098172	-0.2307886	0.4835848	-1.0651415	0.0050827	-0.1313286	
0.4464481	0.6853730	0.3527600	0.7597195	0.3014778	0.0165628	1.6928307	-1.2830596	-0.2589283	-0.2479659	
-0.0177682	-0.0535349	-0.5310490	0.8133681	0.0098172	0.2307886	-0.4835848	1.0651415	0.0050827	-0.1313286	
0.4464481	0.6853730	0.3527600	-0.7597195	0.3014778	0.0165628	-1.6928307	1.2830596	0.2589283	0.2479659	
-0.0177682	-0.0535349	-0.5310490	0.8133681	0.0098172	-0.2307886	0.4835848	-1.0651415	0.0050827	0.1313286	
-0.0177682	-0.0535349	-0.5310490	0.8133681	-0.0098172	-0.2307886	0.4835848	-1.0651415	-0.0050827	0.1313286	

**Table 11. (Continued)**

Table 12. MO expansions for  ${}^1A_g$  ground state at  $\Delta R = 1.5$  a.u.

0.6854625	-0.1438818	0.0993970	0.0728357	-0.4374710	0.1667756	0.0061891	0.6852351	-0.1445466	+0.2463633
0.C765417	0.4580514	-C.2971011	-0.2003108	C.9485341	-0.4095879	-1.6548608	0.0770191	C.4639210	0.6210977
0.0055148	-0.0366945	C.0417880	0.0295719	-0.0422501	0.5991783	1.2672583	0.0053444	-C.0205853	+0.1369402
0.C	0.C	0.0	0.0	0.0	0.0	0.0	0.0	0.0	0.0
0.C	0.0	0.0	0.0	0.0	0.0	0.0	0.0	0.0	0.0
0.0	0.0	0.0	0.0	0.0	0.0	0.0	0.0	0.0	0.0
0.C	0.0	0.0	0.0	0.0	0.0	0.0	0.0	0.0	0.0
0.0021222	-0.1767808	C.5317875	-0.2951705	0.2945972	-0.1936997	-0.3711384	C.0031027	C.1470391	-0.7451764
0.0004411	0.0053663	-0.0358944	-0.5641962	-0.4634998	0.2742077	0.3236788	0.0003753	0.0089328	0.0148875
0.6854625	-0.1438818	0.0993970	0.0728357	-0.4374710	0.1667756	0.0061891	-0.6852351	C.1445466	0.2463633
0.C765417	0.4580514	-C.2971011	-0.2003108	C.9485341	-0.4095879	-1.6548608	0.0770191	-C.4639210	0.6210977
0.0055148	-0.0366945	C.0417880	0.0295719	-0.0422501	0.5991783	1.2672583	-0.0053444	0.0205853	0.1369402
0.C	0.0	0.0	0.0	0.0	0.0	0.0	0.0	0.0	0.0
0.0	0.0	0.0	0.0	0.0	0.0	0.0	0.0	0.0	0.0
0.C	0.0	0.0	0.0	0.0	0.0	0.0	0.0	0.0	0.0
-0.0021222	-0.1767808	-C.5317875	0.2951705	-0.2945972	0.1936997	0.3711384	0.0031027	C.1470391	-0.7451764
-0.0004411	-0.0053663	0.0358944	0.5641962	0.4634998	-C.2742077	-0.3236788	0.0003753	0.0089328	0.0148875
-0.0045C12	-0.20C1664	-C.0913244	-0.3045854	0.5491156	-0.3549133	-0.7772957	0.2048429	0.2015331	-0.0988554
C.0002611	-0.0042029	C.0056402	-0.0482337	-0.1C86942	-0.1304984	C.6166845	-0.0002254	0.0028040	0.0021598
-0.C045012	-0.20C1664	-C.0913244	-0.3045854	0.5491156	-0.3549133	-0.7772957	0.0048425	C.2015331	-0.0988554
C.0002611	-0.0042029	C.0056402	-0.0482337	-C.1086942	-0.1304984	0.8766845	-0.0002254	C.0028040	0.0021598
-0.C045012	-0.20C1664	-C.0913244	-0.3045854	0.5491156	-0.3549133	-0.7772957	0.0048425	-C.2015331	0.0988554
C.0002611	-0.0042029	C.0056402	-0.0482337	-C.1086942	-0.1304984	0.8766845	0.0002254	-0.0028040	-0.0021598
-C.0045C12	-0.20C1664	-C.0913244	-0.3045854	0.5491156	-0.3549133	-0.7772957	-0.0048425	-0.2015331	0.0988554
C.0002611	-0.0042029	C.0056402	-0.0482337	-C.1086942	-0.1304984	0.8766845	0.0002254	-0.0028040	-0.0021598
-C.0045C12	-0.20C1664	-C.0913244	-0.3045854	0.5491156	-0.3549133	-0.7772957	-0.0048425	-0.2015331	0.0988554
C.0002611	-0.0042029	C.0056402	-0.0482337	-C.1086942	-0.1304984	0.8766845	0.0002254	-0.0028040	-0.0021598

**Table 12 (Continued)**

-0.5881684	0.2716824	C.2301616	1.4277503	0.0	0.0	0.0	0.0	0.0	0.0	C.C	C.C
1.3205064	-0.6155778	-D.5967233	-3.0130477	0.0	0.0	0.0	0.0	0.0	0.0	C.C	C.C
-C.6452767	C.8E41275	C.9294126	2.5143924	0.0	0.0	0.0	0.0	0.0	0.0	C.C	C.C
0.0	0.0	0.0	0.0	0.0	0.0	0.0	0.0	0.0	0.0	0.0	0.0
C.0	0.0	0.0	0.0	0.0	0.0	0.0	0.0	0.0	0.0	C.C	C.C
0.0	0.0	0.0	0.0	0.0	0.0	0.0	0.0	0.0	0.0	0.0	0.0
0.0	0.0	0.0	0.0	0.0	0.0	0.0	0.0	0.0	0.0	0.0	0.0
0.0100423	1.C6E8554	C.4303189	0.1148179	0.0	0.0	0.0	0.0	0.0	0.0	0.0	0.0
0.636058	-1.25E4471	-D.4096265	-0.1182174	0.0	0.0	0.0	0.0	0.0	0.0	C.C	C.C
0.5881684	-0.2716824	-C.2301616	-1.4277503	0.0	0.0	0.0	0.0	0.0	0.0	C.C	C.C
-1.3205064	0.6155778	D.5967233	3.0130477	0.0	0.0	0.0	0.0	0.0	0.0	C.C	C.C
C.6452767	-0.E841275	-C.9294126	-2.5143924	0.0	0.0	0.0	0.0	0.0	0.0	C.C	C.C
0.0	0.0	0.0	0.0	0.0	0.0	0.0	0.0	0.0	0.0	0.0	0.0
C.0	0.0	0.0	0.0	0.0	0.0	0.0	0.0	0.0	0.0	C.C	C.C
0.0	0.0	0.0	0.0	0.0	0.0	0.0	0.0	0.0	0.0	0.0	0.0
0.0	0.0	0.0	0.0	0.0	0.0	0.0	0.0	0.0	0.0	0.0	0.0
0.0100423	1.C9E88594	C.4303189	0.1148179	0.0	0.0	0.0	0.0	0.0	0.0	0.0	0.0
0.636058	-1.25E4471	-D.4096265	-0.1182174	0.0	0.0	0.0	0.0	0.0	0.0	C.C	C.C
-0.4951757	-0.5439476	-D.0059792	0.8152140	-0.2952605	0.0480155	1.4093340	-1.1382567	1.2813249	-0.2699676		
0.0344586	0.0688680	G.3583633	-0.8711152	0.0105583	0.2100798	-0.44059096	1.0275763	-0.0996896	-0.1099247		
-C.4655757	-0.5439476	-D.0059792	0.8152140	0.2952605	-0.0480155	-1.4553340	1.1382567	-0.2893249	0.2699676		
0.0344586	0.0688680	G.3583633	-0.8711152	-0.0105583	-0.2100798	0.44059096	-1.0275763	0.0396396	0.1099247		
0.4951757	0.5439476	D.0059792	-0.8152140	-0.2952605	0.0480155	1.4093340	-1.1382567	-0.2813249	0.2699676		
-0.0344586	-0.0688680	-G.3583633	0.8711152	0.0105583	0.2100798	-0.44059096	1.0275763	0.0396896	0.1099247		
0.4951757	0.5439476	D.0059792	-0.8152140	0.2952605	-0.0480155	-1.4553340	1.1382567	-0.2813249	0.2699676		
-0.0344586	-0.0688680	-G.3583633	0.8711152	-0.0105583	-0.2100798	0.44059096	-1.0275763	-0.0396896	-0.1099247		

**Table 12 (Continued)**

0.0	0.0	0.0	0.0	0.0	0.0
0.0	0.0	0.0	0.0	0.0	0.0
C.C	C.C	0.0	0.0	0.0	0.0
0.0	0.0	0.6591665	0.1650961	0.7564019	-0.1404920
C.C	0.0	-0.0757221	0.6280609	-0.0568398	0.8518895
-0.6548328	0.6891832	0.0	0.0	0.0	0.0
C.ECCE356	-0.6219926	0.0	0.3	0.0	0.0
0.0	C.C	0.0	0.0	0.0	C.C
C.C	0.0	0.0	0.0	0.0	0.0
0.0	0.0	C.C	0.0	0.0	0.0
0.0	C.C	0.0	0.0	0.0	0.0
0.0	0.0	0.6591665	0.1650961	-0.7564019	0.1404920
C.C	0.0	-0.0757221	0.6280609	0.0568398	-0.8518895
-C.6548328	0.6891832	0.0	0.0	0.0	0.0
C.ECCE356	-0.6219926	C.C	0.0	0.0	0.0
0.0	0.0	C.C	0.0	0.0	0.0
0.0	0.0	0.0	0.0	0.0	0.0
C.9006324	-0.74C8377	0.0	0.0	0.0	0.0
-C.23C7E33	C.8833726	0.0	0.0	0.0	0.0
-C.9006324	C.74C8377	C.C	0.0	C.C	0.0
C.23C7E33	-C.8833726	0.0	0.0	C.C	0.0
-C.9006324	C.74C8377	C.C	0.0	0.0	C.C
C.23C7E33	-C.8833726	0.0	0.0	0.0	0.0
C.9006324	-C.74C8377	0.0	0.0	0.0	C.C
-C.23C7E33	C.8833726	C.C	0.0	0.0	0.0

Table 13. MO expansions for  $1_{A_q}$  ground state at  $\Delta R = 2.5$  a.u.

Table 13 (continued)

Table 1.3 (continued)

Table 14. MO expansions for  ${}^1A_g$  ground state at  $\Delta R = 3.0$  a.u.

0.6853300	-0.1507237	0.1205414	-0.1032932	-0.3765413	-0.1900174	0.3316614	0.5950764	-0.1510484	0.1733015	
0.0768826	0.4776930	-0.3205257	0.2452594	0.8410938	0.4333301	-1.6895920	0.0774491	0.4760491	0.4532687	
0.0004323	-0.0021764	0.0611065	-0.0576512	-0.0018145	-0.0030349	1.2676536	0.0050275	-0.0345747	0.1031360	
0.0	0.0	0.0	0.0	0.0	0.0	0.0	0.0	0.0	0.0	
0.0	0.0	0.0	0.0	0.0	0.0	0.0	0.0	0.0	0.0	
0.0021400	0.1601090	0.5684713	0.1162460	0.2563216	0.2176779	-0.4244121	0.0921500	0.1277066	0.6746805	
0.0004128	0.0057831	-0.0451251	0.5233934	-0.3550957	-0.2412165	0.3985546	0.0004731	0.0984137	0.0537640	
0.6853300	-0.1507237	0.1205414	-0.1032932	-0.3765413	-0.1900174	0.4316614	-0.6450764	0.1510484	0.1733015	
0.0768826	0.4776930	-0.3205257	0.2452594	0.8410938	0.4333301	-1.6895920	0.0774491	-0.4760491	0.4532687	
0.0004323	-0.0021764	0.0611065	-0.0576512	-0.0018145	-0.0030349	1.2676536	-0.0050275	0.0345742	0.1031360	
0.0	0.0	0.0	0.0	0.0	0.0	0.0	0.0	0.0	0.0	
0.0	0.0	0.0	0.0	0.0	0.0	0.0	0.0	0.0	0.0	
-0.0021400	-0.1601090	-0.5684713	-0.1162460	-0.2563216	-0.2176779	0.4244121	0.0921600	0.1277066	0.6746805	
-0.0004128	-0.0057831	0.0451251	-0.5233934	0.3550957	0.2412165	-0.3985546	0.0004731	0.0984137	0.0537640	
-0.0047132	-0.1601077	-0.0951547	0.2778194	0.5552740	0.3510042	-0.7622722	0.0047997	0.1075972	-0.1005563	
0.0002437	-0.0039506	0.0051562	0.0359031	-0.0323604	0.1210445	0.3760045	-0.0302298	0.0030376	0.0042961	
-0.0047132	-0.1601077	-0.0951547	0.2778194	0.5552740	0.3510042	-0.7622722	0.0047997	-0.1975979	0.1005563	
0.0002437	-0.0039506	0.0051562	0.0359031	-0.0323604	0.1210445	0.3760045	0.0030376	-0.0030376	-0.0042961	
-0.0047132	-0.1601077	-0.0951547	0.2778194	0.5552740	0.3510042	-0.7622722	-0.0047997	-0.175979	0.1005563	
0.0002437	-0.0039506	0.0051562	0.0359031	-0.0323604	0.1210445	0.3760045	0.0030376	-0.0047997	0.175979	

Table 14 (Continued)

0.3726540	0.1049230	0.1614101	1.0966819	0.0	0.0	0.0	0.0	0.0	0.0	0.0	0.0
-0.6534936	-0.2004972	-0.4240676	-2.2958663	0.0	0.0	0.0	0.0	0.0	0.0	0.0	0.0
0.3322149	-0.402771	0.7304123	1.09016752	0.0	0.0	0.0	0.0	0.0	0.0	0.0	0.0
0.0	0.0	0.0	0.0	0.0	0.0	0.0	0.0	0.0	0.0	0.0	0.0
0.0	0.0	0.0	0.0	0.0	0.0	0.0	0.0	0.0	0.0	0.0	0.0
0.0	0.0	0.0	0.0	0.0	0.0	0.0	0.0	0.0	0.0	0.0	0.0
0.0	0.0	0.0	0.0	0.0	0.0	0.0	0.0	0.0	0.0	0.0	0.0
-0.1941809	-0.5971310	0.0227142	-0.1370936	0.0	0.0	0.0	0.0	0.0	0.0	0.0	0.0
-0.5361531	0.9261634	-0.0075468	0.0911776	0.0	0.0	0.0	0.0	0.0	0.0	0.0	0.0
-0.3726540	-0.1049230	-0.1614101	-1.0966819	0.0	0.0	0.0	0.0	0.0	0.0	0.0	0.0
0.6534936	0.2004972	0.4240676	2.2958663	0.0	0.0	0.0	0.0	0.0	0.0	0.0	0.0
-0.3322149	0.402771	-0.7304123	-1.09016752	0.0	0.0	0.0	0.0	0.0	0.0	0.0	0.0
0.0	0.0	0.0	0.0	0.0	0.0	0.0	0.0	0.0	0.0	0.0	0.0
0.0	0.0	0.0	0.0	0.0	0.0	0.0	0.0	0.0	0.0	0.0	0.0
0.0	0.0	0.0	0.0	0.0	0.0	0.0	0.0	0.0	0.0	0.0	0.0
0.0	0.0	0.0	0.0	0.0	0.0	0.0	0.0	0.0	0.0	0.0	0.0
-0.1941809	-0.5971310	0.0227142	-0.1370936	0.0	0.0	0.0	0.0	0.0	0.0	0.0	0.0
-0.5361531	0.9261634	-0.0075468	0.0911776	0.0	0.0	0.0	0.0	0.0	0.0	0.0	0.0
0.4751892	0.4595261	0.2273152	0.9306676	-0.2924585	0.1408131	1.2591462	-0.9356635	0.2890675	0.3010417		
-0.0246708	-0.0332205	0.2178103	-0.9076142	0.0114196	0.1658894	-0.3661412	0.4735977	-0.0114546	0.0983694		
0.4751892	0.4595261	0.2273153	0.8306676	0.2924585	-0.1408131	-1.2591462	0.9856585	-0.2890575	0.3010417		
-0.0246708	-0.0332205	0.2178103	-0.9076142	-0.0114196	-0.1658894	0.3661412	-0.5735977	0.0114646	0.0885694		
-0.4751892	-0.4595261	-0.2273153	-0.8306676	-0.2924585	0.1408131	1.2591462	-0.2890675	-0.5735977	0.3010417		
0.0246708	0.0332205	-0.2178103	0.9076142	0.0114196	0.1558894	-0.3661412	0.5735977	0.0114646	0.0885694		
-0.4751892	-0.4595261	-0.2273153	-0.8306676	0.2924585	-0.1408131	-1.2591462	0.9456635	0.2890675	0.3010417		
0.0246708	0.0332205	-0.2178103	0.9076142	-0.0114196	-0.1658894	0.1661412	-0.5735977	0.0114646	0.0885694		

Table 14 (Continued)

Table 15. MO expansions for  ${}^1A_g$  ground state at  $\Delta R = 3.5$  a.u.

0.6853136	-0.1515660	0.1250228	-0.1344925	-0.3584989	-0.1881573	0.8359810	0.6850933	-0.1515528	-0.1628787
0.0769187	0.4900463	0.3382521	0.3130144	0.8024476	0.4497825	-1.6966261	0.0774534	0.9810006	0.4283466
0.0053225	-0.0429170	0.0521182	-0.0580353	0.0065811	-0.6412861	1.2568164	0.0049942	-0.0367401	-0.0951034
0.0	0.0	0.0	0.0	0.0	0.0	0.0	0.0	0.0	0.0
0.0	0.0	0.0	0.0	0.0	0.0	0.0	0.0	0.0	0.0
0.0	0.0	0.0	0.0	0.0	0.0	0.0	0.0	0.0	0.0
0.0	0.0	0.0	0.0	0.0	0.0	0.0	0.0	0.0	0.0
0.0021596	0.1360173	-0.5784098	0.3241752	0.2456503	0.2186585	-0.4222193	0.0020728	0.1268240	-0.6579606
0.0003687	0.0105173	-0.0444726	0.4962688	-0.3838489	-0.2826910	0.4132841	0.0005104	0.0088889	0.0528134
0.6853136	-0.1515660	0.1250228	-0.1344925	-0.3584989	-0.1881573	0.8359810	-0.6850933	0.1515528	0.1628787
0.0769187	0.4900463	0.3382521	0.3130144	0.8024476	0.4497825	-1.6966261	-0.0774534	-0.4810006	-0.4283466
0.0053225	-0.0429170	0.0521182	-0.0580353	0.0065811	-0.6412861	1.2568164	-0.0049942	0.0367401	0.0951034
0.0	0.0	0.0	0.0	0.0	0.0	0.0	0.0	0.0	0.0
0.0	0.0	0.0	0.0	0.0	0.0	0.0	0.0	0.0	0.0
0.0	0.0	0.0	0.0	0.0	0.0	0.0	0.0	0.0	0.0
0.0021596	-0.1360173	-0.5784098	-0.3241752	-0.2456503	-0.2186585	0.4222193	0.0020728	0.1268240	-0.6579606
-0.0003687	-0.0105173	0.0444726	-0.4962688	0.3838489	0.2826910	-0.4132841	0.0005104	0.0088889	0.0528134
-0.0047431	-0.1976387	-0.0946485	0.3086794	0.5358858	0.3545675	-0.7567898	0.0047836	0.1974093	-0.1010186
0.0002478	-0.0040435	0.0043968	0.0307720	-0.0838096	0.1171771	0.8717363	-0.0002228	0.0031377	0.0047370
-0.0047431	-0.1976387	-0.0946485	0.3086794	0.5358858	0.3545675	-0.7567898	-0.0047336	-0.1974093	0.1010186
0.0002478	-0.0040435	0.0043968	0.0307720	-0.0838096	0.1171771	0.8717363	0.0002228	-0.0031377	-0.0047370
-0.0047431	-0.1976387	-0.0946485	0.3086794	0.5358858	0.3545675	-0.7567898	-0.0047336	-0.1974093	0.1010186
0.0002478	-0.0040435	0.0043968	0.0307720	-0.0838096	0.1171771	0.8717363	-0.0002228	-0.0031377	-0.0047370

**Table 15** (Continued)

Table 15 (Continued)

0.0	0.0	0.0	0.0	0.0	0.0
0.0	0.0	0.0	0.0	0.0	0.0
0.0	0.0	0.0	0.0	0.0	0.0
0.0	0.0	0.0944744	0.0905398	0.7168981	0.0071253
0.0	0.0	-0.0698818	0.6657548	-0.0721963	0.7515997
-0.9755537	0.6978188	0.0	0.0	0.0	0.0
0.0850280	-0.6190124	0.0	0.0	0.0	0.0
0.0	0.0	0.0	0.0	0.0	0.0
0.0	0.0	0.0	0.0	0.0	0.0
0.0	0.0	0.0	0.0	0.0	0.0
0.0	0.0	0.0	0.0	0.0	0.0
0.0	0.0	0.0944744	0.0905398	-0.7168981	-0.0071253
0.0	0.0	-0.0698818	0.6657548	0.0721963	-0.7515997
-0.9755537	0.6978188	0.0	0.0	0.0	0.0
0.0850280	-0.6190124	0.0	0.0	0.0	0.0
0.0	0.0	0.0	0.0	0.0	0.0
0.0	0.0	0.0	0.0	0.0	0.0
0.9270271	-0.7051493	0.0	0.0	0.0	0.0
-0.2390741	0.8513146	0.0	0.0	0.0	0.0
-0.9270271	0.7051493	0.0	0.0	0.0	0.0
0.2390741	-0.8513146	0.0	0.0	0.0	0.0
-0.9270271	0.7051493	0.0	0.0	0.0	0.0
0.2390741	-0.8513146	0.0	0.0	0.0	0.0
0.9270271	-0.7051493	0.0	0.0	0.0	0.0
-0.2390741	0.8513146	0.0	0.0	0.0	0.0

Table 16. MO expansions for  ${}^1A_g$  ground state at  $\Delta R = 7.5$  a.u.

0.6853088	-0.1529559	-0.1375565	0.2391950	0.3037026	0.1737433	0.2546910	0.6852370	-0.1529927	0.1402727
0.0769545	0.4839266	0.3676408	-0.5503443	-0.6277838	-0.4241251	-1.7434993	0.771093	0.4840645	0.3740407
0.0053721	-0.0429115	-0.0690928	0.0521991	0.0165340	0.6609906	1.3075968	0.0052137	-0.0425668	0.0734599
0.0	0.0	0.0	0.0	0.0	0.0	0.0	0.0	0.0	0.0
0.0	0.0	0.0	0.0	0.0	0.0	0.0	0.0	0.0	0.0
0.0	0.0	0.0	0.0	0.0	0.0	0.0	0.0	0.0	0.0
0.0	0.0	0.0	0.0	0.0	0.0	0.0	0.0	0.0	0.0
0.0021026	0.12E5940	-0.6110356	-0.3368544	-0.2572716	-0.1733525	-0.3730956	0.0020936	0.1278471	0.6163099
0.0003479	0.0110055	0.0457940	-0.3017436	0.5925876	0.1949416	0.3732267	0.0004020	0.0109702	-0.0470568
0.6853088	-0.1529559	-0.1375565	0.2391950	0.3037026	0.1737433	0.2546910	-0.6852370	0.1529927	-0.1402727
0.0769545	0.4839266	0.3676408	-0.5503443	-0.6277838	-0.4241251	-1.7434993	0.771093	0.4840645	0.3740407
0.0053721	-0.0429115	-0.0690928	0.0521991	0.0165340	0.6609906	1.3075968	-0.0052137	0.0425668	-0.0734599
0.0	0.0	0.0	0.0	0.0	0.0	0.0	0.0	0.0	0.0
0.0	0.0	0.0	0.0	0.0	0.0	0.0	0.0	0.0	0.0
0.0	0.0	0.0	0.0	0.0	0.0	0.0	0.0	0.0	0.0
0.0	0.0	0.0	0.0	0.0	0.0	0.0	0.0	0.0	0.0
0.0	0.0	0.0	0.0	0.0	0.0	0.0	0.0	0.0	0.0
-0.0021026	-0.12E5940	0.6110356	0.3368544	0.2572716	0.1733525	0.3730956	0.0020936	0.1278471	0.6163099
-0.0003479	-0.0110055	-0.0457940	0.3017436	-0.5925876	-0.1949416	-0.3732267	0.0004020	0.0109702	-0.0470568
-0.0048295	-0.1966823	0.0954534	-0.4328312	-0.4838931	-0.3186155	-0.7477185	0.0047791	0.1966617	0.0975544
0.0003026	-0.0478117	-0.0030627	-0.0160337	0.1110162	0.1373420	0.8614431	-0.002506	0.0339648	-0.2239781
-0.0048295	-0.1566828	0.0954534	-0.4328312	-0.4838931	-0.3186155	-0.7477185	0.0047791	0.1966617	0.0975544
0.0003026	-0.0478117	-0.0030627	-0.0160337	0.1110162	0.1373420	0.8614431	-0.002506	0.0339648	-0.2239781
-0.0048295	-0.1566828	0.0954534	-0.4328312	-0.4838931	-0.3186155	-0.7477185	0.0047791	0.1966617	0.0975544
0.0003026	-0.0478117	-0.0030627	-0.0160337	0.1110162	0.1373420	0.8614431	-0.002506	0.0339648	0.0975544
-0.0048295	-0.1566828	0.0954534	-0.4328312	-0.4838931	-0.3186155	-0.7477185	0.0047791	0.1966617	0.0975544
0.0003026	-0.0478117	-0.0030627	-0.0160337	0.1110162	0.1373420	0.8614431	-0.002506	0.0339648	0.0975544

Table 16 (continued)

Table 16 (Continued)

Table 17. MO expansions for  ${}^1A_g$  ground state at  $\Delta R = 15.0$  a.u.

0.6852772	-0.1530569	0.1788684	0.2490365	0.3213974	0.1413423	0.9620400	0.6852772	-0.1530574	0.1343658
0.0770226	0.4842342	-0.3706249	-0.5723950	-0.7023750	-0.3569945	-1.2609275	0.0770226	0.4842356	-0.3706193
0.0053027	-0.0427686	0.0718276	0.0465199	0.0634445	0.6378502	1.3495393	0.0053026	-0.0427699	0.0718169
0.0	0.0	0.0	0.0	0.0	0.0	0.0	0.0	0.0	0.0
0.0	0.0	0.0	0.0	0.0	0.0	0.0	0.0	0.0	0.0
0.0	0.0	0.0	0.0	0.0	0.0	0.0	0.0	0.0	0.0
0.0020898	0.1278643	-0.6137158	-0.1328314	-0.2740875	-0.1498453	-0.3676038	0.0020922	0.1273625	0.6137216
0.0002755	0.0110865	-0.0466134	-0.3799007	0.6435257	0.1349815	0.3448315	0.0002756	0.0110575	-0.0466074
0.6852772	-0.1530569	0.1388684	0.2490365	0.3213974	0.1413423	0.9620400	0.6852772	0.1530574	-0.1343658
0.0770226	0.4842342	-0.3706249	-0.5723950	-0.7023750	-0.3569945	-1.2609275	0.0770226	0.4842356	-0.3706193
0.0053027	-0.0427686	0.0718276	0.0465199	0.0634445	0.6378502	1.3495393	0.0053026	-0.0427699	0.0718165
0.0	0.0	0.0	0.0	0.0	0.0	0.0	0.0	0.0	0.0
0.0	0.0	0.0	0.0	0.0	0.0	0.0	0.0	0.0	0.0
0.0	0.0	0.0	0.0	0.0	0.0	0.0	0.0	0.0	0.0
0.0020898	0.1278643	-0.6137158	-0.1328314	-0.2740875	-0.1498453	-0.3676038	0.0020922	0.1273625	0.6137216
0.0002755	0.0110865	-0.0466134	-0.3799007	0.6435257	0.1349815	0.3448315	0.0002756	0.0110575	-0.0466074
-0.0048033	-0.1966008	-0.0966074	-0.460430	-0.4998089	-0.2796791	-0.7512470	0.0048033	0.1966006	0.0966069
0.002796	-0.0040141	0.0035397	-0.0054016	0.1194321	-0.1632273	-0.5618697	-0.002795	0.0040143	-0.035374
-0.0048033	-0.1966008	-0.0966074	-0.460430	-0.4998089	-0.2796791	-0.7512470	0.0048033	0.1966006	0.0966069
0.0002796	-0.0040141	0.0035397	-0.0054016	0.1194321	-0.1632273	-0.5618697	-0.002795	0.0040143	-0.035374
-0.0048033	-0.1966008	-0.0966074	-0.460430	-0.4998089	-0.2796791	-0.7512470	0.0048033	0.1966006	0.0966069
0.0002796	-0.0040141	0.0035397	-0.0054016	0.1194321	-0.1632273	-0.5618697	-0.002795	0.0040143	-0.035374
-0.0048033	-0.1966008	-0.0966074	-0.460430	-0.4998089	-0.2796791	-0.7512470	0.0048033	0.1966006	0.0966069
0.0002796	-0.0040141	0.0035397	-0.0054016	0.1194321	-0.1632273	-0.5618697	-0.002795	0.0040143	-0.035374

Table 17 (Continued)

**Table 17** (continued)

Table 18. MO expansions for  ${}^1\text{Ag}$  first excited state at  $\Delta R = 0.0$  a.u.

Table 18 (continued)

**Table 18** (Continued)

Table 19. MO expansions for  $^1A_g$  first excited state at  $\Delta R = 1.00$  a.u.

0.6855229	-0.1476487	-0.0675276	0.1233210	0.4661512	0.1756734	0.9124124	0.6853730	-0.1495917	-0.2821337
0.0764414	0.4741637	0.2227155	-0.3260056	-0.9735945	-0.4252078	-1.6709507	0.0766962	0.4736923	0.6942755
0.0055765	-0.0379416	-0.0127881	0.0183213	0.0663085	0.5826179	1.2970139	0.0053777	-0.0241819	-0.1515169
0.0	0.0	0.0	0.0	0.0	0.0	0.0	0.0	0.0	0.0
0.0	0.0	0.0	0.0	0.0	0.0	0.0	0.0	0.0	0.0
0.0	0.0	0.0	0.0	0.0	0.0	0.0	0.0	0.0	0.0
0.0	0.0	0.0	0.0	0.0	0.0	0.0	0.0	0.0	0.0
0.0027621	0.1176528	-0.5412902	-0.3030934	-0.3370166	-0.1867363	-0.3474795	0.0033263	0.1362901	-0.9091486
0.0004202	0.0074002	0.0143679	-0.5065343	0.6136918	0.2832037	0.3192572	0.0005258	0.0138447	0.1167478
0.6855229	-0.1476487	-0.0675276	0.1233210	0.4661512	0.1756734	0.9124124	-0.6853730	0.1495917	0.2821337
0.0764414	0.4741637	0.2227155	-0.3260056	-0.9735945	-0.4252078	-1.6709507	0.0766962	-0.4736923	0.6942755
0.0055765	-0.0379416	-0.0127881	0.0183213	0.0663085	0.5826179	1.2970139	-0.0053777	0.0241819	0.1515169
0.0	0.0	0.0	0.0	0.0	0.0	0.0	0.0	0.0	0.0
0.0	0.0	0.0	0.0	0.0	0.0	0.0	0.0	0.0	0.0
0.0	0.0	0.0	0.0	0.0	0.0	0.0	0.0	0.0	0.0
0.0	0.0	0.0	0.0	0.0	0.0	0.0	0.0	0.0	0.0
-0.0027621	-0.1176528	0.5412902	0.3030934	0.3370166	0.1867363	0.3474795	0.0033263	0.1362901	-0.9091486
-0.0004202	-0.0074002	-0.0143679	0.5065343	-0.6136918	-0.2832037	-0.3192572	0.0005258	0.0138447	0.1167478
-0.0048323	-0.1919345	0.1126295	-0.3844687	-0.5060277	-0.3688007	-0.7931202	-0.0050509	-0.2041409	0.0081822
0.0002885	-0.0029171	-0.0030853	-0.0391823	0.1384745	-0.1364545	0.8750792	0.0002846	-0.0012404	0.0354065
-0.0048323	-0.1919345	0.1126295	-0.3844687	-0.5060277	-0.3688007	-0.7931202	-0.0050509	-0.2041409	0.0081822
0.0002885	-0.0029171	-0.0030853	-0.0391823	0.1384745	-0.1364545	0.9750792	0.0002846	-0.0012404	0.0354065
-0.0048323	-0.1919345	0.1126295	-0.3844687	-0.5060277	-0.3688007	-0.7931202	0.0050509	0.2041409	-0.0081822
0.0002885	-0.0029171	-0.0030853	-0.0391823	0.1384745	-0.1364545	0.8750792	-0.0002846	0.0012404	-0.0354065
-0.0048323	-0.1919345	0.1126295	-0.3844687	-0.5060277	-0.3688007	-0.7931202	0.0050509	0.2041409	-0.0081822
0.0002885	-0.0029171	-0.0030853	-0.0391823	0.1384745	-0.1364545	0.8750792	-0.0002846	0.0012404	-0.0354065

**Table 19 (Continued)**

0.7306401	0.3843693	-0.3366190	1.6309357	0.0	0.0	0.0	0.0	0.0	0.0	0.0
-1.6146704	-0.8143638	0.8216249	-3.4066654	0.0	0.0	0.0	0.0	0.0	0.0	0.0
0.8616594	0.9463142	-1.0857882	2.8562416	0.0	0.0	0.0	0.0	0.0	0.0	0.0
0.0	0.0	0.0	0.0	0.0	0.0	0.0	0.0	0.0	0.0	0.0
0.0	0.0	0.0	0.0	0.0	0.0	0.0	0.0	0.0	0.0	0.0
0.0	0.0	0.0	0.0	0.4314197	0.0383190	-2.1454565	1.4808607	0.4033261	-0.4467795	
0.0	0.0	0.0	0.0	0.0128862	0.8624444	1.9022722	-1.2856980	0.0319199	-0.4835833	
0.1473076	1.2301201	-0.6986474	0.2369142	0.0	0.0	0.0	0.0	0.0	0.0	0.0
-0.7691276	-1.3071103	0.6354062	-0.2141563	0.0	0.0	0.0	0.0	0.0	0.0	0.0
-0.7306401	-0.3843693	0.3366190	-1.6309357	0.0	0.0	0.0	0.0	0.0	0.0	0.0
1.6146704	0.8143638	-0.8216249	3.4066654	0.0	0.0	0.0	0.0	0.0	0.0	0.0
-0.8616594	-0.9463142	1.0857882	-2.8562416	0.0	0.0	0.0	0.0	0.0	0.0	0.0
0.0	0.0	0.0	0.0	0.0	0.0	0.0	0.0	0.0	0.0	0.0
0.0	0.0	0.0	0.0	0.0	0.0	0.0	0.0	0.0	0.0	0.0
0.0	0.0	0.0	0.0	-0.4314197	-0.0383190	2.1454565	-1.4808607	0.4033261	-0.4467795	
0.0	0.0	0.0	0.0	-0.0128862	-0.8624444	-1.9022722	1.2856980	0.0319199	-0.4835833	
0.1473076	1.2301201	-0.6986474	0.2369142	0.0	0.0	0.0	0.0	0.0	0.0	0.0
-0.7691276	-1.3071103	0.6354062	-0.2141563	0.0	0.0	0.0	0.0	0.0	0.0	0.0
-0.4376477	0.6632774	-0.1520313	-0.7814821	0.2895791	-0.0134666	1.5826771	-1.2014573	0.2646299	0.2527976	
0.0199913	-0.0881287	0.4386520	0.8419781	-0.0075052	-0.2228357	-0.4520109	1.0435073	-0.0055068	0.1211629	
-0.4376477	0.6632774	-0.1520313	-0.7814821	-0.2895791	0.0134666	-1.5826771	1.2014573	-0.2646299	0.2527976	
0.0199913	-0.0881287	0.4386520	0.8419781	0.0075052	0.2228357	0.4520109	-1.0435073	0.0055068	-0.1211629	
0.4376477	-0.6632774	0.1520313	0.7814821	-0.2895791	0.0134666	-1.5826771	1.2014573	0.2646299	0.2527976	
-0.0199913	0.0881287	-0.4386520	-0.8419781	0.0075052	0.2228357	0.4520109	-1.0435073	-0.0055068	0.1211629	
0.4376477	-0.6632774	0.1520313	0.7814821	0.2895791	-0.0134666	1.5826771	-1.2014573	-0.2646299	0.2527976	
-0.0199913	0.0881287	-0.4386520	-0.8419781	-0.0075052	-0.2228357	-0.4520109	1.0435073	0.0055068	-0.1211629	

**Table 19 (Continued)**

Table 20. MO expansions for  ${}^1A_g$  first excited state at  $\Delta R = 1.4$  a.u.

0.6853771	-0.1834310	0.0731203	-0.0754919	-0.4431993	0.1701544	0.8081223	0.685585	-0.1526305	-0.2402580
0.0718666	0.4181858	-0.2224070	0.2119319	0.9654496	-0.4169069	-1.1600969	0.0772295	0.829774	0.6067901
0.0035159	-0.0110459	0.0275397	-0.0228811	-0.0524169	0.5991628	1.2899872	0.0053009	-0.286332	0.1503017
0.0	0.0	0.0	0.0	0.0	0.0	0.0	0.0	0.0	0.0
0.0	0.0	0.0	0.0	0.0	0.0	0.0	0.0	0.0	0.0
0.0	0.0	0.0	0.0	0.0	0.0	0.0	0.0	0.0	0.0
0.0022348	0.1143601	0.5510307	0.2944977	0.3085698	-0.1932421	-0.3704536	0.0029226	0.1243268	0.8552782
0.0004124	0.0105136	-0.0346302	0.5604586	-0.4913343	0.2748330	0.3261259	0.0003574	0.131351	0.1295759
0.6853771	-0.1534310	0.0731203	-0.0764949	-0.4431993	0.1701544	0.8081223	-0.685585	0.1526305	0.2402580
0.0718666	0.4365898	-0.2224070	0.2119319	0.9654496	-0.4169069	-1.1600969	-0.0772295	0.829774	0.6067901
0.0035159	-0.0110459	0.0275397	-0.0228811	-0.0524169	0.5991628	1.2899872	-0.0053009	0.286332	0.1503017
0.0	0.0	0.0	0.0	0.0	0.0	0.0	0.0	0.0	0.0
0.0	0.0	0.0	0.0	0.0	0.0	0.0	0.0	0.0	0.0
0.0	0.0	0.0	0.0	0.0	0.0	0.0	0.0	0.0	0.0
-0.0022348	-0.1143601	-0.5510307	-0.2944977	-0.3085698	0.1932421	0.3704536	0.0029226	0.1243268	0.8552782
-0.0004124	-0.0105136	0.0346302	-0.5604586	0.4913343	-0.2748330	-0.3261259	0.0003574	0.131351	0.1295759
-0.0047933	-0.1891339	-0.1117223	0.3135444	0.5493592	-0.3601430	-0.7809620	-0.0049525	-0.2005024	0.0286271
0.0002742	-0.0365533	0.0029321	0.0492401	-0.1156129	-0.1301910	0.3771048	0.0002925	-0.020544	0.0255058
-0.0047933	-0.1891339	-0.1117223	0.3135444	0.5493592	-0.3601430	-0.7809620	-0.0049525	-0.2005024	0.0286271
0.0002742	-0.0365533	0.0029321	0.0492401	-0.1156129	-0.1301910	0.8771048	0.0002925	-0.020544	0.0255058
-0.0047933	-0.1891339	-0.1117223	0.3135444	0.5493592	-0.3601430	-0.7809620	-0.0049525	-0.2005024	0.0286271
0.0002742	-0.0365533	0.0029321	0.0492401	-0.1156129	-0.1301910	0.8771048	-0.0002925	0.020544	0.0255058
-0.0047933	-0.1891339	-0.1117223	0.3135444	0.5493592	-0.3601430	-0.7809620	0.0049525	0.2005024	-0.0286271
0.0002742	-0.0365533	0.0029321	0.0492401	-0.1156129	-0.1301910	0.8771048	-0.0002925	0.020544	0.0255058

Table 20 (Continued)

-0.6126958	-0.2165011	-0.2527611	1.4761797	0.0	0.0	0.0	0.0	0.0	0.0	0.0
1.3728127	0.4112914	0.6462588	-3.1188319	0.0	0.0	0.0	0.0	0.0	0.0	0.0
-0.7095174	-0.7101918	-0.9664186	2.5943229	0.0	0.0	0.0	0.0	0.0	0.0	0.0
0.0	0.0	0.0	0.0	0.0	0.0	0.0	0.0	0.0	0.0	0.0
0.0	0.0	0.0	0.0	0.0	0.0	0.0	0.0	0.0	0.0	0.0
0.0	0.0	0.0	0.0	0.4159034	0.0994465	-1.3764682	1.3539349	0.3965054	0.4605205	0.4754966
0.0	0.0	0.0	0.0	0.0251987	0.8109007	1.7389465	-1.1911715	0.0365302	0.4754966	0.4754966
-0.0654523	-1.0569132	-0.4887564	0.1613357	0.0	0.0	0.0	0.0	0.0	0.0	0.0
0.7245369	1.2271945	0.4601474	-0.1522035	0.0	0.0	0.0	0.0	0.0	0.0	0.0
0.6126958	0.2165011	0.2527611	-1.4761797	0.0	0.0	0.0	0.0	0.0	0.0	0.0
-1.3728127	-0.4112914	-0.6462588	3.1188319	0.0	0.0	0.0	0.0	0.0	0.0	0.0
0.7095174	0.7101918	0.9664186	-2.5943229	0.0	0.0	0.0	0.0	0.0	0.0	0.0
0.0	0.0	0.0	0.0	0.0	0.0	0.0	0.0	0.0	0.0	0.0
0.0	0.0	0.0	0.0	0.0	0.0	0.0	0.0	0.0	0.0	0.0
0.0	0.0	0.0	0.0	-0.4159034	-0.0994465	1.3764682	-1.3539349	0.3965054	0.4605205	0.4754966
0.0	0.0	0.0	0.0	-0.0251987	-0.8109007	-1.7389465	1.1911715	0.0365302	0.4754966	0.4754966
-0.0654523	-1.0569132	-0.4887564	0.1613357	0.0	0.0	0.0	0.0	0.0	0.0	0.0
0.7245369	1.2271945	0.4601474	-0.1522035	0.0	0.0	0.0	0.0	0.0	0.0	0.0
0.4489439	-0.6134210	-0.0304286	-0.8090616	0.2918587	-0.0417904	1.5026310	-1.1427641	0.2762407	0.2657019	0.2657019
-0.0245435	0.0860637	0.3714960	0.8675077	-0.0092055	-0.2119120	-0.4439195	1.0277654	-0.0085908	0.1115279	0.1115279
0.4489439	-0.6134210	-0.0304286	-0.8090616	-0.2918587	0.0417904	-1.5026310	1.1427641	-0.2762407	0.2657019	0.2657019
-0.0245435	0.0860637	0.3714960	0.8675077	0.0092055	0.2119120	0.4439195	-1.0277654	0.0085908	0.1115279	0.1115279
-0.4489439	0.6134210	0.0304286	0.8090616	-0.2918587	0.0417904	-1.5026310	1.1427641	0.2762407	0.2657019	0.2657019
0.0245435	-0.0860637	-0.3714960	-0.8675077	0.0092055	0.2119120	0.4439195	-1.0277654	-0.0085908	0.1115279	0.1115279
-0.4489439	0.6134210	0.0304286	0.8090616	0.2918587	-0.0417904	1.5026310	-1.1427641	-0.2762407	0.2657019	0.2657019
0.0245435	-0.0860637	-0.3714960	-0.8675077	-0.0092055	-0.2119120	-0.4439195	1.0277654	0.0085908	0.1115279	0.1115279

Table 20 (continued)

Table 21. MO expansions for  ${}^1A_g$  first excited state at  $\Delta R = 1.5$  a.u.

0.6853570	-0.1544277	0.0757424	0.0655898	0.4461685	0.1717142	0.8098718	0.6851417	-0.1529575	-0.2327768
0.0769154	0.4884509	-0.2268228	-0.1850187	-0.9573505	-0.4202962	-1.6623789	0.0772988	0.4839581	0.5910413
0.0055039	-0.0417112	0.0315708	0.0232875	0.0518594	0.6047912	1.2896518	0.0052992	-0.0291515	-0.1477734
0.0	0.0	0.0	0.0	0.0	0.0	0.0	0.0	0.0	0.0
0.0	0.0	0.0	0.0	0.0	0.0	0.0	0.0	0.0	0.0
0.0	0.0	0.0	0.0	0.0	0.0	0.0	0.0	0.0	0.0
0.0	0.0	0.0	0.0	0.0	0.0	0.0	0.0	0.0	0.0
0.0022614	0.1042657	0.5517304	-0.2932590	-0.3044981	-0.1986037	-0.3808643	0.0028635	0.1234569	-0.8398138
0.0004132	0.0113201	-0.0378893	-0.5694252	0.4647483	-0.2755694	0.3335591	0.0003478	0.0128332	0.1299017
0.6853570	-0.1544277	0.0757424	0.0655898	0.4461685	0.1717142	0.8098718	-0.6851417	0.1529575	0.2327768
0.0769154	0.4884509	-0.2268228	-0.1850187	-0.9573505	-0.4202962	-1.6623789	-0.0772988	-0.4839581	0.5910413
0.0055039	-0.0417112	0.0315708	0.0232875	0.0518594	0.6047912	1.2896518	-0.0052992	0.0291515	0.1477734
0.0	0.0	0.0	0.0	0.0	0.0	0.0	0.0	0.0	0.0
0.0	0.0	0.0	0.0	0.0	0.0	0.0	0.0	0.0	0.0
0.0	0.0	0.0	0.0	0.0	0.0	0.0	0.0	0.0	0.0
0.0	0.0	0.0	0.0	0.0	0.0	0.0	0.0	0.0	0.0
-0.0022614	-0.1042657	-0.5517304	0.2932590	0.3044981	0.1986037	0.3808643	0.0028635	0.1234569	-0.8398138
-0.0004132	-0.0113201	0.0378893	0.5694252	-0.4647483	-0.2755694	-0.3335591	0.0003478	0.0128332	0.1299017
-0.0047876	-0.1887915	-0.1108606	-0.2951656	-0.5609230	-0.3609073	-0.7799888	-0.0049300	-0.1994036	0.0353600
0.002687	-0.0039167	0.0028450	-0.0518571	0.1135863	-0.1275984	0.9784157	0.002306	-0.0023652	0.0228865
-0.0047876	-0.1887915	-0.1108606	-0.2951656	-0.5609230	-0.3609073	-0.7799888	-0.0049300	-0.1994036	0.0353600
0.0002687	-0.0039167	0.0028450	-0.0518531	0.1135863	-0.1275984	0.8784157	0.002306	-0.0023652	0.0228865
-0.0047876	-0.1887915	-0.1108606	-0.2951656	-0.5609230	-0.3609073	-0.7799888	0.0049300	0.1994036	-0.0353600
0.0002687	-0.0039167	0.0028450	-0.0518531	0.1135863	-0.1275984	0.9784157	-0.002306	0.0023652	-0.0228865
-0.0047876	-0.1887915	-0.1108606	-0.2951656	-0.5609230	-0.3609073	-0.7799888	0.0049300	0.1994036	-0.0353600
0.0002687	-0.0039167	0.0028450	-0.0518531	0.1135863	-0.1275984	0.8784157	-0.002306	0.0023652	-0.0228865

**Table 21 (Continued)**

-0.5852361	-0.1783426	-0.2379985	1.4415236	0.0	0.0	0.0	0.0	0.0	0.0	0.0
1.3149755	0.4040971	0.6140305	-3.0448659	0.0	0.0	0.0	0.0	0.0	0.0	0.0
-0.6742551	-0.7533790	-0.9407860	2.5340731	0.0	0.0	0.0	0.0	0.0	0.0	0.0
0.0	0.0	0.0	0.0	0.0	0.0	0.0	0.0	0.0	0.0	0.0
0.0	0.0	0.0	0.0	0.0	0.0	0.0	0.0	0.0	0.0	0.0
0.0	0.0	0.0	0.0	0.4128368	0.1162335	-1.9775794	1.3178486	0.3954643	0.4641321	
0.0	0.0	0.0	0.0	0.0277696	0.7963305	1.6920708	-1.1631454	0.0375924	0.4723063	
-0.0425219	-1.0366012	-0.4421449	0.1335445	0.0	0.0	0.0	0.0	0.0	0.0	0.0
0.7147316	1.2100112	0.4190930	-0.1294685	0.0	0.0	0.0	0.0	0.0	0.0	0.0
0.5852361	0.1783426	0.2379985	-1.4415236	0.0	0.0	0.0	0.0	0.0	0.0	0.0
-1.3149755	-0.4040971	-0.6140305	3.0448659	0.0	0.0	0.0	0.0	0.0	0.0	0.0
0.6742551	0.7533790	0.9407860	-2.5340731	0.0	0.0	0.0	0.0	0.0	0.0	0.0
0.0	0.0	0.0	0.0	0.0	0.0	0.0	0.0	0.0	0.0	0.0
0.0	0.0	0.0	0.0	0.0	0.0	0.0	0.0	0.0	0.0	0.0
0.0	0.0	0.0	0.0	-0.4128368	-0.1162335	1.9775794	-1.3178486	0.3954643	0.4641321	
0.0	0.0	0.0	0.0	0.0277696	0.7963305	-1.6920708	1.1631454	0.0375924	0.4723063	
-0.0425219	-1.0366012	-0.4421449	0.1335445	0.0	0.0	0.0	0.0	0.0	0.0	0.0
0.7147316	1.2100112	0.4190930	-0.1294685	0.0	0.0	0.0	0.0	0.0	0.0	0.0
0.4483028	-0.6085207	-0.0037717	-0.8164581	0.2927754	-0.0509599	1.4734813	-1.1230336	0.2787772	-0.2701610	
-0.0243901	0.0882711	0.3563431	0.8742027	-0.0097724	-0.2080111	-0.4354400	1.0215245	-0.0093395	-0.1087602	
0.4483028	-0.6085207	-0.0037717	-0.8164581	-0.2927754	0.0509599	-1.4734813	1.1230336	-0.2787772	0.2701610	
-0.0243901	0.0882711	0.3563431	0.8742027	0.0097724	0.2080111	0.4354400	-1.0215245	0.0093395	0.1087602	
0.4483028	0.6085207	0.0037717	0.8164581	-0.2927754	0.0509599	-1.4734813	1.1230336	-0.2787772	-0.2701610	
0.0243901	-0.0882711	-0.3563431	-0.8742027	0.0097724	0.2080111	0.4354400	-1.0215245	-0.0093395	-0.1087602	
-0.4483028	0.6085207	0.0037717	0.8164581	0.2927754	-0.0509599	1.4734813	-1.1230336	-0.2787772	0.2701610	
0.0243901	-0.0882711	-0.3563431	-0.8742027	-0.0097724	-0.2080111	-0.4354400	1.0215245	0.0093395	0.1087602	

Table 21 (continued)

Table 22. MO expansions for  ${}^1A_g$  first excited state at  $\Delta R = 1.7$  a.u.

0.6856763	-0.1491434	0.1033793	-0.0068765	-0.5282801	0.2574084	0.9417872	0.6853941	-0.1445469	-0.2499366
0.0759628	0.4720683	-0.3041133	-0.0219657	1.1430106	-0.5976976	-1.7195227	0.0765077	0.4612626	0.6457683
0.0056890	-0.0393474	0.0500900	-0.0372460	-0.1500211	0.7127287	1.2971176	0.0054917	-0.0272530	-0.1681958
0.0	0.0	0.0	0.0	0.0	0.0	0.0	0.0	0.0	0.0
0.0	0.0	0.0	0.0	0.0	0.0	0.0	0.0	0.0	0.0
0.0	0.0	0.0	0.0	0.0	0.0	0.0	0.0	0.0	0.0
0.0	0.0	0.0	0.0	0.0	0.0	0.0	0.0	0.0	0.0
0.0026821	0.1413673	0.5189602	-0.2875455	0.4487018	-0.3180531	-0.5210524	0.0032841	0.1574235	-0.7707914
0.0004517	0.0178425	-0.0385461	-0.6096113	-0.4819194	0.3383915	0.4650594	0.0000577	0.0108132	0.1516606
0.6856763	-0.1491434	0.1033793	-0.0068765	-0.5282801	0.2574084	0.9417872	-0.6853941	0.1445469	0.2499366
0.0759628	0.4720683	-0.3041133	-0.0219657	1.1430106	-0.5976976	-1.7195227	-0.0765077	0.4612626	0.6457683
0.0056890	-0.0393474	0.0500900	-0.0372460	-0.1500211	0.7127287	1.2971176	-0.0054917	0.0272530	-0.1681958
0.0	0.0	0.0	0.0	0.0	0.0	0.0	0.0	0.0	0.0
0.0	0.0	0.0	0.0	0.0	0.0	0.0	0.0	0.0	0.0
0.0	0.0	0.0	0.0	0.0	0.0	0.0	0.0	0.0	0.0
0.0	0.0	0.0	0.0	0.0	0.0	0.0	0.0	0.0	0.0
-0.0026821	-0.1413673	-0.5189602	0.2875455	-0.4487018	0.3180531	0.5210524	0.0032841	0.1574235	-0.7707914
-0.0004517	-0.0178425	0.0385461	0.6096113	0.4819194	-0.3383915	-0.4650594	0.0000577	0.0108132	0.1516606
-0.0048470	-0.1921984	-0.1032023	-0.1962647	0.6378968	-0.4586276	-0.7920496	-0.0046070	-0.1939551	0.0631989
0.0002615	-0.0055870	-0.0007291	-0.0940561	-0.1702116	-0.0667465	0.9949395	0.0031061	-0.0055432	0.0202077
-0.0048470	-0.1921984	-0.1032023	-0.1962647	0.6378968	-0.4586276	-0.7920496	-0.0046070	-0.1939551	0.0631989
0.0002615	-0.0055870	-0.0007291	-0.0940561	-0.1702116	-0.0667465	0.9949395	0.0031061	-0.0055432	0.0202077
-0.0048470	-0.1921984	-0.1032023	-0.1962647	0.6378968	-0.4586276	-0.7920496	0.0046070	0.1939551	-0.0631989
0.0002615	-0.0055870	-0.0007291	-0.0940561	-0.1702116	-0.0667465	0.9949395	-0.0001061	0.0055432	-0.0202077
-0.0048470	-0.1921984	-0.1032023	-0.1962647	0.6378968	-0.4586276	-0.7920496	0.0046070	0.1939551	-0.0631989
0.0002615	-0.0055870	-0.0007291	-0.0940561	-0.1702116	-0.0667465	0.9949395	-0.0001061	0.0055432	-0.0202077
-0.0048470	-0.1921984	-0.1032023	-0.1962647	0.6378968	-0.4586276	-0.7920496	0.0046070	0.1939551	-0.0631989
0.0002615	-0.0055870	-0.0007291	-0.0940561	-0.1702116	-0.0667465	0.9949395	-0.0001061	0.0055432	-0.0202077

**Table 2.2** (Continued)

Table 2.2 (Continued)

Table 23. MO expansions for  $^1A_g$  first excited state at  $\Delta R = 2.0$  a.u.

0.6857496	-0.1420535	0.1262549	-0.0123922	0.5287008	0.2720117	-0.8510447	0.6856013	-0.1369165	-0.2457065
0.0756281	0.4541503	-0.3022619	-0.0050372	-1.1490483	-0.6271064	1.3353276	0.0759077	0.441391	0.6422279
0.0056397	-0.0359385	-0.677565	-0.00368230	-0.1600783	-1.7356121	-1.3044116	0.0057339	-0.0176528	-0.1657102
0.0	0.0	0.0	0.0	0.0	0.0	0.0	0.0	0.0	0.0
0.0	0.0	0.0	0.0	0.0	0.0	0.0	0.0	0.0	0.0
0.0	0.0	0.0	0.0	0.0	0.0	0.0	0.0	0.0	0.0
0.0	0.0	0.0	0.0	0.0	0.0	0.0	0.0	0.0	0.0
0.0027371	0.1690530	0.5021359	-0.02938980	-0.4715593	-0.3502147	0.5607291	0.0035056	0.1806670	-0.7230243
0.0000810	0.0179594	-0.0376611	-0.0606097	0.4673994	0.3518686	-0.489544	-0.0005705	0.055626	0.1487945
0.6857496	-0.1426335	0.1262549	-0.0123922	0.5287008	0.2720117	-0.8510447	-0.686013	0.1369165	0.2457065
0.0756281	0.4541503	-0.3022639	-0.0050372	-1.1480483	-0.6271064	1.7353276	-0.0759077	-0.413591	-0.6422279
0.0056397	-0.0359385	-0.677565	-0.00368230	-0.1600783	-1.7356121	-1.3044116	-0.0057339	0.176429	0.1657102
0.0	0.0	0.0	0.0	0.0	0.0	0.0	0.0	0.0	0.0
0.0	0.0	0.0	0.0	0.0	0.0	0.0	0.0	0.0	0.0
0.0	0.0	0.0	0.0	0.0	0.0	0.0	0.0	0.0	0.0
0.0	0.0	0.0	0.0	0.0	0.0	0.0	0.0	0.0	0.0
0.0	0.0	0.0	0.0	0.0	0.0	0.0	0.0	0.0	0.0
0.0	0.0	0.0	0.0	0.0	0.0	0.0	0.0	0.0	0.0
-0.0027871	-0.1690530	-0.0521359	0.2938980	0.4715593	0.2502147	-0.507291	0.0035056	-0.1906670	-0.7230243
-0.0000810	-0.0179594	0.0376611	0.606097	-0.4673994	-0.3518686	0.699544	-0.0005705	0.055625	0.1487945
-0.0047302	-0.1973772	-0.162667	-0.197685	-0.7050890	-0.4749552	0.7954947	-0.004106	-0.194369	-0.745660
0.001742	-0.0058507	0.028653	-0.075144	0.1743176	-0.0566115	-0.8996132	0.0000082	-0.065219	0.0135913
-0.0047302	-0.1973772	-0.162667	-0.197685	-0.7050890	-0.4749552	0.7954947	-0.004106	-0.194369	-0.745660
-0.0001742	-0.0058507	-0.028653	-0.075144	0.1743176	-0.0566115	-0.8996132	0.0000082	-0.065219	0.0135913
-0.0001742	-0.0058507	-0.028653	-0.075144	0.1743176	-0.0566115	-0.8996132	0.0000082	-0.065219	0.0135913
-0.0047302	-0.1973772	-0.162667	-0.197685	-0.7050890	-0.4749552	0.7954947	-0.004106	-0.194369	-0.745660
-0.0001742	-0.0058507	-0.028653	-0.075144	0.1743176	-0.0566115	-0.8996132	0.0000082	-0.065219	0.0135913
-0.0047302	-0.1973772	-0.162667	-0.197685	-0.7050890	-0.4749552	0.7954947	-0.004106	-0.194369	-0.745660
-0.0001742	-0.0058507	-0.028653	-0.075144	0.1743176	-0.0566115	-0.8996132	0.0000082	-0.065219	0.0135913
-0.0001742	-0.0058507	-0.028653	-0.075144	0.1743176	-0.0566115	-0.8996132	0.0000082	-0.065219	0.0135913

**Table 2.3 (Continued)**

Table 23 (Continued)

Table 24. MO expansions for  ${}^1A_g$  first excited state at  $\Delta R = 2.4$  a.u.

0.6857864	-0.1341010	0.1469054	0.0087495	0.5311174	-0.2640754	-0.8758117	0.6857866	-0.1286017	-0.2311044
0.0753893	0.4313690	-0.4154467	-0.0444301	-1.0943831	0.6095469	1.7834249	0.0755500	0.4203401	0.6136967
0.0055547	-0.0313118	0.0807676	-0.0169161	0.1392173	-0.7256298	-1.3354014	0.0058052	-0.0127517	-0.1565381
0.0	0.0	0.0	0.0	0.0	0.0	0.0	0.0	0.0	0.0
0.0	0.0	0.0	0.0	0.0	0.0	0.0	0.0	0.0	0.0
0.0	0.0	0.0	0.0	0.0	0.0	0.0	0.0	0.0	0.0
0.0	0.0	0.0	0.0	0.0	0.0	0.0	0.0	0.0	0.0
0.0028498	0.2012738	0.4949782	-0.3107124	-0.4556400	0.3552792	0.5963122	0.034660	0.2068227	-0.6557952
-0.0002464	0.0166146	-0.0400654	-0.5817101	0.436794	-0.3490538	-0.5324342	-0.0009345	0.0018467	0.1227112
0.6857864	-0.1341013	0.1469054	0.0087495	0.5011174	-0.2640754	-0.8758117	-0.6857856	0.1285017	0.2311044
0.0753893	0.4313690	-0.4154467	-0.0444301	-1.0943831	0.6095469	1.7834249	-0.0755500	-0.4203401	0.6136967
0.0055547	-0.0313118	0.0807676	-0.0169161	0.1392173	-0.7256298	-1.3354014	-0.0058052	0.0127517	0.1565381
0.0	0.0	0.0	0.0	0.0	0.0	0.0	0.0	0.0	0.0
0.0	0.0	0.0	0.0	0.0	0.0	0.0	0.0	0.0	0.0
0.0	0.0	0.0	0.0	0.0	0.0	0.0	0.0	0.0	0.0
0.0	0.0	0.0	0.0	0.0	0.0	0.0	0.0	0.0	0.0
0.0028498	-0.2012738	-0.4949782	0.3107124	0.4556400	-0.3552792	-0.5963122	0.0034550	0.2058227	-0.6557952
0.0002464	-0.0166146	0.0400654	0.5817101	-0.436794	0.3490538	0.5324342	-0.0009345	0.0018467	0.1227112
-0.0045162	-0.2026679	-0.0913380	-0.1892387	-0.6924467	0.4660744	0.8201610	-0.0042556	-0.1977449	0.0817725
0.0000860	-0.0061414	0.0346504	-0.0882111	0.1634535	0.0680736	-0.9063995	-0.0000392	-0.0066336	0.0049159
-0.0045162	-0.2026679	-0.0913380	-0.1892387	-0.6924467	0.4550744	0.8201610	-0.0042556	-0.1977449	0.0817725
0.0000860	-0.0061414	0.0046504	-0.0882111	0.1634535	0.0680736	-0.9063995	-0.0000392	-0.0066336	0.0049159
-0.0045162	-0.2026679	-0.0913380	-0.1892387	-0.6924467	0.4660744	0.8201610	0.0042556	0.1977449	-0.0817725
0.0000860	-0.0061414	0.0046504	-0.0882111	0.1634535	0.0680736	-0.9063995	0.0000392	0.0066336	-0.0049159
-0.0045162	-0.2026679	-0.0913380	-0.1892387	-0.6924467	0.4660744	0.8201610	0.0042556	0.1977449	-0.0817725
0.0000860	-0.0061414	0.0046504	-0.0882111	0.1634535	0.0680736	-0.9063995	0.0000392	0.0066336	-0.0049159

**Table 2.4** (Continued)

**Table 24 (Continued)**

Table 25. MO expansions for  $^1A_g$  first excited state at  $\Delta R = 3.0$  a.u.

0.6858565	-0.1230156	0.1621936	-0.0442313	0.4730772	-0.2562846	0.9056878	0.6858137	-0.1181518	-0.2197217
0.0750600	0.4017489	-0.4592554	0.1174888	-1.0366114	0.5927760	-1.3428466	0.0751760	0.3926981	0.5935544
0.0054862	-0.0260373	0.0851347	-0.0016695	0.1162478	-0.7112737	1.3683396	0.0057429	-0.0080462	-0.1437979
0.0	0.0	0.0	0.0	0.0	0.0	0.0	0.0	0.0	0.0
0.0	0.0	0.0	0.0	0.0	0.0	0.0	0.0	0.0	0.0
0.0	0.0	0.0	0.0	0.0	0.0	0.0	0.0	0.0	0.0
0.0	0.0	0.0	0.0	0.0	0.0	0.0	0.0	0.0	0.0
0.0028898	0.2393248	0.4910467	0.3317762	-0.4346923	0.3516342	-0.6236119	0.0032581	0.2398385	-0.6132341
-0.0004342	0.0135632	-0.0464626	0.5492626	0.4321156	-0.3451505	0.5688653	-0.0009130	-0.0002559	0.0981646
0.6858565	-0.1230156	0.1621936	-0.0442813	0.4730772	-0.2562846	0.9056878	0.6858137	0.1181518	0.2197217
0.0750600	0.4017489	-0.4592554	0.1174888	-1.0366114	0.5927760	-1.3428466	0.0751760	0.3926981	0.5935544
0.0054862	-0.0260373	0.0851347	-0.0016695	0.1162478	-0.7112737	1.3683396	0.0057429	0.0080462	0.1437979
0.0	0.0	0.0	0.0	0.0	0.0	0.0	0.0	0.0	0.0
0.0	0.0	0.0	0.0	0.0	0.0	0.0	0.0	0.0	0.0
0.0	0.0	0.0	0.0	0.0	0.0	0.0	0.0	0.0	0.0
0.0	0.0	0.0	0.0	0.0	0.0	0.0	0.0	0.0	0.0
-0.0028898	-0.2393248	-0.4910467	-0.3317762	0.4346923	-0.3516342	0.6236119	0.0032581	0.2398385	-0.6132341
0.0004342	-0.0135632	0.0464626	-0.5492626	-0.4321156	0.3451505	-0.5688653	-0.0009130	-0.0002559	0.0981646
-0.0042306	-0.3066467	-0.0723416	0.2187294	-0.6736009	0.4564583	-0.8495280	-0.0041236	-0.2028661	0.0786767
0.0000177	-0.0069442	0.0033873	0.0757198	0.1556850	0.0821498	0.7141036	-0.0000333	-0.0064834	-0.0006375
-0.00042306	-0.2066467	-0.0723416	0.2187294	-0.6736009	0.4564583	-0.8495280	-0.0041236	-0.2028661	0.0786767
0.0000177	-0.0069442	0.0033873	0.0757198	0.1556850	0.0821498	0.7141036	-0.0000333	-0.0064834	-0.0006375
-0.00042306	-0.2066467	-0.0723416	0.2187294	-0.6736009	0.4564583	-0.8495280	0.0041236	0.2028661	-0.0786767
0.0000177	-0.0069442	0.0033873	0.0757198	0.1556850	0.0821498	0.7141036	0.0000333	0.0064834	0.0006375
-0.00042306	-0.2066467	-0.0723416	0.2187294	-0.6736009	0.4564583	-0.8495280	0.0041236	0.2028661	-0.0786767
0.0000177	-0.0069442	0.0033873	0.0757198	0.1556850	0.0821498	0.7141036	0.0000333	0.0064834	0.0006375
-0.0000177	-0.0069442	0.0033873	0.0757198	0.1556850	0.0821498	0.7141036	0.0000333	0.0064834	0.0006375

Table 25 (continued)

Table 25 (continued)

Table 26. MO expansions for  ${}^1\text{A}_q$  first excited state at  $\Delta R = 5.0$  a.u.

**Table 26 (Continued)**

**Table 26** (Continued)